2008

INVESTIGATION OF BLAST MITIGATION PROPERTIES OF CARBON AND POLYURETHANE BASED FOAMS

Bradley E. Toon
University of Kentucky, brad.toon@uky.edu

ABSTRACT OF THESIS

INVESTIGATION OF BLAST MITIGATION PROPERTIES OF CARBON AND POLYURETHANE BASED FOAMS

Solid foams have been studied for years for their ability to mitigate damage from sudden impact. Small explosive attacks threaten to damage or destroy key structures in some parts of the world. A newly developed material, carbon foam, may offer the ability to mitigate the effects of such blasts. This project investigates the energy absorbing properties of carbon and polyurethane based foams in dynamic compression to illustrate their viability to protect concrete structures from the damaging effects of pressure waves from a small blast. Cellular solid mechanics fundamentals and a survey of the microscopic cellular structure of each type of foam are discussed. Experiments were performed in three strain rate regimes: low strain rate compression testing, middle strain rate impact testing, and high strain rate blast testing to reveal mechanical behavior. Experiments show a 7.62 cm (3") thick hybrid composite layered foam sample can protect a concrete wall from a small blast.

KEYWORDS: carbon foam, cellular solids, energy absorption, blast mitigation, impact testing

Bradley E. Toon

April 14, 2008

INVESTIGATION OF BLAST MITIGATION PROPERTIES OF CARBON AND POLYURETHANE BASED FOAMS

By

Bradley E. Toon

Rodney J. Andrews, Ph.D
Co-Director of Thesis

Kozo Saito, Ph.D.
Co-Director of Thesis

L. Scott Stephens, Ph.D
Director of Graduate Studies

April 14, 2008

RULES FOR THE USE OF THESES

Unpublished theses submitted for the Master's degree and deposited in the University of Kentucky Library are, as a rule open for inspection, but are to be used only with due regard to the rights of the authors. Bibliographical references may be noted, but quotations or summaries of parts may be published only with the permission of the author, and with the usual scholarly acknowledgments.

Extensive copying or publication of the thesis in whole or in part also requires the consent of the Dean of the Graduate School of the University of Kentucky.

Name Date

_____

_____

_____

_____

_____

_____

_____

_____

_____

_____

_____

_____

_____

_____

_____

_____

THESIS

Bradley E. Toon

The Graduate School
University of Kentucky
2008

INVESTIGATION OF BLAST MITIGATION PROPERTIES OF CARBON AND POLYURETHANE BASED FOAMS

THESIS

A thesis submitted in partial fulfillment of the requirements
for the degree of Master of Science in Mechanical
Engineering in the College of Engineering at the
University of Kentucky

By

Bradley Edward Toon

Lexington, Kentucky

Co-Director: Dr. Rodney J. Andrews, Associate Professor of Mechanical Engineering
Co-Director: Dr. Kozo Saito, Professor of Mechanical Engineering

Lexington, Kentucky

2008

Acknowledgements

I would like to thank my advisor, Dr. Rodney Andrews, for the opportunity to complete research at the Center for Applied Energy Research and for setting this study in motion. I would like to thank the members of my review committee, Dr. Kozo Saito and Dr. Raymond LeBeau, Jr..

This project would not have been possible without the efforts of many members of the Center for Applied Energy Research (CAER) Carbon Group, especially Dr. Mark Meier, Dr. Matt Weisenberger, Mr. David Jacques, and Mr. Terry Rantell. I am grateful for their insight throughout this project and for sharing their knowledge of carbon materials.

Blast testing would have been impossible without the direction of Dr. Tom Thurman of Eastern Kentucky University. Every test was performed safely thanks to his guidance. Also, I am grateful for all the work of Dr. Paul Yeary of Alice Lloyd College. Special thanks go to all the members of the Institute of Research for Technology Development for helping to guide my graduate education and research.

I would like to thank all the CAER staff members who helped with the construction of test components and contributed to this project.

I greatly appreciate Koppers, Inc. for providing funding for my graduate studies. The Department of Homeland Security, through the National Institute of Hometown Security, is also recognized for funding this project.

Personally, I must thank my family and friends for their support during this process. Special thanks my mother, Carol Toon, and the Merimee family.

Table of Contents

List of Tables

List of Figures

List of Files

BToonThesis.pdf……4.9 MB

Nomenclature

F	Applied Force
d	Cell Diameter
ρ	Density
X	Distance from Explosion
E	Elastic Modulus
En	Energy
Y	Explosive Yield Factor
ρ_f	Foam Density
E_f	Foam Elastic Modulus
u_f	Foam Front Velocity
H_c	Heat of Combustion
h	Height
υ_f	Ideal Foam Poisson's Ratio
δ	Ideal Ligament Deflection
l	Ideal Ligament Length
t	Ideal Ligament Thickness
J	Impulse
KE	Kinetic Energy
M	Mach Number
m	Mass
P	Overpressure
Φ	Porosity
ρ_s	Pre-Foaming Density
P_{xy}	Pressure Ratio
I	Second Moment of Inertia
m_s	Sled Mass
E_s	Solid Elastic Modulus
Γ	Specific Heat Ratio
ε	Strain
γ	Strain Energy Density
σ	Stress
En_{lost}	Sum of Energy Lost and Energy Absorbed by Foam
m_t	Target Mass
t	Time
σ_d	Total Densified Stress or Maximum Stress
v	Velocity
u_w	Wave Front Velocity
w	Width
σ_y	Yield Stress

Abbreviations

KFOAML	Koppers, Inc. carbon foam type L
KFOAML1	Koppers, Inc. carbon foam type L1
KFOAMLF	Koppers, Inc. carbon foam type LF
KFOAMLF1	Koppers, Inc. carbon foam type LF1
4 lb. PU	Polyurethane foam of density 4 pounds per cubic foot
8 lb. PU	Polyurethane foam of density 8 pounds per cubic foot
16 lb. PU	Polyurethane foam of density 16 pounds per cubic foot
4 lb. Ceno	Polyurethane foam of density 4 pounds per cubic foot with 25% Cenosphere additives by mass
8 lb. Ceno	Polyurethane foam of density 8 pounds per cubic foot with 25% Cenosphere additives by mass
16 lb. Ceno	Polyurethane foam of density 16 pounds per cubic foot with 25% Cenosphere additives by mass
4 lb. UFA	Polyurethane foam of density 4 pounds per cubic foot with 50% Ultra fine Fly Ash additives by mass
8 lb. UFA	Polyurethane foam of density 8 pounds per cubic foot with 50% Ultra fine Fly Ash additives by mass
16 lb. UFA	Polyurethane foam of density 16 pounds per cubic foot with 50% Ultra fine Fly Ash additives by mass

Chapter 1 Introduction

1.1 Motivation

The Department of Homeland Security described attacks on United States interest around the world over the past 25 years in a document entitled "The National Plan for Research and Development In Support of Critical Infrastructure Protection." [1] Recent bomb attacks on US buildings and military vehicles have motivated the effort to find new materials to mitigate the destructive effects of explosives. Several studies are underway to develop better ways to design buildings and reinforce existing at-risk structures. [2]

This project, supported by the Department of Homeland Security and Koppers, Inc., investigated the mechanical properties of carbon foam and identified foam materials that are best suited to mitigate the effects of a small blast on building walls. A multifunctional material that provides blast mitigation, chemical and radiation protection, and shielding from electromagnetic interference was desired. Thick steel panels may meet these protection requirements, but in most cases existing structures can not support the extreme weight at protective steel panels demand. Therefore, the material must be lightweight and easily retrofitted to existing structures. This project focused on the ability of carbon foam to mitigate the effects of blasts. This study does not intend to investigate blast mitigation for large explosions, like the Oklahoma City bombing in 1995. The goal was to uncover a method of protecting buildings and vehicles from the most prevalent threat of small explosions.

Koppers, Inc. (Pittsburgh, Pennsylvania, USA) produced the carbon foam that was central to this project. They have already established a number of novel uses for the foam including its ability to shield electromagnetic interference. Its properties may meet the other multifunctional requirements for chemical and radiation protection; however these attributes will not be elaborated here. Carbon foam is lightweight and permeable but strong, making it a candidate for acoustic and structural applications. [3]

Additionally, new impact and explosion testing methods were developed through this project. Although several testing methods already exist, new methods allowed the blast size of interest to be reproduced.

1.2 Introduction

The project objective was to investigate the effectiveness of using carbon foam to mitigate blasts in light of the requirement to retrofit existing structures with coverings that protect against radiation, chemical exposure, and electromagnetic interference. The results of this study provided information for a wall covering that is lightweight, shields electromagnetic interference, resists flame, radiation, and chemicals, and protects against small explosions. The protective material must be installed without affecting the integrity of existing structures. The investigation focused on the ability of carbon foam to mitigate the pressure wave from a small blast. The prevailing threat to vital structures around the world is small explosives.

Koppers, Inc., who provided some of the funding for this study, produced the carbon foams that were studied. Four types of carbon foam were investigated: L, L1, LF and LF1. All four types were pitch based foams. Types L1 and LF1 contained 2% multiwalled carbon nanotubes by weight. Multiwalled carbon nanotubes have been shown to enhance strength properties in some materials. Types L and L1 were carbonized while LF and LF1 were graphitized after carbonization. Carbon foam will be described further in Chapter 2. [3, 4]

Although carbon foam was the central material of this project, polyurethane and polystyrene foams were included for comparison. Polyurethane foam has been studied for its energy absorbing characteristics under impact for many years. Density is one of the characteristics that determine the yield stress and how much energy foam will absorb. Three nominal densities of polyurethane foam were studied: 4, 8 and 16 pounds per cubic foot. Studying three densities provided an understanding of the material selection process for impacts. Denser foams absorb more energy; however, yield stress increases with density which may not be ideal for all impact events. Specifically, if the impact pressure is less than the yield stress, the foam will not absorb much energy and the object the foam

is meant to protect experiences most of the impact pressure. This behavior will be discussed further in Chapters 4 and 5.

Polyurethane foam can be made by combining two components, polyol and toluene diisocyanate. When the two are thoroughly mixed carbon dioxide gas is released. As the gas rises out of the liquid, it forms elongated pores in solid foam. Carbon foam is created from pitch that is carbonized at a high temperature after foaming.[4] The material properties will be discussed further in Chapter 2. Since the polyurethane foam components exist in liquid form, they can be mixed with additives with known properties to create different types of polyurethane foam. Specifically, non-flammable additives were mixed with polyol and toluene diisocyanate to create polyurethane foam that resisted flame. Ultra fine fly ash, or UFA, and cenospheres are the remains of high temperature (>1500°C (>2732°F)) coal combustion, and resist flame ignition. Fly ash is mostly silica and lime spheres of diameter between 0.5 and 300 μm (0.02 and 11.7 mil). Cenospheres are alumina and silica spherical remains between 10 and 300 μm (0.39 and 11.7 mil). UFA and cenospheres were added at the highest possible concentration that would allow polyurethane to foam.[5] This limit was uncovered empirically. When the concentration of UFA or cenospheres was too great, the polyurethane mixture became viscous and impossible to properly mix. The resulting foam contained pockets of UFA and cenospheres. These components must be combined so that the particles are embedded in the polyurethane foam structure. Enlarged photos of properly mixed polyurethane foam will illustrate this in Chapter 3.

A brief experiment showed the addition of UFA and cenospheres to polyurethane enhanced its resistance to flame. Carbon and polyurethane based foams were cut into cubes measuring 2.54 cm X 2.54 cm 2.54 cm (1” X 1” X 1”) and exposed to flame from a propane torch for 5 seconds. Polyurethane with UFA and cenosphere burned for less time and a significantly greater mass remained after extinction compared to the polyurethane foam without non-flammable additives. Carbon foam samples did not ignite. Polystyrene foam burned completely during the flammability test. Since polystyrene foam is a typical commercial wall covering, it was included with other compression tests. Moreover, it

fails elastically, unlike polyurethane and carbon foams. Results of the flame test are shown in Table 2.3.

1.3 Background of Cellular Solids

A thorough literature search was conducted on impact and blast testing, and fundamentals of cellular solids. The search yielded several helpful resources. On the most fundamental level, foam properties are determined by the material that makes up the foam and the cellular structure. Cellular solids are divided into two groups, open and closed cell foams. Open cell foams are a web-like connection of ligaments and edges. Closed cell foams are similar to open cell foams except cell walls divide each cell from the next. Polyurethane foam has open cells, and polystyrene foam resembles tightly packed bubbles or closed cells. Carbon foam is a unique case; because the cells appear to be closed but the cell walls usually are not complete. Since carbon foam cell walls contain holes they cannot support stress and are treated as open cell foams.

To understand how each type of foam differs on a fundamental level and to investigate how cell structure affects mechanical properties, a survey of each type of foam was conducted using a 10X magnifying aperture and microscope. (Leica Microsystem GmbH, Wetzlar, Germany) Imaging software allowed the ligament, edge and cell wall thickness to be measured. (Advanced Spot, Diagnostic Instruments Inc., Sterling Heights, Michigan, USA) Five images were captured from each type of foam. Three ligament, edge and cell diameter measurements were taken from each image. The average results were later compared to compression test data. Images and survey results are discussed in Chapter 3.

Cellular structure is determined during the foaming process. The size and shape of cells is seemingly random. For polyurethane foam, the reaction between polyol and toluene diisocyanate releases of carbon dioxide gas that bubbles to the surface. Competitive pressures that result from the release of gas determine the cellular structure. Because cellular structures are random, assumptions must be made to simulate the mechanical behavior of foam. Gibson and Ashby provide two examples, honeycomb and a matrix of

uniform cubic cells, that can be rigorously modeled and simulated.[6] Creating a simulation that predicts the foam mechanical behavior was beyond the scope of this project. However, illustrating how an ideal cellular solid might be modeled explains the mechanical behavior of foam on a cellular level. A description of one modeling process is provided in Chapter 3.

After exploring the fundamentals of cellular solid mechanic, a regiment of empirical tests was performed to investigate foam response to impact. Foams were studied under three strain rate regimes. Low rate, or compression, testing was performed using a MTS compression device (MTS, Eden Prairie, Minnesota, USA) and followed guidelines provided by ASTM D695. Five 2.54 cm (1") cube samples of each type of foam were stressed between two plates. The resulting data provided stress-strain curves. Elasticity, yield stress, strain energy density, and maximum stress were gathered from this curve. Also, the shape of the curve and behavior during the test indicated the failure mode.[6]

The stress-strain curve for polyurethane foam exhibited plastic failure. The curve followed a straight line initially, and then sharply turned as the sample yielded. As the sample densified, the stress increased. As a result, the maximum stress was greater than the yield stress. Polyurethane foam with cenospheres behaved similarly, but polyurethane foam with UFA failed to densify, or show increased stress after yielding. The stress-strain curves for carbon foams were very jagged, indicating brittle failure. Finally, polystyrene foam nearly returns to its original shape after being slowly deformed, indicating elastic failure.

Each failure mode can be visualized on a macroscopic or cellular level. For example, when polystyrene foam is compressed the individual cell walls bend like a hinge and then return to their original shape when relieved. Similarly, the jagged edges of a brittle failure stress-strain curves represents the failure of a series of cells. Plastic failure can be viewed as cell ligaments that deform and then fail.[6]

Although compression tests can provide a great deal of information about each type of foam, they cannot predict exactly how foams will behave under impact or blast since yield stress is a function of strain rate. Many articles have discussed this phenomenon. [2, 6-8] To demonstrate this behavior a brief test was performed using the MTS compression device. Strain rate was increased from 1 to 1000 mm/min (0.039 to 39.4 inches/min). Tests showed that yield stress increased from 1.2 to 1.6 MPa (174 to 232 psi) from the lowest to the highest strain rate.

Since foam responds differently to high strain rate compression, impact tests were performed. Several different methods of impact testing exist. Previous studies have used the dual hammer method, drop darts, gas guns, the Hopkinson bar, and impact pendulum. An original approach was designed for this study. An impact sled, consisting of a 10.16 cm X 10.16 cm X 34.56 cm (4"X4"X13.5") steel block and weighing 33.8 kg (74.5 lbs.), was suspended from a curved rail. During each test, the impact sled, or impacter, was hoisted to the top of a ramp 4.3 vertical meters (14 vertical feet) above a horizontal section of rail. A magnetic latch held the impacter in place. When released, gravity pulled the impacter down the inclined rail. At the end of the incline, it reached a speed of about 8.81 m/s (28.9 ft/s). Along the horizontal rail section, the impacter collided with a steel target mass weighing 118.4 kg (261 lbs.). The collision stopped the impacter and sends the target mass into a stack of sandbags to end the movement.

When foam was placed between the impacter and target mass, the energy imparted to the target was mitigated. To measure this mitigation, the velocity of the impact sled immediately before impact and the target mass velocity after collision was measured. The velocities were measured using photogates and picket fences from Pasco Scientific (Roseville, California, USA). A picket fence is a rectangular sheet of rigid plastic with dark lines evenly spaced along the length. When this sheet passes through the photogate, speed is immediately recorded on a computer. By attaching picket fences to the impacter and target mass, the speeds mentioned were measured.

The target mass kinetic energy after collision was subtracted from the kinetic energy of the impacter to find the energy absorbed by material between the two components and energy lost to the environment. Repeated tests showed consistent kinetic energy differences for each type of foam. A great deal of time was dedicated to the development of this device, and more reliable measurement techniques are being considered by the Carbon Group at the Center for Applied Energy Research (CAER).

A high speed camera (Fastec Trouble Shooter, Factec Imaging, San Diego, California, USA) was used to capture the impact test event. The camera obtained images at 1000 frames per second. One test with carbon foam and a low density polyurethane foam sample revealed a key property of layered composite hybrid foam samples. During impact the carbon foam layer facing the target mass was observed being crushed before the low density polyurethane. Since the low density polyurethane has a lower yield stress than carbon foam, it was expected to crush before carbon foam. Since the carbon foam crushed first, the front layer of the hybrid composite layered sample endured the impact pressure before the rest of the composite. Jang, *et al*. experimented with this phenomena and documented the finding in the article "Impact Resistance and Energy Absorption Mechanisms in Hybrid Composites." Jang, *et al*. concluded that the hybrid composite layered samples initially exhibit mechanical properties of the material facing the impact.[9]

Blast testing reveals how foam sample behave under actual blast conditions. To recreate the conditions of a small bomb explosion, mock walls were constructed from cinder blocks and concrete mortar. Compression tests showed that the face of cinder blocks fail at a stress of about 6.9 MPa (1000 psi) at the weakest part of the wall face. Foam samples must mitigate the pressure of a blast to prevent the wall face from experiencing this pressure. During blast tests, the mock walls were supported by a steel frame to prevent the wall from tipping over. A steel sheet with a 30.72 cm (1') square window was mounted over the face of the mock wall. Sixteen different samples were mounted in this space. The samples included layered composites of carbon foam and polyurethane of different densities. Each sample received a dry wall cover to match the construction of a

typical commercial wall. A 125 g (0.275 lbs.) charge of C4 explosives was hung by duct tape from a wire stretched across the site. The charge was offset 15.36 cm (6") from front of the face of the mock wall. The ability of each sample to mitigate the effects of the blast was accessed by photographs take before and after detonation. The final condition of the mock walls was identified as "Intact," "Cracked," or "Broken." The blast experimental procedure will be explained further in Chapter 4.

Finally, impact tests were repeated using samples identical to those used during blast testing. Instead of colliding with the target mass, a mock wall was set-up in its place. This simulation of blast testing using the impacter provided an empirical comparison of the two test methods. Results showed the condition of the mock wall after blast testing was mirrored by the impact simulation. Calculations showed that the pressure due to collision with the impact sled was about 12.9 MPa (1870.5 psi) while the blast wave resulted in about 140.9 MPa (20,426 psi) of pressure on the foam sample front. Results from impact and blast testing were mostly congruent since both pressures were high and occurred over a short time period (<0.005 s).

The results of the cell structure survey, compression tests, impact tests, and simulations through blast and impact were analyzed. The behavior of each type of foam sample mentioned is discussed in Chapter 6. With respect to the objective of this project, experiments showed that a hybrid layered composite foam sample consisting of a 2.56 cm (1") thick carbon foam type L or L1 sample followed by an 8 lb./ft^3 and 4 lb./ft^3 polyurethane foam sample regularly mitigated the effects of a blast from 125 g (0.275 lbs.) of C4 offset 15.36 cm (6") from the face of the mock wall and left the wall intact.

1.4 Development of Novel Impact Testing Approach

Much of the preparation for this project focused on the development of the middle strain rate impact tester. The goal was to build a testing device that could simulate impacts similar to the pressure experienced during a small explosive blast. The tests must be repeatable.

The Carbon Group at CAER decided to build a rail and target based impacter. Several challenges were encountered during the development of this device. First, efforts to create a static target were unsuccessful. A backdrop weighing more than 83.9 kg (185 lbs.) was weighed down with more than 907.2 kg (1 ton) of sandbags in an effort to establish a static target. Every impact displaced the target, leaving an unrepeatable system. A thorough literature search revealed that similar impact tests, like those conducted at the Protective Technologies Research and Development Center at the Ben Gurion University, utilized extensive steel structures to establish a static target.[2, 8] Creating such a target was beyond the scope, budget and time table for this project. Instead, an inertia based collision system was chosen.

Figure 1.1 Rail and Target Based Impact Testing Device

To establish a collision based system, the steel backdrop was mounted to a cart with low-friction wheels. Ideally, the impacter would collide with the cart and the initial impacter speed and final cart speed would be recorded. Unfortunately, the cart did not maintain a uniaxial path during tests. Extraneous side-to-side movement ensured that this method was not repeatable. Also, any movement outside the axis of collision would result in

untraceable lost energy. The cart was abandoned and replaced by a 118.4 kg (261 lbs.) steel block measuring 30.5 cm X 30.5 cm X 34.3 cm (12”X12”X13.5”) suspended from the rail. Since the block was suspended from the rail, it could only move along a single axis.

The development of the impact sled itself proved to be the most challenging aspect. Originally, the kinetic energy of the impact sled was intended to vary by adding lead weights to a hopper inside the sled. The requirement to have this hopper led to a box-like impact sled design held together with more than 15 screws. The original sled consisted of a box constructed of 0.635 cm (1/4”) steel panels with a 1.91 cm (3/4”) steel front panel. The top of the sled could be removed and a mixture of 0.32 cm (1/8”) and 0.64 cm (1/4”) steel screws held the sled together. The bottom panel covered the edges of the four side panels. During a collision the front and side panels would abruptly stop but bottom panel would push forward. This arrangement resulted in the repeated shearing of screws holding the bottom panel to the side panels. Also, bolts holding the front and rear panels to the side sheared repeatedly. Moreover, screws holding the arms connecting the box to the wheels above sheared.

Also, two steel rods connecting the sled to the wheel assembly above were severely bent after several impacts. In short, the original sled design was not robust enough to endure the impact force necessary for the desired experimental strain rate.

The initial sled design was replaced by a 10.2 cm X 10.2 cm X 30.5 cm (4” X 4” X 12”) solid block of steel. Grade 8, 1.91 cm (¾”) steel bolt were used to fix the impacter arms to the wheel assembly above. Two rods attaching the impact sled to the wheel assembly were replaced with oil harden steel rods. Also, the original sled held these rods in place with 0.64 cm (¼”) spiral clips. Since the clips failed after every impact, they were replaced by cotter pins inserted in 0.64 cm (¼”) holes in the harden steel rods. Figure 1.2 shows the sled used during successful tests. This impacter has survived more than 100 tests and should continue to perform for some time.

Additional problems were revealed after reviewing high speed videos. Videos showed the sled bouncing on impact. A third wheel on the underside of the rail was installed to prevent the sled from moving upward. With the impacter fixed directly to the rail wheels, the sled was closer to the rail and the wheel assembly weight acted with the rest of the sled. [10, 11] This adjustment eliminated most the upward movement and mitigated extraneous movement of the impact sled on collision.

Figure 1.2 Final Impact Sled Used During Middle Strain Rate Tests. (Light gates that obtain the sled speed are shown.)

Finding the best foam sample size posed another issue. Initially the impact sled was equipped with a 5.08 cm (2") diameter steel nose. Foam samples 2.54 cm (1") thick, and 5.08 cm (2") in diameter were attached to the nose. Since the force of impact was concentrated on such a small area, the resulting pressure was too great to allow 2.54 cm (1") to mitigate the impact. Tests showed no measurable difference between samples. The 5.08 cm (2") diameter nose was replaced by a 15.24 cm (6") square harden steel panel, increasing the impact area. Now, the impact pressure was less than 1/10 of the previous pressure allowing a noticeable energy absorption difference.

The new impacter design eliminated the ability to change the initial kinetic energy by adding weight. Also, the size of the impact sled face is constrained by the target block

shape. The target block face is 20.48 cm X 20.48 cm (8” X 8”) square. To compensate, this design may be modified so that the sled can be released from different heights, thereby allowing the velocity of the sled to be varied. This will allow the kinetic energy and impact pressure to be varied.

Chapter 2 Background

2.1 Material Selection

Four types of carbon foam were produced by Koppers, Inc. for this project. Polyurethane foam was selected since it can be produced on site and mixed with flammability reducing additives. Also, it is frequently used to absorb impact. Polystyrene foam was included in this study since it is often used to absorbed energy in impact and already exists as a commercial wall covering.

2.1.1 Koppers Carbon Foam

Koppers Inc. produced four types of carbon foam for impact testing. The specific production method is patented, but a general outline of the process is provided in section 2.1.1.1.

2.1.1.1 General Production Method

Koppers, Inc. licensed rights from Oak Ridge National Laboratory to a carbon foam production process. Some cellular solids require the introduction of a gas during formation to create openings. The production of carbon foam differs from other types of production since no blowing required. In general, pitch powder is loaded into molds and heated above 500ºC (932°F) at pressures as high as 10.3 MPa (1500 psi). The foam is allowed to cool and then is carbonized at a higher temperature for several days as shown in Figure 2.1. The overall mass and volume decrease by about 10% during this step. Type L1 and LF1 foam is further graphitized. Type LF and LF1 include pitch mixed with carbon nanotubes before the process begins to create a completely different cellular structure. The specific steps involved in creating carbon foam are proprietary. [4]

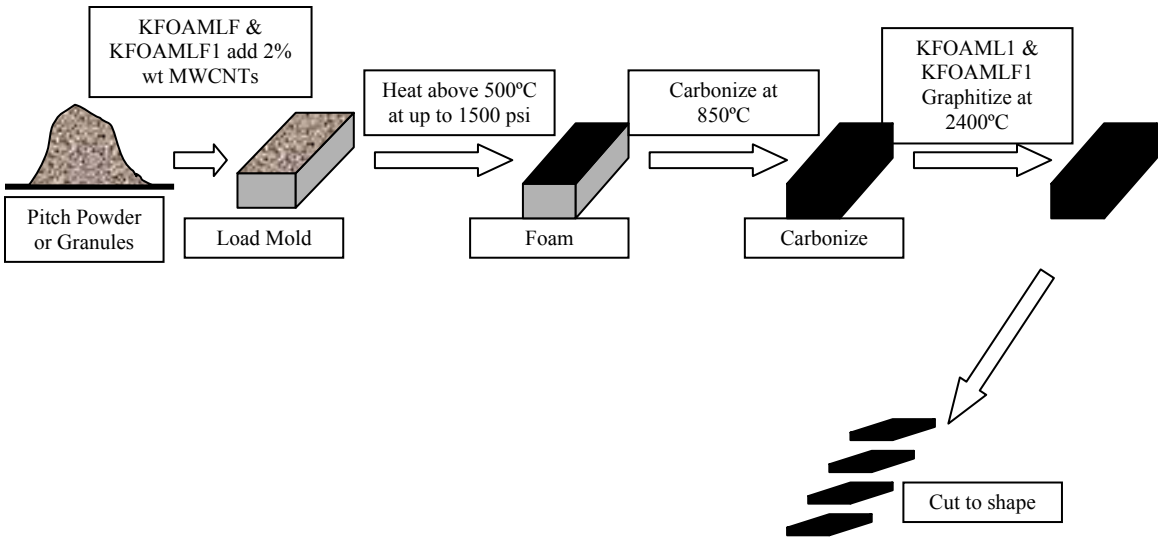

Figure 2.1 General Process to Create Carbon Foam

2.1.1.2 Carbon Foam Sample Descriptions

Table 2.1 provides a general description of the difference between the four carbon foam samples. KFOAML and KFOAML1 cells are densely packed and rough to the touch. KFOAMLF and KFOAMLF1 contain many pores and resemble a rigid web. KFOAML1 and KFOAMLF1 exhibit higher thermal conductivity making the samples cooler when touched.[3]

Table 2.1 Carbon Foam Description

Sample	Firing Method	Base Mixture
KFOAML	Carbonized at 850ºC	Pitch
KFOAML1	Graphitized at 2400ºC	Pitch
KFOAMLF	Carbonized at 850ºC	Pitch with 2% Multiwall Carbon Nanotubes by weight
KFOAMLF1	Graphitized at 2400ºC	Pitch with 2% Multiwall Carbon Nanotubes by weight

2.1.2 Polyurethane-based Foams

Polyurethane foam was studied for several reasons. First, polyurethane foam has been used in energy absorption for many years. It is easily accessible and can be infused with other materials to change material properties. Three different polyurethane foam densities, 4 lb./ft^3, 8 lb./ft^3, and 16 lb./ft^3, were used in combination with 2 additives:

cenospheres and ultra-fine fly ash. Table 2.2 lists all the samples studied and the abbreviations used.

Table 2.2 List of Foam Samples and Abbreviations

Abbreviation	Foam Sample
KFOAML	Koppers, Inc. carbon foam type L
KFOAML1	Koppers, Inc. carbon foam type L1
KFOAMLF	Koppers, Inc. carbon foam type LF
KFOAMLF1	Koppers, Inc. carbon foam type LF1
4 lb. PU	Polyurethane foam of density 4 pounds per cubic foot
8 lb. PU	Polyurethane foam of density 8 pounds per cubic foot
16 lb. PU	Polyurethane foam of density 16 pounds per cubic foot
4 lb. Ceno	Polyurethane foam of density 4 pounds per cubic foot with 25% Cenosphere additives by mass
8 lb. Ceno	Polyurethane foam of density 8 pounds per cubic foot with 25% Cenosphere additives by mass
16 lb. Ceno	Polyurethane foam of density 16 pounds per cubic foot with 25% Cenosphere additives by mass
4 lb. UFA	Polyurethane foam of density 4 pounds per cubic foot with 50% Ultra fine Fly Ash additives by mass
8 lb. UFA	Polyurethane foam of density 8 pounds per cubic foot with 50% Ultra fine Fly Ash additives by mass
16 lb. UFA	Polyurethane foam of density 16 pounds per cubic foot with 50% Ultra fine Fly Ash additives by mass
Polystyrene Foam	Polystyrene Foam Insulation (Georgia-Pacific, Atlanta, Georgia, USA)

2.1.2.1 General Production Method

Polyurethane foam from US Composites (West Palm Beach, Florida, USA) was used for this project. The two liquid parts are simply labeled Part A and Part B, but their chemical names are polyol and toluene diisocyanate. To produce solid foam, the two liquid parts are vigorously mixed at a one-to-one ratio by mass for 45 seconds. Then, the mixture is poured into a disposable mold as shown in Figure 2.2. The two parts react, releasing carbon dioxide gas. The mixture expands or foams, hardens and then is cut to shape. Cenospheres and fly ash are added to each liquid part at 25% and 50% respectively by mass, before mixing. Three different “Part B’s” are specially formulated to create three different nominal densities, 4, 8 and 16 pounds per cubic foot.

Each foam sample is examined for uniformity. Since the two liquid parts must be thoroughly mixed in a short time before hardening, sometimes inconsistencies are found inside a single foam batch. For example, some foam mixtures with UFA show a dark swirl after hardening. Only uniform samples are used, all other are discarded. Since the foams are measured and mixed manually, some variation occurs from batch to batch. Since no two batches are identical, some experimental error results from the manual production of polyurethane foam.

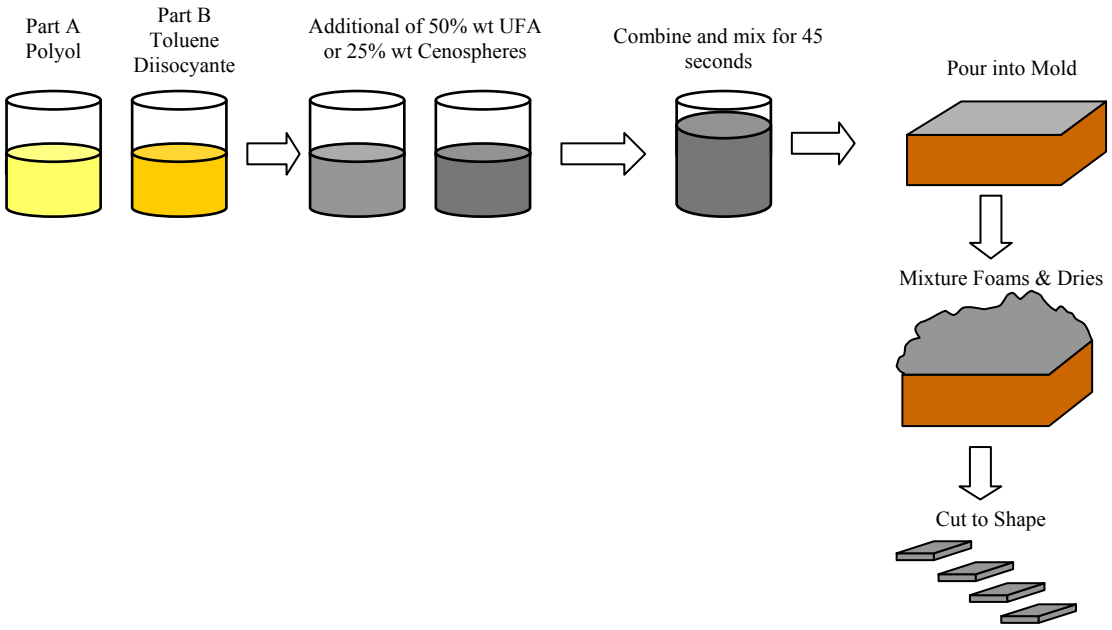

Figure 2.2 General Process to Create Polyurethane Foam

2.1.2.2 Polyurethane Foam Sample Description

Three different polyurethane foam densities were produced: 4 lbs./ft^3, 8 lbs./ft^3 and 16 lbs./ft^3 (64.1 kg/m, 128.1 kg/m, and 256.3 kg/m). Density is one indication of the foam structure. Higher density foam generally has a high yield stress and can absorb more energy. However, a high yield stress is not desirable when the impact stress is less than yield stress.

Since fire often accompanies an explosion, the blast mitigation material must be resistant to flame. Polyurethane foam alone is flammable, therefore nonflammable coal combustion by-products were mixed with polyurethane to create a material with the desired properties. Ultra fine fly ash is a by-product of coal combustion. Obviously, it has non-flammable properties since it survives high temperature combustion (<1500°C (2732°F)). Ultra fine fly ash was mixed with the liquid polyurethane components at 50% by weight. The resulting foam is dark gray and resists flame as described in Section 2.2.

Cenospheres are mixed with the three foam densities at 25% by weight. Cenospheres, hollow silica-aluminum spheres between 10 and 300 μm (0.393 and 11.8 mil) in diameter, are another by-product of coal combustion. The resulting foam is light grey and does not resist flame as well as the 50% UFA mixtures.

Naturally, the maximum concentration of UFA and cenospheres in polyurethane foam are desired. Viscosity increases greatly as UFA and cenospheres are added to liquid polyurethane. More viscous mixtures are more difficult to mix in a short amount of time. Polyurethane mixtures that were not properly combined resulted in non-uniform and weak foams. The concentrations of non-flammable additives used for this project, 25% cenosphere and 50% UFA, were empirically found to create uniform foam with desirable strength properties. [12, 13]

2.1.3 Other Samples

Georgia-Pacific (Atlanta, Georgia, USA) polystyrene foam insulation boards of 2.54 cm (1”) thickness were obtained and cut to shape. Polystyrene foam has closed cells and exhibits more elastic properties then all other foam samples tested.

2.2 Flammability & Material Selection

Since the foam samples may be exposed to fire, the flammability properties were studied. An experiment was conducted to reveal whether each sample will catch fire when exposed to flame. Five different 2.54 cm (1”) cube specimens were exposed to a propane torch flame for 5 seconds. Once the flame was removed, the foam samples were observed

to determine if ignition took place, burning duration and how much of the total mass combusted after extinction.

Table 2.3 Flammability Results

Sample	Combustion Initiated	Average Burn Time (s)	Percent Mass Consumed by Fire (%)
KFOAML	No	---	---
KFOAML1	No	---	---
KFOAMLF	No	---	---
KFOAMLF1	No	---	---
8 lb. PU	Yes	39.6	43
8 lb. Ceno	Yes	35.2	15
8 lb. UFA	Yes	23.2	0.63
Polystyrene Foam	Yes	9.4	100

Table 2.3 shows the results of this test. The carbon foam samples did not catch fire, and the polyurethane foams with cenospheres and ultra-fine fly ash performed best among the remaining samples. Polyurethane foam with 50% ultra-fine fly ash lost less than 1% of its total mass. The 8 lb. UFA samples outperformed the 8 lb. Ceno samples since 8 lb. UFA has a higher concentration of non-flammable material. Almost half of the mass of the 8 lb. PU sample burned away showing the necessity of non-flammable additive to increase foam survival when exposed to flame. Because polystyrene foam caught fire and burned completely and quickly, it is not an ideal material for blast mitigation since blasts result in fire. However, because its mechanical properties differ greatly from the other foams, polystyrene foam was included during other tests.

2.3 Past Projects with Energy Absorption from Aluminum Foam

A great deal of work has been performed to analyze and model the effects of blast on structures. The Norwegian Defense Construction Service has achieved extensive computer modeling and empirical results from concrete structures exposed to blasts.[2] Since carbon foam is a fairly new material, its behavior is not well documented in literature. However, substantial work has been reported on the blast mitigation properties of a similar material, aluminum foam. Aluminum foam research provided a benchmark for this project and some perspective on blast mitigation testing methods. [2, 7, 8, 14]

In 2005, a group from the Protective Technologies Research and Development Center at the Ben Gurion University of the Negev, Beer Sheva, Israel, published the results of their blast investigation with aluminum foam. [2, 8]

First, to generate data for finite element code the group used a ballistic pendulum to simulated blast pressure on reinforced concrete beams.[8] The ballistic pendulum can vary in mass (250 – 1000 kg or 551.2 – 2204.6 kg) and velocity (0 – 4 m/s or 0 – 13.1 ft/s) and a load cell attached to the impacting front measures force. Ballistic pendulum tests provide the stress-strain response from aluminum foams under impact.

In a separate experiment, the group investigated the dynamic properties of aluminum foam at different strain rates using an Instron (Instron, Norwood, Massachusetts, USA) compression testing matching (0.001 m/s & 2 m/s (0.0033 & 6.56 ft/s)), shock tube testing (equivalent to ~22 m/s (72.16 ft/s)), and the described pendulum (1 m/s (3.28 ft/s)). The results of the shock tube and compression tests indicated higher stress levels at higher strain rates. [8]

The group set the pendulum weight to 400 kg (881.8 lbs.) and varied the impact velocity on reinforced concrete beams. The beam was simply supported, creating a bending failure experimental set-up. Tests were conducted with a beam covered first with a 9 mm (0.354 in) sheet of wood and later with aluminum foam. Impact velocities were 0.5 m/s (1.64 ft/s) and lower. Results indicated little difference between the wood covered and aluminum covered beam until aluminum foam covers of at least 7.62 cm (3”) thickness were used. [2, 8] Subsequent explosion tests performed on concrete plates indicated a 7.62 cm (3”) aluminum foam thickness as the threshold for protecting a concrete wall.

The Ben Gurion University group performed two explosion tests using reinforced concrete walls similar to those used during impact tests. Two 1.2m X 1.3m x 0.2 m (3.94 ft X 4.26 ft X 0.66 ft) walls were placed 10 m (32.8 ft) from a 100 kg (220.5 lbs.) TNT charge. One wall was covered with aluminum foam and the other was left bare. In a

second test, two 1.4 m X 3.2 m X 0.2 m (4.59 ft X 10.5 ft X 0.66 ft) concrete plates were placed 21 m (68.9 ft) from a 900 kg (1984.1 lbs.) charge. The results clearly showed both the protected and unprotected plates received some damage. However, the exposed walls had more than 10 times as many cracks and were visibly more damaged than the aluminum foam covered wall. [8, 14, 15]

The work discussed by Sadot and Schenker, *et al.* provided a nearly parallel project in objective and approach to this project. While the study of carbon foam utilizes a novel testing approach and investigates new materials, the similarities to other projects can provide a benchmark for experimental method and evaluation of results. For example, the use of a pendulum for impact testing in the Ben Gurion University tests emphasized that the velocity of impact is a greater consideration in foam energy absorption than mass. The work of Sadot and Schenker, *et al*. provides insight and comparison to other studies in protecting key structure from blast.

Chapter 3 Properties and Mechanics of Cellular Solids

Almost any material can be formed into foam. Examples of foams or cellular materials exist in nature. Wood, bones, wasp nests, and honeycomb are examples of naturally occurring solid foams. Honeycomb is frequently studied because it exhibits a naturally occurring, two dimensional, homogenous cellular array. These characteristics allow mechanical behavior governing equation to be applied since the cellular solid is uniform throughout. Studying how honeycomb and other simplified cellular solids behave in compression helps illustrate the mechanical behavior of all solid foam. [6, 16]

3.1 Foam Structure

The structural properties of solid foams are of particular interest, specifically the ability of foam to absorb energy. The mechanical behavior of solid foam is fundamentally determined by its material make-up and the shape and arrangement of cells. [6]

Cells are the three dimensional shapes that make up solid foam. Cells can be closed or open. Closed cells, like the cells formed by soap bubbles, are made of walls of material completely separating each cell from the next. Open cells have no material in the cell face, instead they are a web of ligaments connecting at edges. The ligament and edge thickness determines the strength of foam, along with the material make-up and shape of the cells. [6] Figure 3.1 and 3.2 show a magnified view of 16 lb. PU and polystyrene foam that have open and closed cells respectively.

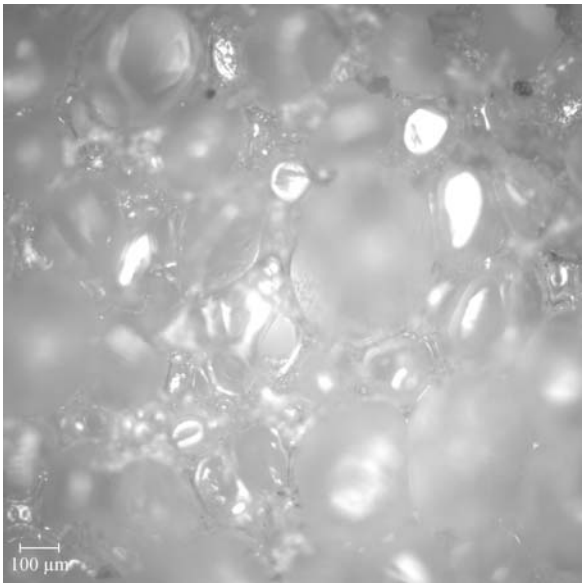

Figure 3.1 Magnified View of 16 lb. Polyurethane Foam with Cenospheres (Open cell foam with connectivity of three since three ligaments meet an edge.)

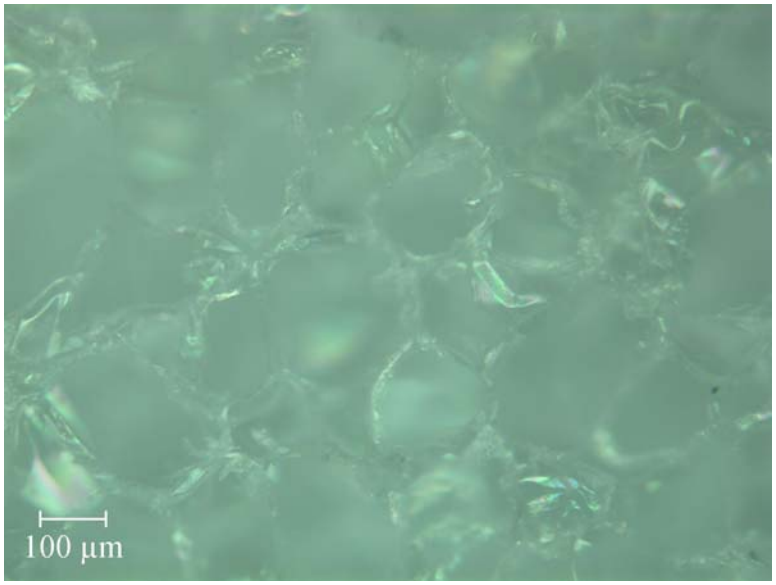

Figure 3.2 Magnified View of Polystyrene Foam (Closed cell foam with cell walls connecting at edge instead of ligaments.)

The arrangement of cells helps determine the structural properties of foam. The size of each cell is not as important as it placement with respect to other cells. The connectivity, or number of cells that meet at an edge, defines what type of shapes the cells create. [6]

Not all empty space in foam lies inside cells. Pores also form during foaming. A pore is a closed shape inside the foam structure that does not match the rest of the cellular geometry. A deep crevasse or split in the cellular structure may be considered a pore. Typically, a pore diameter is much larger than the diameter of even the largest cell in a single foam sample. Figure 3.3 shows an elongated pore that developed in 8 lb. polyurethane with cenospheres sample. [6]

Figure 3.3 Elongated pores formed in 8 lb. polyurethane foam with cenospheres

Foam structure can be described on a bulk level by its density, relative density, and porosity. The relative density and porosity provide a bulk value for the empty space in foam. The relative density is the ratio of the foam density with respect to the density of its solid material, or pre-foaming density. Porosity is simply unity minus the relative density. Since polyurethane samples used for this project start in liquid form, and foam immediately after mixing, the liquid density is shown instead of a solid density in the case of all polyurethane based foams in Table 3.1. Since carbon dioxide is released during foaming the relative density is not exact. The mass of carbon dioxide released accounts for very little of the total liquid mass. The solid density of carbon foams was found by crushing a foam sample and compressing the remains at 0.69 MPa (100 psi). [6]

Relative Density

$$\rho_f \Big/ \rho_s \tag{3.1}$$

Porosity

$$\Phi = 1 - \rho_f / \rho_s \tag{3.2}$$

Table 3.1 Foam Density Characteristics

Foam Type	Pre-foaming Density (g/mL)	Foam Density (g/mL)	Relative Density	Porosity
KFOAML	0.731	0.355	0.486	0.514
KFOAML1	0.779	0.420	0.539	0.462
KFOAMLF	0.762	0.290	0.381	0.620
KFOAMLF1	0.750	0.348	0.464	0.536
4 lb. PU	1.2	0.066	0.054	0.946
8 lb. PU	1.1	0.084	0.076	0.924
16 lb. PU	1.1	0.203	0.188	0.812
4 lb. Ceno	1.0	0.084	0.087	0.913
8 lb. Ceno	0.8	0.082	0.098	0.902
16 lb. Ceno	0.9	0.212	0.226	0.774
4 lb. UFA	1.3	0.092	0.070	0.930
8 lb. UFA	1.4	0.166	0.119	0.881
16 lb. UFA	1.3	0.220	0.170	0.830
Polystyrene Foam	0.062	0.022	0.350	0.650

The linear elastic behavior of foam is determined by the bending of cell walls (closed cell foam) or ligaments (open cell foam). Many types of foam contain viscous fluid that must be considered when examining the compressive strength of a cellular solid. All the foam samples for this project contain only air. While the effect of fluid inside foam can be calculated, the effect of air on yield strength and other parameters of interest is negligible. [6]

Since the strength of foam depends on the cell structure and the material make-up, mechanical behavior can be modeled and simulated in compression. First, the cellular structure must be simplified. If the cellular structure is imagined to resemble a three dimensional cubic matrix, or a so-called ideal foam, the mechanical behavior can be predicted based on the properties of the ligaments and edges. If a single open cell is defined as cube with ligaments of length, *l*, and square thickness, *t,* than the following state equations can predict the mechanical behavior. [6]

The relative density will be directly proportional to the aspect ratio of the ligaments [6]:

$$\frac{\rho_f}{\rho_s} \propto \left(\frac{t}{l}\right)^2 \tag{3.2}$$

The second moment of inertia of a single ligament will be proportional to the thickness of the ligament [6]:

$$I \propto t^4 \tag{3.3}$$

Structural mechanics provides a means to determine the deflection of horizontal ligaments in the matrix, δ, associated with a force, F, applied to the foam [6]:

$$\delta \propto \frac{Fl^3}{IE_s} \tag{3.4}$$

Obviously, the force applied to a cell equals the stress, σ, multiplied by the area over which it acts:

$$F = \sigma l^2 \tag{3.5}$$

Strain, ε, is defined as the displacement, δ, that result from some stress divided by the original length, l:

$$\varepsilon = \frac{\delta}{l} \tag{3.6}$$

Combining the equations above with the elastic stress formula provides an expression for the elastic modulus of foam [6]:

$$E_f = \frac{\sigma}{\varepsilon} = \frac{C_1 E_s I}{l^4} \tag{3.7}$$

Poisson's ratio, υ, compares the lateral strain and axial strain. Typically, Poisson's ratio for foam, υ_f, is taken to be 1/3. [6]

$$\upsilon_f \cong 1/3 \tag{3.8}$$

Empirical data from many open cell foams indicates the ratio of the foam elasticity to the solid elasticity is proportional to the relative density [6]:

$$\frac{E_f}{E_s} \approx \left(\frac{\rho_f}{\rho_s}\right)^2 \tag{3.9}$$

Since foam ligaments are typically too small to test, bulk empirical data is used to describe foam mechanics. Of course, the equations above only apply to ideal foam with open, cubic, stacked cell. Since actual cells are roughly spherical, Gibson and Ashby suggest the optimal geometric representations for foam cells are either the pentagonal dodecahedron or tetrakaidecahedron.[6] These shapes provide a good model for cells since they are constructed from straight ligaments and three ligaments connect at each edge, just like polyurethane foam cells. [6]

By making assumptions about the geometry of cellular solids and considering the material properties of what makes up foam, some researchers have written computer programs to simulate the behavior of foam under stress. In reality, it is not possible to exactly predict mechanical behavior because cellular structures are seldom homogeneous in shape and size or consistent from sample to sample.

3.1.1 Cellular Structure Development

Generally, foam cells are non-uniform and cellular structure is random. This random structure results from competitive pressures during foaming. As mentioned in the introduction, polyurethane foam results from the mixture of polyol and toluene diisocyanate. Carbon dioxide gas released during foaming, results in gas bubbles that move through the liquids. These bubbles often result in elongated pores in the solid foam. If the cell growth during foaming occurs at the same rate and simultaneously throughout

the mixture, the cell size and distribution will be nearly uniform. [6] In reality, the cell formation occurs randomly throughout the material. The result is foam with non-uniform sized cells and random distribution. Gibson and Ashby described the random distribution of cell diameters to be similar to the competitive development of coral in the ocean. Stronger pressures during foaming prevail just like stronger organisms. [17]

As mentioned, polyurethane foams were measured and mixed by hand for this project. Not only do foam properties differ from batch-to-batch, but the different regions of a single foam sample differ. For example, the upper portion of polyurethane foams tends to have larger cells than the bottom as a result of the pressure gradient developed by the weight of the liquid polyurethane.

3.1.2 Microscopic Foam Structure

As mentioned, foam strength is determined by the cellular structure and the material that makes up the foam. Magnified images provide fundamental information about the foam structure. Specifically, the face and edge thickness, face and edge connectivity and cell diameters can be measured.

To obtain key dimensions of individual foam cells, 1 cm (0.393”) cube samples were set in resin. The samples were polished and mounted to be viewed by a microscope (Leica Microsystem GmbH, Wetzlar, Germany) with a 10X aperture. Some of the images, like Figure 3.13, show scratch marks across the foam surface. This results from resin that hardens inside the cell structure. During polishing, the hard resin was scratched and remained visible.

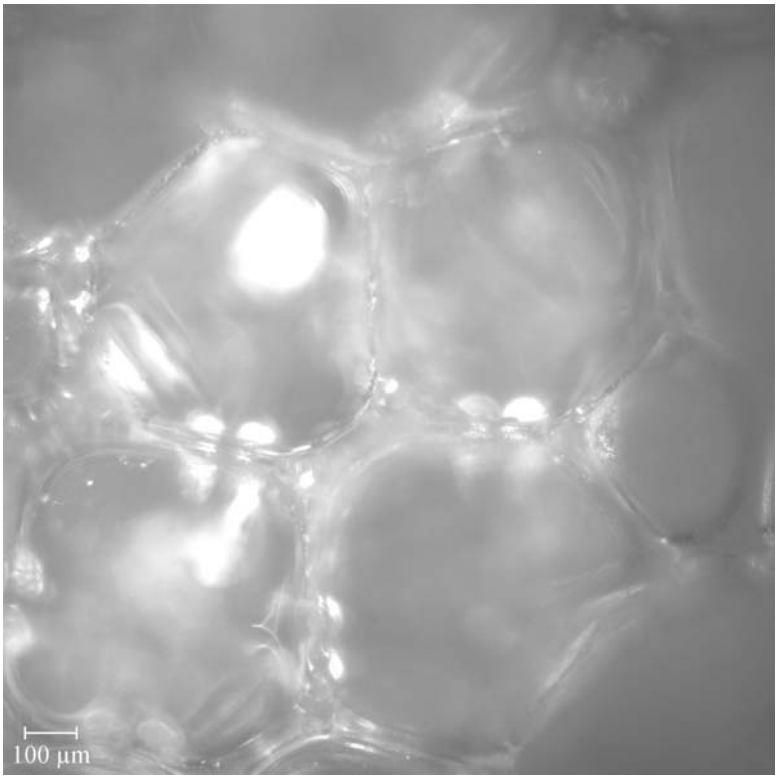

Figure 3.4 Typical 4 lb. Polyurethane Cell Structure

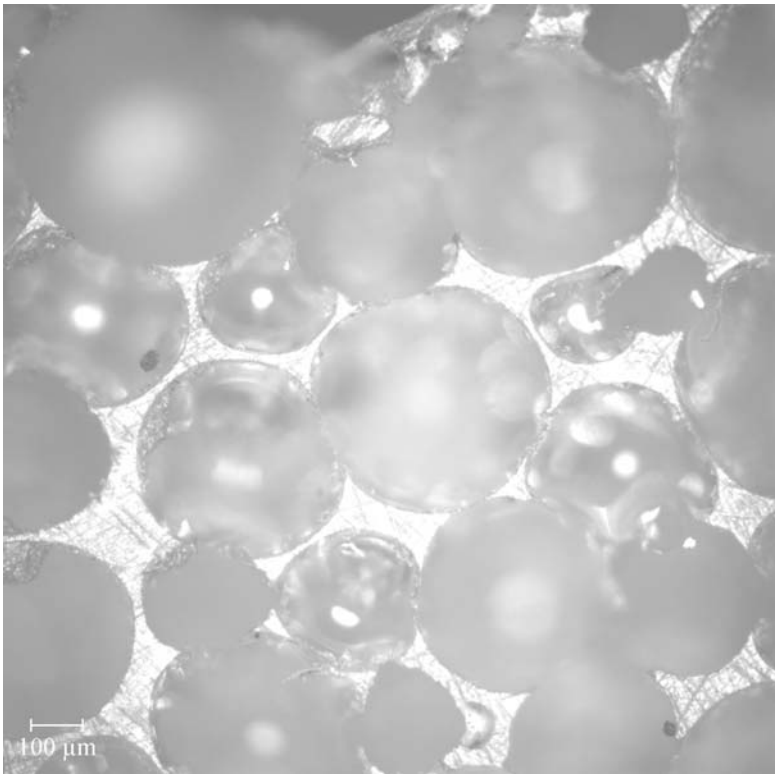

Figure 3.5 Typical 8 lb. Polyurethane Cell Structure

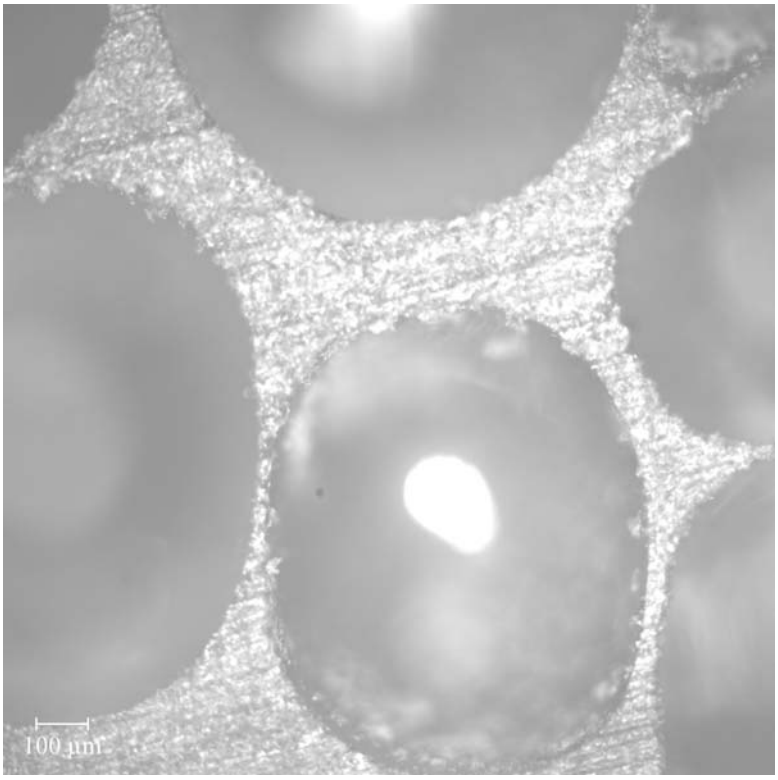

Figure 3.6 Typical 16 lb. Polyurethane Foam Cell Structure

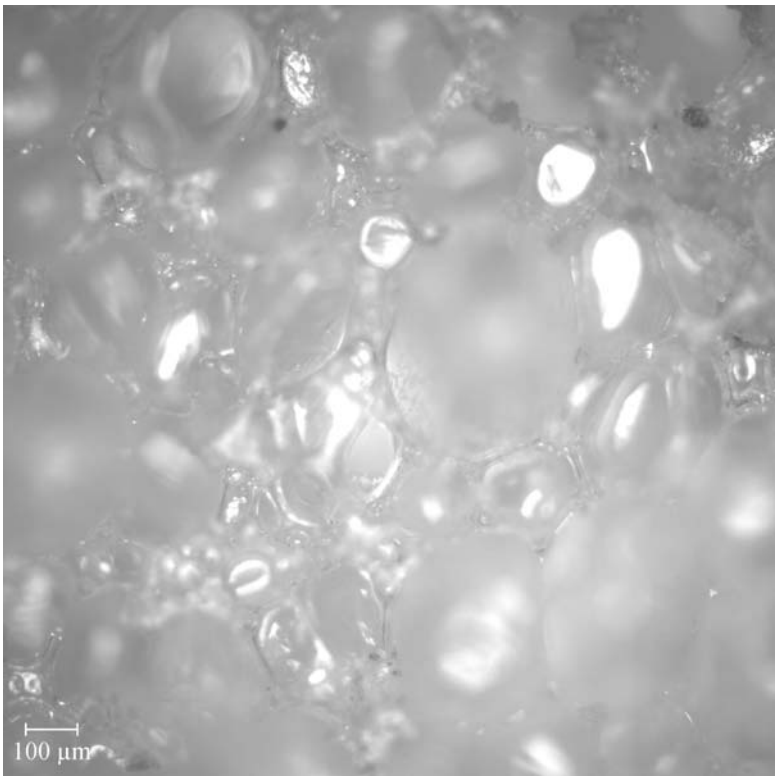

Figure 3.7 Typical 4 lb. Polyurethane with Cenospheres Cell Structure

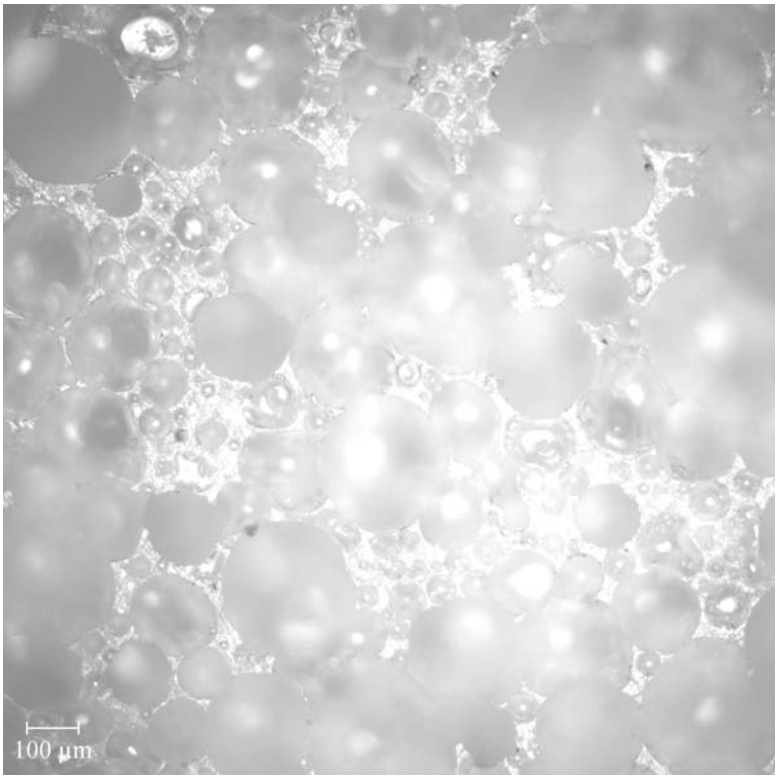

Figure 3.8 Typical 8 lb. Polyurethane with Cenospheres Cell Structure

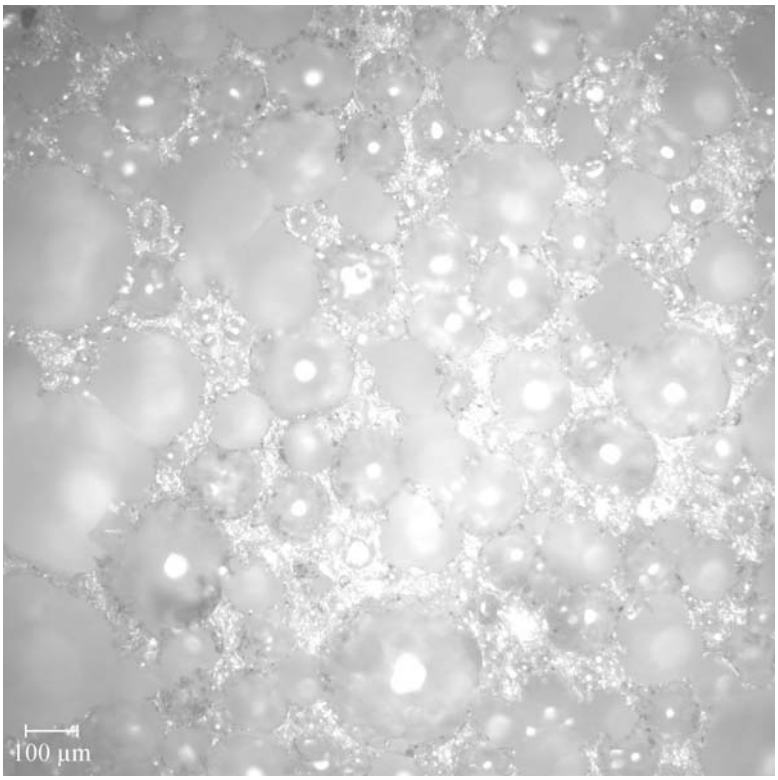

Figure 3.9 Typical 16 lb. Polyurethane with Cenospheres Cell Structure

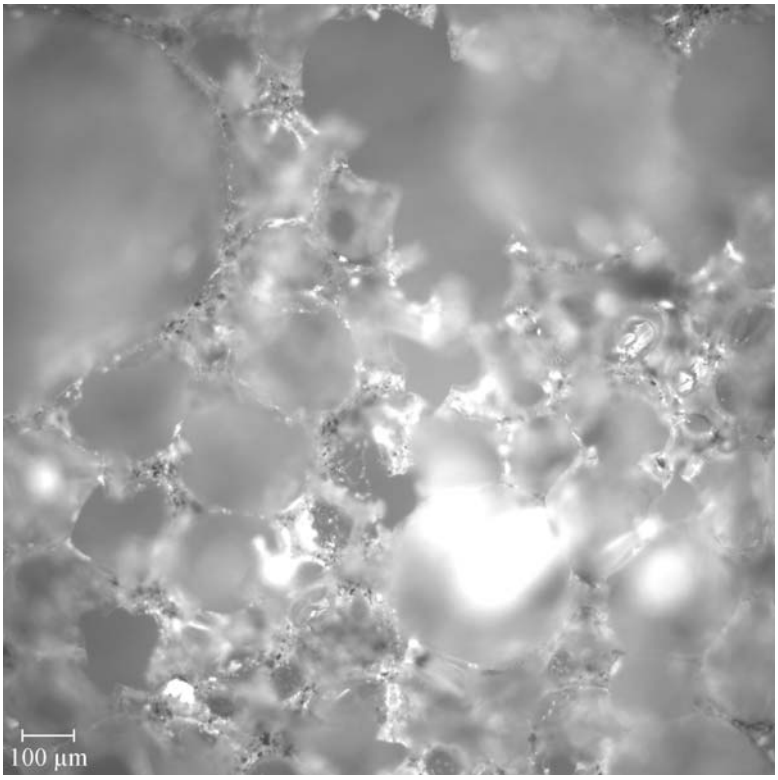

Figure 3.10 Typical 4 lb. Polyurethane with Ultra Fine Fly Ash Cell Structure

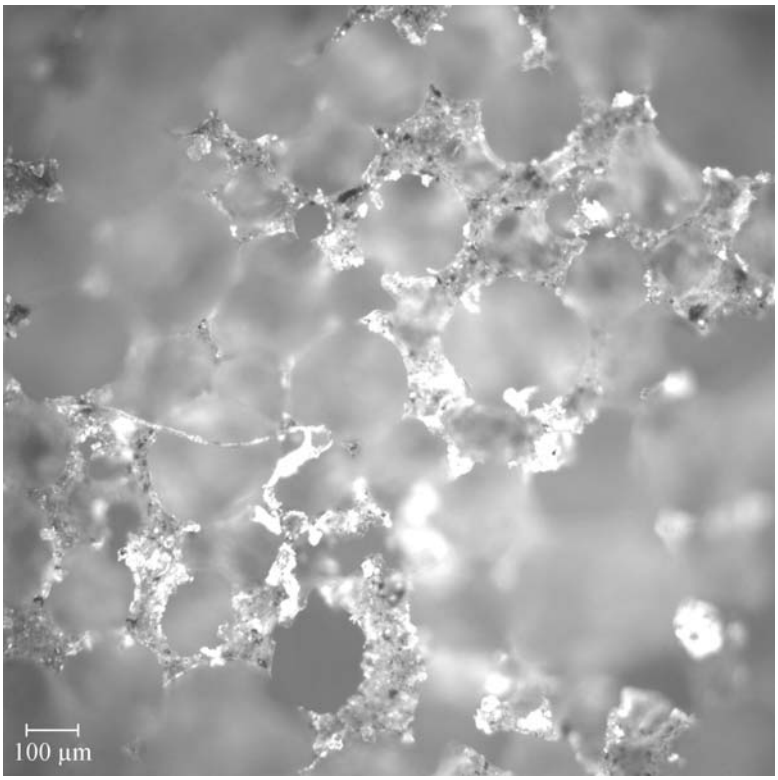

Figure 3.11 Typical 8 lb. Polyurethane with Ultra Fine Fly Ash Cell Structure

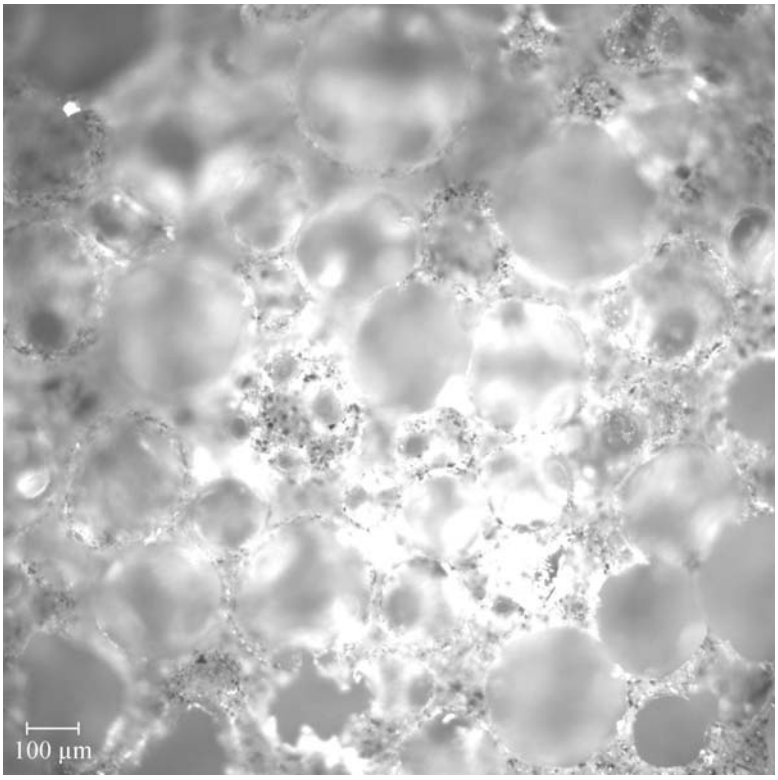

Figure 3.12 Typical 16 lb. Polyurethane with Ultra Fine Fly Ash Cell Structure

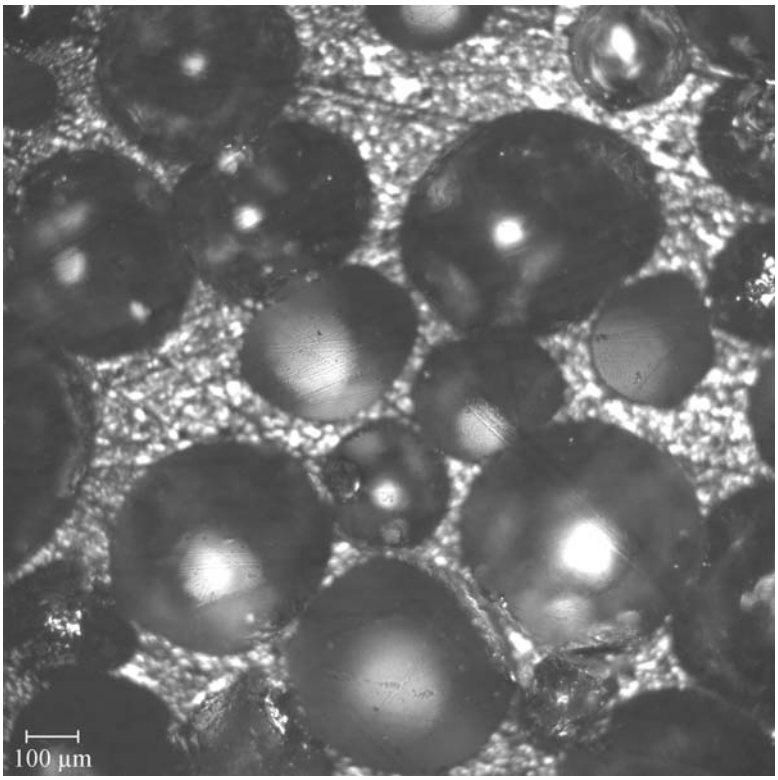

Figure 3.13 Typical KFOAML Cell Structure

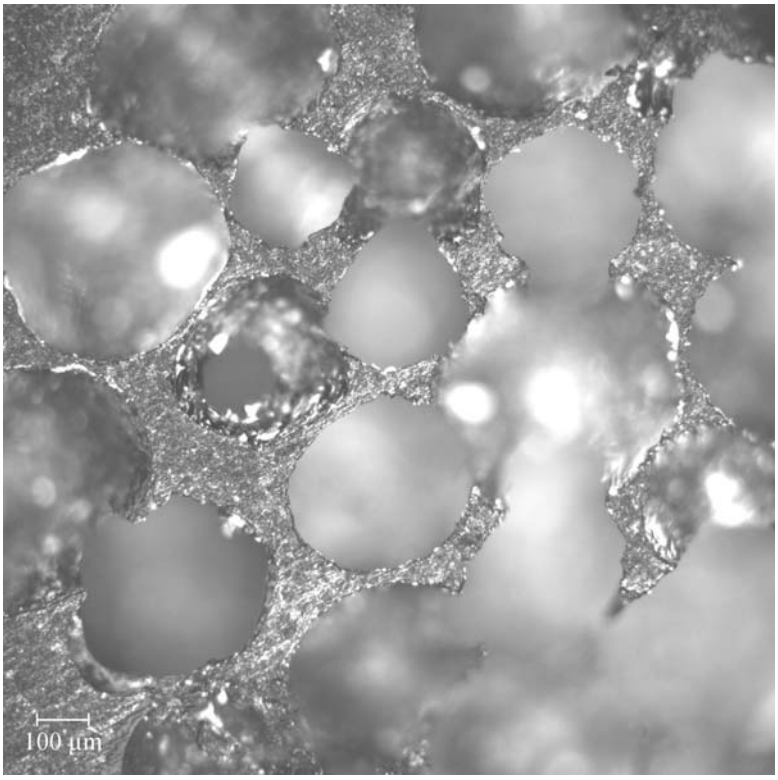

Figure 3.14 Typical KFOAML1 Cell Structure

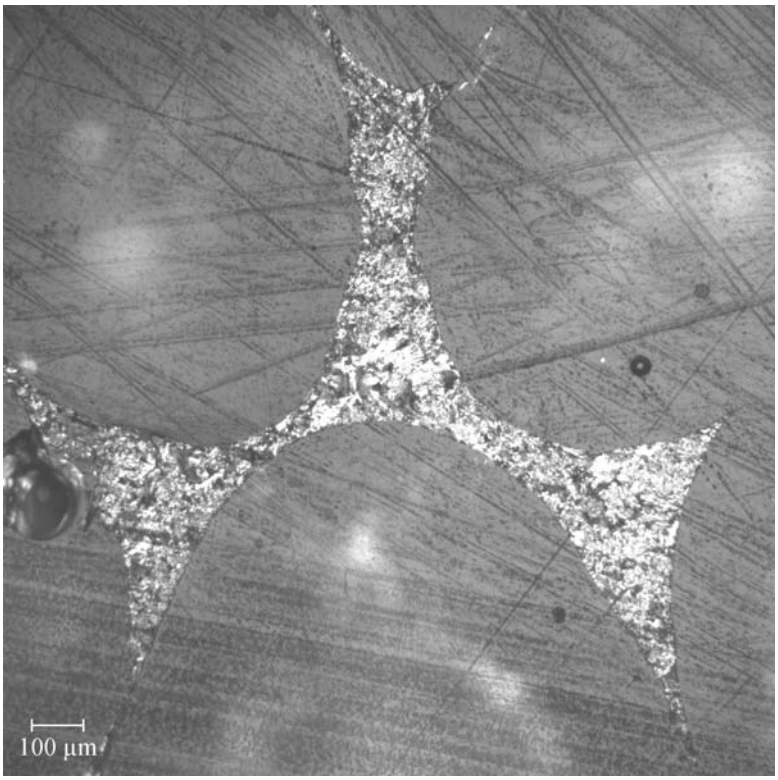

Figure 3.15 Typical KFOAMLF Cell Structure

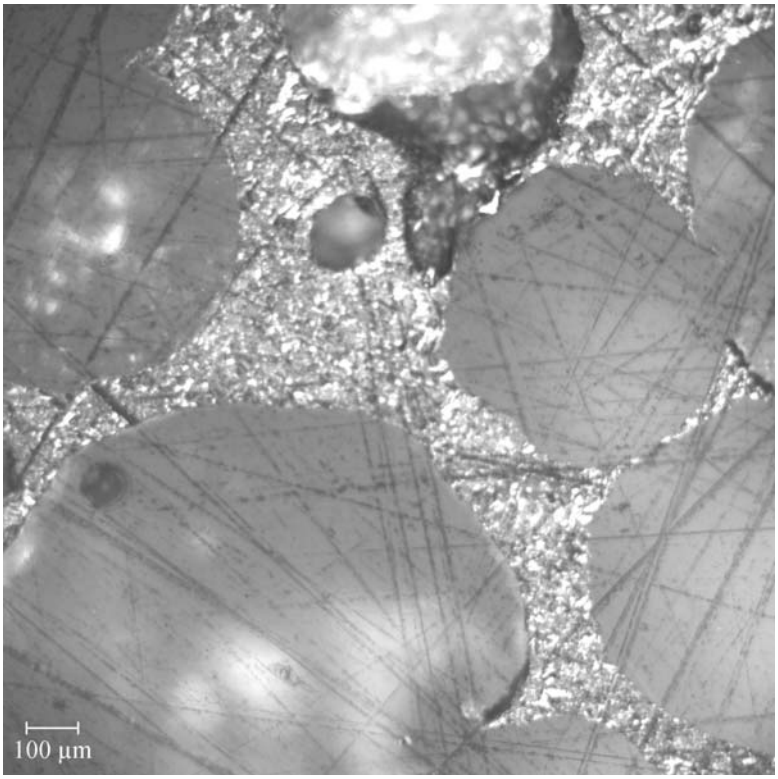

Figure 3.16 Typical KFOAMLF1 Cell Structure

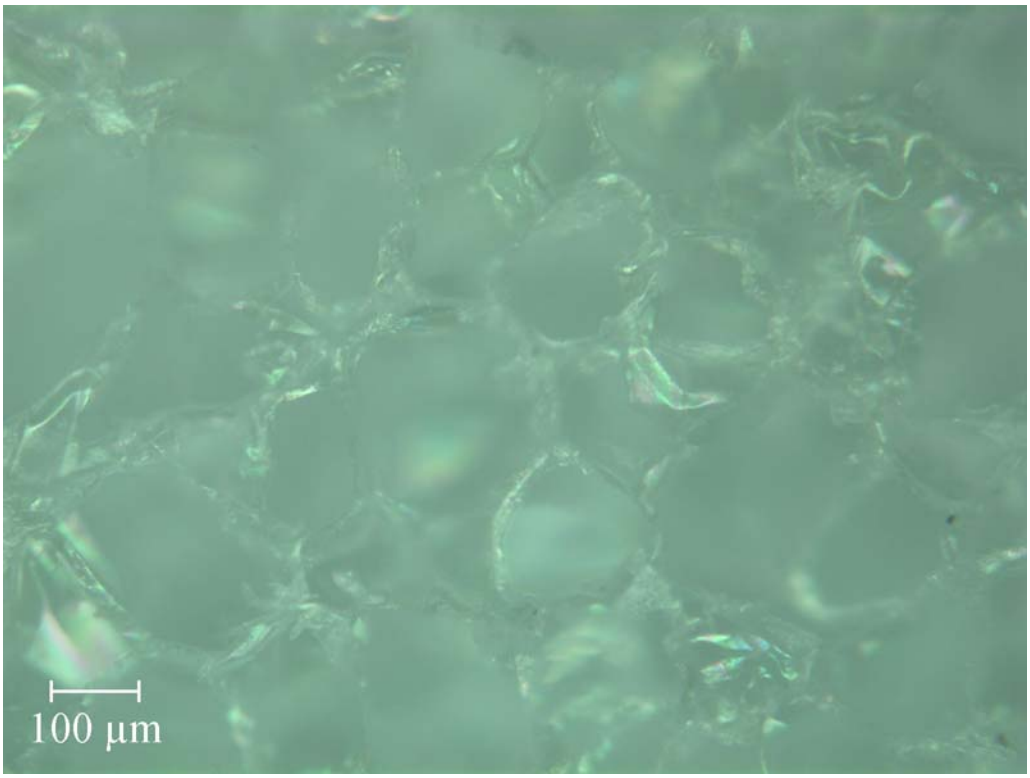

Figure 3.17 Typical Polystyrene Foam Cell Structure

To collect data from these images, five photos were taken from different parts of the foam surface. Three edge and face thickness and cell diameter measurements were made using the Advanced Spot software (Diagnostic Instruments Inc., Sterling Heights, Michigan, USA) from each image. The average thicknesses and cell diameters are reported below. Next, the geometric data was compared to compression testing results.

Table 3.2 Results of Foam Cell Survey of Average Cell Diameter Using 10x Aperture

Sample	Average Cell Diameter (µm)	Largest Cell Diameter (µm)	Smallest Cell Diameter (µm)
KFOAML	345	554	177
KFOAML1	394	623	248
KFOAMLF	851	1427	590
KFOAMLF1	641	1026	272
4 lb. PU	527	782	280
8 lb. PU	383	575	239
16 lb. PU	695	1044	225
4 lb. Ceno	200	371	85
8 lb. Ceno	207	331	102
16 lb. Ceno	150	220	79
4 lb. UFA	188	354	100
8 lb. UFA	205	277	148
16 lb. UFA	230	358	151
Polystyrene Foam	179	257	110

Table 3.3 Results from Foam Cell Survey of Face and Edge Thickness Using 10x Aperture

Sample	Average Face Thickness (μm)	Average Edge Thickness (μm)
KFOAML	148.4	66.0
KFOAML1	94.9	39.3
KFOAMLF	277.5	144.1
KFOAMLF1	226.6	71.3
4 lb. PU	97.9	44.5
8 lb. PU	67.1	20.1
16 lb. PU	172.2	58.5
4 lb. Ceno	80.0	29.8
8 lb. Ceno	82.0	43.6
16 lb. Ceno	46.9	18.1
4 lb. UFA	58.4	25.3
8 lb. UFA	53.1	24.0
16 lb. UFA	70.5	24.7
Polystyrene Foam	55.2	21.2

3.1.3 Anisotropic Mechanical Behavior

Both the polyurethane and carbon based foams exhibit anisotropic properties. Specifically, the foams tend to be stronger in the direction of formation, or along the major axis (larger of the two axis that divide a shape in half) of elongated pores. Both the polyurethane and carbon based foams show elongated cells and pores that indicate the rise of gas bubbles during formation. This is the most common irregularity in foam production. The major axis direction exhibits the highest compressive strength in the foam.

To demonstrate that the polyurethane foams are anisotropic and that the major axis direction is the strongest in compression, a brief test was performed on the MTS compression device. Figure 3.18 indicates the simple compression tests results for polyurethane foam oriented along the major and minor axis directions.

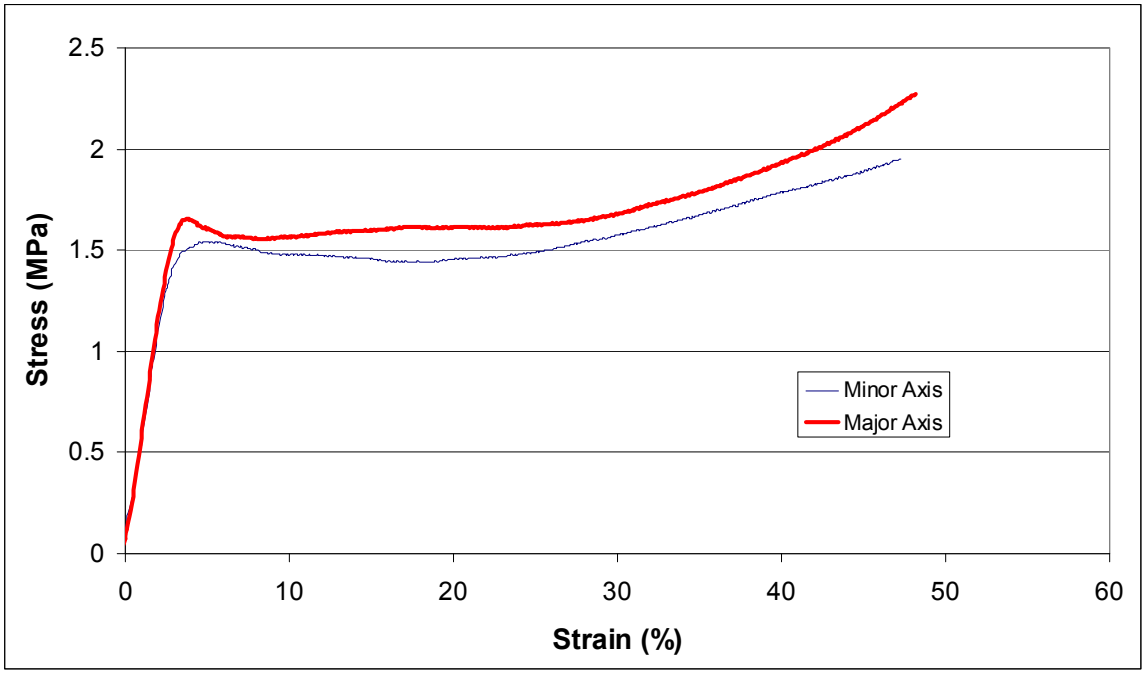

Figure 3.18 Non-isotropic Behavior Evidence in 8 lb. Ceno Along Major and Minor Axis of Elongated Pores

Compression tests indicate higher yield stress and strain energy density (area under the stress-strain curve) along the major axis of elongated pores.

3.1.4 Mechanical Behavior of Layered Composites

Each type of foam was tested in compression and impact. Several different samples were combined in hybrid composite layers to create 5.08 cm (2") and 7.62 cm (3") samples. It was believe that hybrid composite layered samples would exhibit the behavior of the weakest type of foam in the sample, however experiment showed this was not the case. The mechanical behavior of hybrid layered composites varied with respect to the order of layering. Specifically, the entire hybrid composite layered sample exhibited properties of the single layer facing impact initially. This observation was discussed by B.Z. Jang, *et al.* in the paper "Impact Resistance and Energy Absorption Mechanisms in Hybrid Composites."[9]

Jang, *et al*. tested nylon and graphite layers in different ordered layers. Compression testing indicated graphite-graphite and graphite-nylon samples initially showed the same elasticity when graphite faced the impacting plate. After some strain, the two samples

differed in behavior. The test was repeated with nylon-nylon and nylon-graphite sample with nylon facing the impacting plate. As expected, the layered sample matched the initial stress-strain response of nylon alone. These experiments showed that layered materials exhibit the properties, of the material facing impact initially.[9]

This phenomenon was observed during blast and impact testing. Videos obtained with a high speed camera confirmed the anticipated behavior of stacked layers of foam. One video showed the impact of a layered composite with 2.54 cm (1") thick KFOAML and 8 lb. PU sample with carbon foam facing the impacter. The impact takes place over 0.005 seconds. At the point of impact the carbon foam sample clearly densifies before the softer polyurethane begins to crush. Intuitively, the weakest foam sample of the hybrid composite layered sample would be expected to densify first, but that was not the case. The blast results were similar. Seven of the sixteen samples tested were hybrid composite layered samples of three types of foam. All samples placed drywall and carbon foam first on the impact, or blast side. Those foam samples were followed by a variety of 8 lb. PU and 4 lb. PU. First, the carbon foam layer experienced severe damage. Then, the lowest density foam was crushed as shown in Figure 3.19. All the test samples that included layers of 4 lb. PU, 8 lb. PU and a carbon foam face exhibited this behavior.

Figure 3.19 Remains from Blast 6 - 4 lb. Ceno, 8 lb. Ceno, KFOAML Layer

Compression testing results indicated the average yield stress of KFOAML and 8 lb. PU to be 3.9 and 1.25 MPa (565.5 and 181.25 psi) respectively. One might expect the foam sample with lower yield stress to be crushed first regardless of the arrangement of layers. This phenomenon is likely the result of the high rate of the incoming force. This behavior can be investigated further; however, the empirical evidence suffices to determine the best order to create hybrid composite layered foam samples to protect a wall from blast or impact. Considering the fourteen types of foam used in this project, the best layered order from the side facing impact to the concrete wall is carbon foam, followed by polyurethane foams of decreasing density.

3.2 Mechanics of Energy Absorption

Energy absorption dynamics are further complicated since yield stress and energy absorption are a function of strain rate. Higher yield stresses result from higher strain rates. This property is echoed through foam behavior literature. [6, 9, 18] Since the strain rate can be modified on the MTS compression testing device, a simple test demonstrated this phenomenon. Figure 3.20 shows the stress-strain curve for 8lb. PU at different strain rates from 1 mm/min to 1000 mm/min (0.039 – 39.4 mil/min). The strain energy density (or area under the stress-strain curve) and yield stress increase with each step in strain rate.

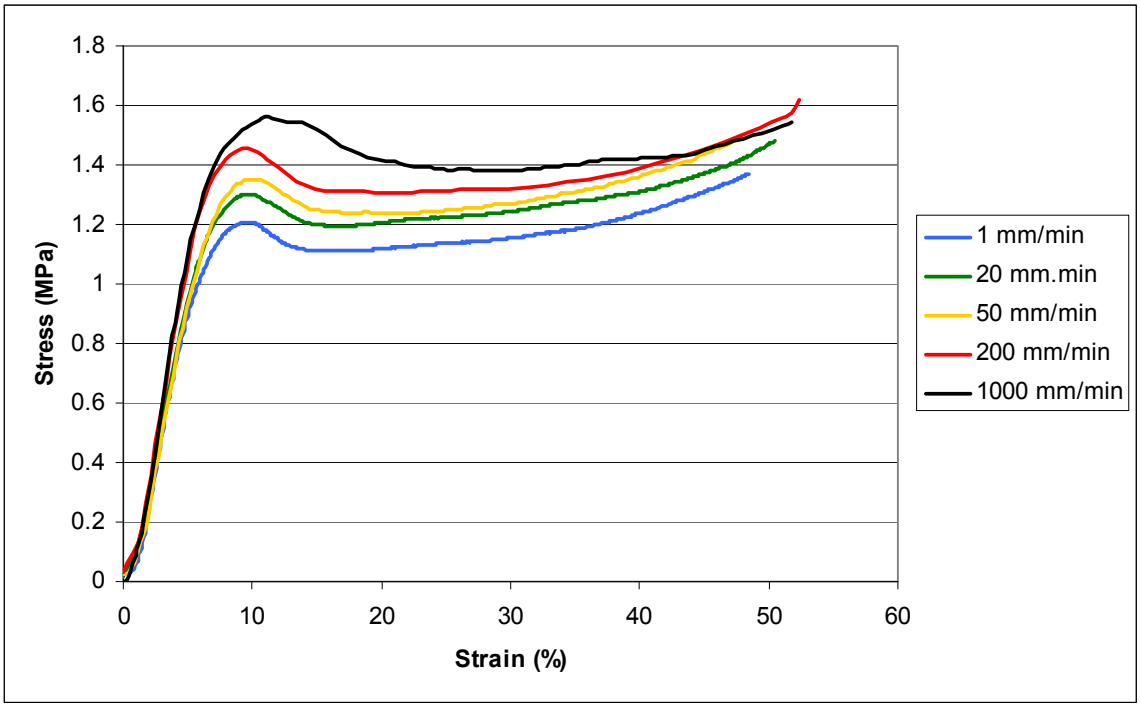

Figure 3.20 Stress-strain Plot at Different Strain Rates of 8 lb. PU

Table 3.4 Yield Stress Changes with Strain Rate

Strain Rate (mm/min)	Yield Stress (MPa)	Strain Energy Density (J/m^2)
1	1.15	10.7
20	1.25	13.3
50	1.32	13.3
200	1.44	15.1
1000	1.49	15.4

The highest strain rate possible using the MTS compression device is 1000 mm/min or 1 m/min (39.4 mil/min). Of course, this strain rate is much lower than that experienced during a blast or impact (8.81 m/s (28.9 ft/s)). Since materials respond differently to higher strain rates, three strain rate regimes were examined in this project. The three strain rates were low rate compression testing, middle rate impact testing and high rate blast testing.

Chapter 4 Experimental Approach

Besides the examination of foams under a microscope, the mechanical properties of each type of foam was tested in 3 strain rate regimes: low rate compression, middle rate impact testing, and high rate blast testing. Table 4.1 lists the four empirical approaches used, the data collected from each approach and information provided by that data.

Table 4.1 Data and Information Obtained from the Foam Cellular Survey and Three Strain Rate Tests

Test Type	Data Yield	Information Gained
Foam Cell Images	• Survey of Cell Structure	• Cell Diameter • Edge Thickness • Ligament Thickness • Types of Cells (Open or Closed)
Compression Testing	• Stress-strain Curve	• Elasticity • Yield Stress • Peak Stress • Strain Energy Density • Failure Mode (General Material Behavior)
Impact Testing	• Kinetic Energy Change • High Speed Camera Video	• Energy Absorbed by Foam and Lost to Environment • Hybrid Composite Layered Foam Behavior • Failure Mode
Blast Testing	• Before & After Images • High Speed Camera Video	• Mock Wall Status: Broken, Cracked, or Intact • Explosion Observations

4.1 Low Strain Rate Compression Testing

Low strain rate testing, also known as static or compression testing, was performed by an MTS universal testing machine (MTS, Eden Prairie, Minnesota, USA) under computer controlled data acquisition according to testing standard ASTM D695.

4.1.1 Simple Compression Experimental Set-up

Cube samples measuring 2.54 cm (1”) on each side were placed between the two parallel plates of the MTS device. The plates moved at a constant rate of 1 mm/min (0.0394 in/min) until 50% strain was achieved. The MTS device measured the resistance to

crushing and provided the resulting stress. The computer recorded data at a frequency of 10 Hz. The resulting stress-strain curve supplied information to determine the elastic modulus, yield stress, peak stress, strain energy density and the mode of failure.

The elastic modulus is the slope of the initial straight portion of the stress-strain curve. If the stress is relieved in this region, the sample returns to its original position. Yield stress indicates the point where the material begins to plastically deform. In brittle materials this can indicate when a sample fractures. Peak stress is the highest stress on the stress-strain curve. If the sample increases in density, or densifies, the peak stress is typically greater than the yield stress. [19]

Strain energy density is the amount of energy a sample absorbs over the deformation length. Strain energy density can be found by integrating the area under the stress-strain curve. The resulting units will be a unit of pressure that can be interpreted as energy per unit volume.[6]

$$\gamma = \int_0^{\varepsilon} \sigma d\varepsilon \tag{4.1}$$

4.1.2 Failure Mode Relation to Material Properties

Failure modes provide an image of the overall foam behavior. For example, Figure 4.1 shows the stress-strain curve of 8 lb. polyurethane foam. The initial slope on the left side of the curve indicates a region of elastic deformation. The yield stress occurs where the curve changes from the initial straight section to curving concave down. At this point the specimen is plastically deformed. [6, 20]

Since most energy absorption takes place under the plateau section of the stress-strain curve after the yield stress is reached, if the pressure from impact is less than the yield stress, the material offers very little impact mitigation. Knowing the yield stress and strain energy density is vital to selecting materials for impact mitigation. These properties are well documented for packaging materials. Some literature exists for the use of

aluminum foam in blast mitigation, but few other materials are documented for this application.

4.1.2.1 Elastic-Plastic Failure

In general, energy is absorbed by foams through the deformation of cells. Polyurethane exhibits elastic-plastic failure because the material initially follows an elastic modulus then plastically deforms and densifies. Figure 4.1 shows elastic-plastic failure.

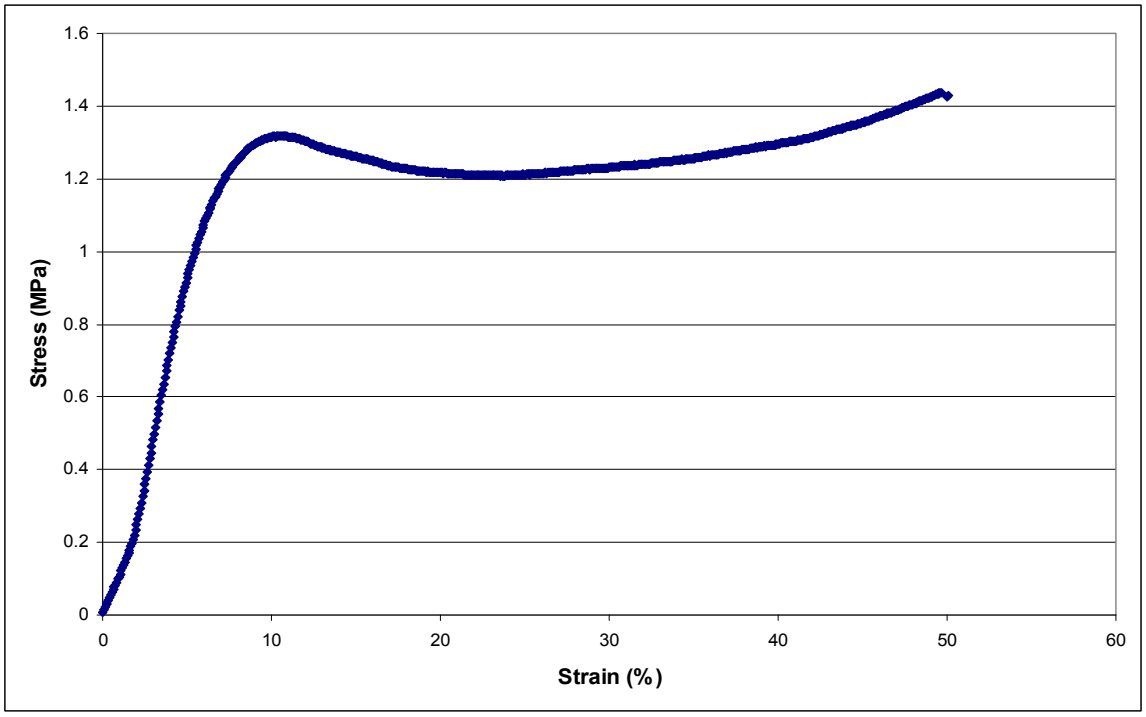

Figure 4.1 Elastic-Plastic Foam – 8lb. PU Average Stress-strain Curve

4.1.2.2 Elastic-Brittle Failure

All four carbon foam samples exhibited elastic-brittle behavior. Each resisted stress along the elastic modulus then failed repeatedly. The brittle failure of foam differs from brittle failure for solid materials. Typically, a brittle solid will follow an elastic curve then yield and abruptly fail. Foam brittle failure occurs on a cellular level. Consequently, repeated sets of cells deform and fail under stress. After a set of cells fail, the stress applies to another set. Figure 4.2 shows the stress-strain curve for KFOAMLF1. The resulting stress-strain jagged curve indicates when sets of cells failed.

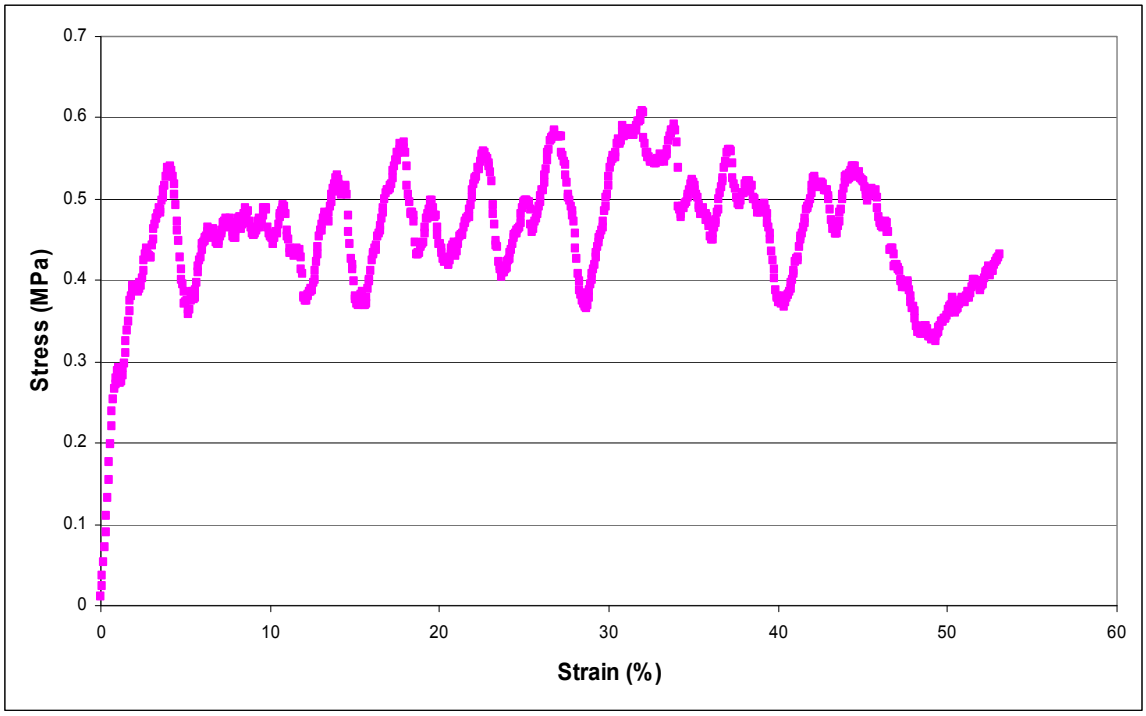

Figure 4.2 Elastic-brittle foam – KFOAMLF1 Specimen Stress-strain Curve

4.1.2.3 Elastic Failure

Polystyrene foam is the only sample in this project that exhibits elastic failure. Cell walls bend like a hinge during compression and when the stress is relieved the cell walls return nearly to their original position. Catastrophic compression failure of polystyrene foam can occur. This was observed under very high pressures during middle strain rate impact testing. When the impact tester was fitted with a 5.08 cm (2") diameter cylindrical shaped nose instead of the 15.24 cm X 15.24 cm (6" X 6") steel plate, the full force of a 8.81 m/s (28.9 ft/s) collision was concentrated on a 2.54 cm (1") thick polystyrene foam sample. The sample burst, leaving a tightly compressed area under the nose and the rest of the sample in small pieces. Immediately after this event, the polystyrene foam sample was noticeably hot and permanently deformed. Part of the sample appeared to have melted under then heat generated during the impact.

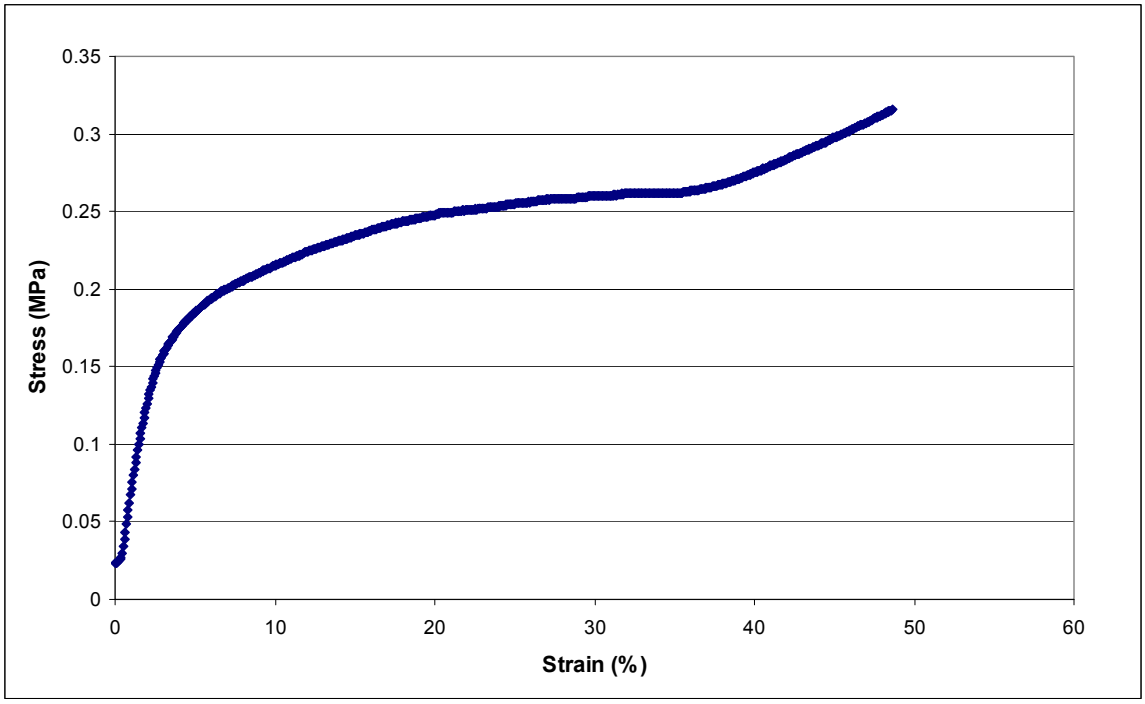

Figure 4.3 Elastic Failure – Polystyrene Foam Stress-strain Curve

Figure 4.3 shows the stress-strain curve for polystyrene foam. Polystyrene foam showed no clear yield stress point and the foam nearly returned to its original shape after unloading. Since polystyrene foam densified and the average stress leveled off between 0.2 and 0.25 MPa (29.0 psi and 36.3 psi), it may be described has having elastic-plastic characteristics.

4.2 Middle Strain Rate Impact Testing

Middle strain rate impact testing increased the strain rate from 10 mm/min (0.393 mil/min) to 8.81 m/s (32.8 ft/s). The response from impact tests mirrored that of a small blast.

Several impact testing methods exist. Drop dart, pneumatic rod, dual hammer, gas gun, and other tests have been used to test materials in impact. This project designed a novel rail and sled device for impact testing. [6, 10, 11, 13, 18]

The impact tester consists of an impact sled and target mass suspended from a rail. During a test run, the impact sled (33.8 kg or 74.5 lbs.) glides along an inclined section of rail falling about 4.27 vertical meters (14 ft). Next, the sled travels along a straight section before colliding with the target mass (118.4 kg or 261 lb) at about 8.81 m/s (18.9 ft/s). Foam samples (15.24 cm X 15.24 cm (6"X6")) are attached to a hardened steel plate on the impact sled before collision. Typically, the duration of impact is about 0.005 seconds when foam samples were in place. The duration of impact is observed using a high speed camera (Fastec Trouble Shooter, Factec Imaging, San Diego, California, USA).

To find the energy the foam absorbs, data is collected during the impact in two primary ways. First, a high speed camera (Fastec Trouble Shooter, Factec Imaging, San Diego, California, USA) captures the event at 1000 frames per second. Second, photo-gates measure the impacter speed before collision and the target mass speed after collision. The difference of the kinetic energy of the impact sled before the impact and the target mass after impact provides the kinetic energy lost and absorbed by the sample during the impact. In the future, an accelerometer will record the force and duration of impacts. This measurement method is discussed further in Chapter 7.

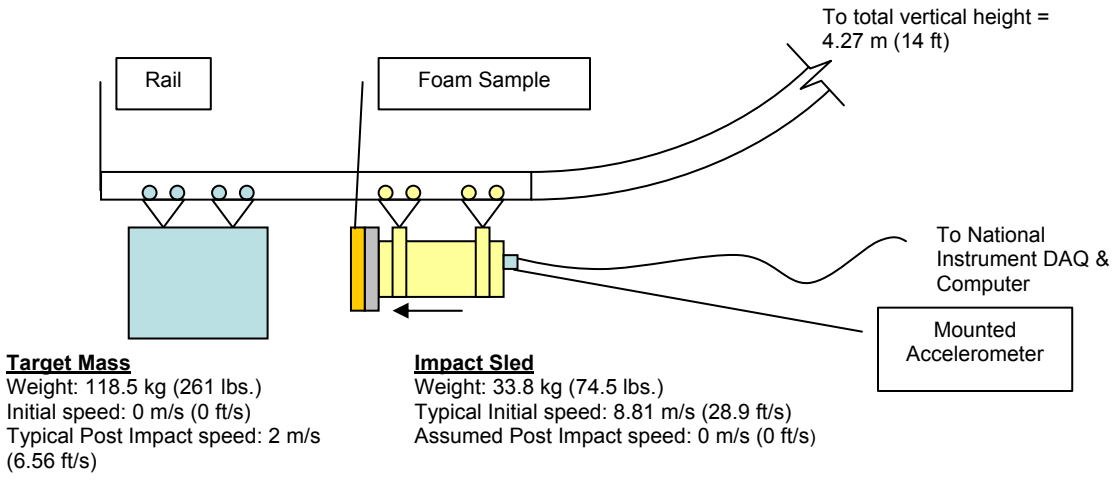

Figure 4.4 Impact Test Experimental Set-up

The percent of energy the foam absorbs is found using conservation of energy. The sled velocity before impact represents the total energy of the system. After collision, the velocity of the target mass is recorded. The difference between these two values is the energy absorbed by the foam sample or lost to the environment. This approach provides a means to quantitatively compare the response of each sample to impact. [21]

Conservation of Energy

$$En_i = En_f \tag{4.2}$$

$$\frac{1}{2} m_s v_i^2 = \frac{1}{2} m_t v_f^2 + En_{lost} \tag{4.3}$$

The calculations assume the velocity of the sled after the impact was zero. Actually, the sled moves backwards after collision most of the time. This is one of many extraneous energy losses that were difficult to quantify. A great deal of effort was made to eliminate known controllable loses as discussed in Section 1.3. Nonetheless, the results provide a comparison between samples rather than strict analytical results.

4.3 High Strain Rate Blast Testing

Blast testing is the only way to directly simulate the effect of a blast on a concrete structure.

4.3.1 Blast Testing Experimental Set-up

Blast testing aims to simulate a small explosion occurring outside the walls of a building. To achieve this, mock concrete walls are constructed from cinder blocks and mortar. The walls consist of two concrete blocks with two half blocks sandwiched between to create the staggered effect found in most concrete block buildings. The concrete walls are constructed in wooden frames to ease transport. To fix the mock walls in position, each wall is strapped to a steel frame planted in the earth by 4 – 0.61 m (2') rods.

A 1.27 cm (1/2") thick steel plate covers the mock wall and leaves a 0.305 m (1') square opening in the middle of the wall. Foam samples are glued or taped to this section.

A 125g (0.276 lbs.) sphere of C4 explosives is suspended directly in front of the square. A high speed camera records the explosion; however, because these tests occur very quickly, little discernable difference between blasts videos can be observed. Photos of the mock wall are taken before and after the blast. Each blast is rated "Broken," "Cracked," or "Intact" to describe the effect on the concrete blocks. Only "Intact" walls pass, while "Cracked" and "Broken" walls fail the test.

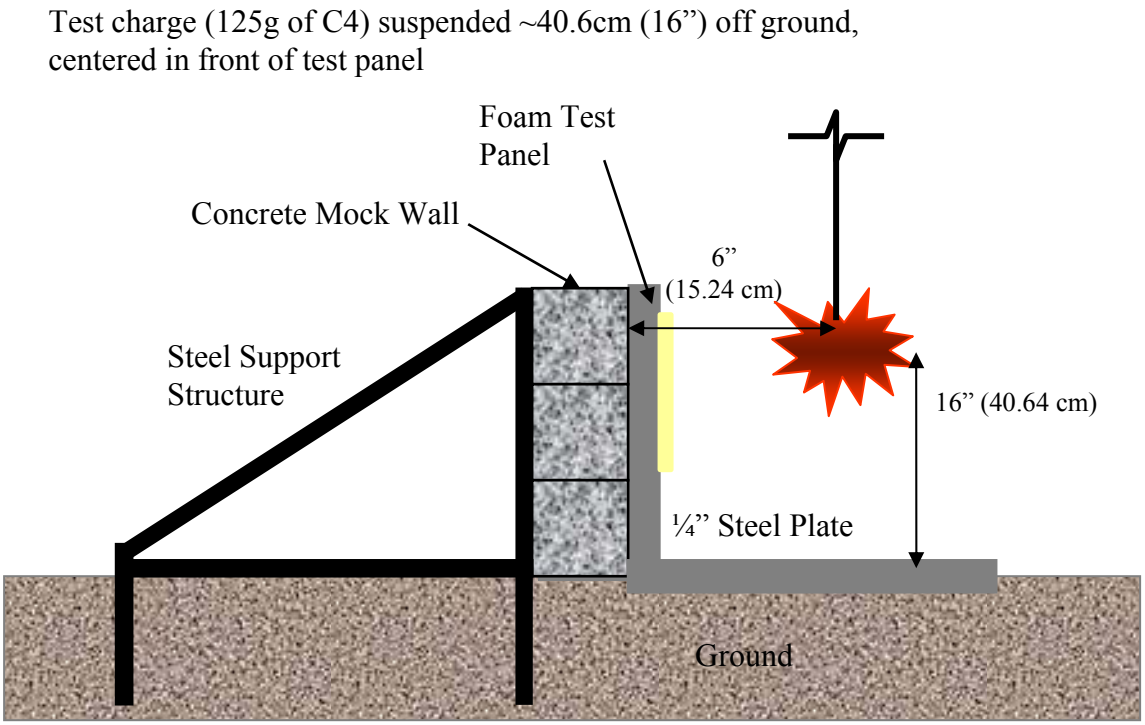

Figure 4.5 Schematic Drawing of Blast Testing Experimental Set-up

4.3.2 Calculating Blast Parameters

Explosions are the result of a great deal of energy released quickly from a source. The rapid increase in temperature and expansion of gas results in a pressure wave that propagates away from the source. The severity of an explosion depends mostly on two parameters: the source of the explosion and the distance from the source. [22]

For this project, a small mass of solid C4 explosives is used. Dr. Tom Thurman, of Eastern Kentucky University, selected this size charge (125 g (0.275 lb.)) since it is similar to the blasts that are the most prevalent threat to US structures. For each test, the

charge was offset about 15.24 cm (6”) from the concrete wall face. The hybrid composite foam layered sample fronts are closer to the blast than the concrete wall. All personnel who helped perform the experiment stayed at least 30.8 m (100ft) away from the blast. Table 4.2 provides information about C4 and two typical solid explosives: TNT (trinitrotoluene) and RDX (Royal Demolition Explosive or cyclotrimethylenetrinitramine). [23]

The velocity of particles going out from the blast source quantifies the severity of an explosion, along with the change in temperature. The detonation velocity and resulting pressure are the primary interest of this project. Table 4.2 provides the detonation velocity of C4 and equations 4.7 and 4.8 provide the pressure applied to the foam sample face during the blast. [24]

Table 4.2 Solid Explosive Parameters [3]

	C4	TNT	RDX
Density (g/cm^3)	1.64	1.65	1.85
Heat of Combustion (MJ/kg)	---	15.02	9.46
Heat of Detonation (MJ/kg)	6.61	4.23	4.54
Gas Volume (cm^3/g) at STP	---	710	780
Detonation Velocity (m/s)	8340	6940	8570
Detonation Pressure (GPa)	25.7	18.9	33.8

Shock tubes and blast testing are often used in the study of material properties under sudden pressure. The following set of equations calculates the pressure acting on the test face with respect to the medium through which the wave propagates. P_{21} is the pressure ratio in front and behind the pressure wave propagating away from a blast source.

In equation 4.6 M represents the Mach number, or the ratio between the wave propagation velocity and the speed of sound in the medium. For this project, the blast wave propagates through air at about 286.5 m (940 ft) above sea level. The speed of sound at this altitude is about 233.5 m/s (759 ft/s). [25] Γ is the ratio of the specific heats of the gas in front and behind the blast pressure wave.

$$M = \frac{u_w}{u_{sound}} \tag{4.4}$$

$$P_{21} = P_2 / P_1 \tag{4.5}$$

$$P_{21} = 1 + \frac{2\Gamma}{(\Gamma + 1)}(M^2 - 1) \tag{4.6}$$

The pressure resulting from a blast is called "overpressure" since it indicates the pressure above ambient. The following equation represents the overpressure on the wall face.

$$P_2 - P_1 = P_1(P_{21} - 1) \tag{4.7}$$

Relating the stress experienced by the front of the foam during a blast test to the loading rate is important to analyze the physical effect of a blast. Several authors provide the following derivation to relate the pressure experienced by the foam to the loading rate of the blast. [8, 18, 26] First, the blast test is assumed to be a one dimensional nonlinear wave that compresses the foam. To develop the equations, the foam must be assumed to be rigid, perfectly plastic, and locking (r-p-p-l). The term perfectly plastic indicates that the material will not deform elastically at any point and any deformation is locked into place. Here, two key stresses are significant: the yield stress, σ_y and the stress of complete densification or when all the cells are collapsed, σ_d. The incident shock wave is assumed to completely densify or collapse all the cells. The foam density before the shock wave reached the face is ρ_o, and after complete densification the density is ρ_f.

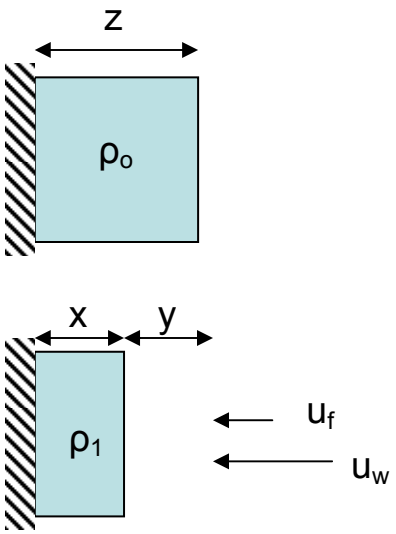

Figure 4.6 Simplified Perfectly Plastic Foam Crushed by Blast Wave

The incoming blast wave velocity, u_w, is imparted on the foam surface causing the front of the foam to compress at a rate, $u_{f,}$ Conservation of mass reveals a relation between the velocity of the blast wave and foam front velocity. The height, h, and width, w, of the foam remain unchanged during the event.

$$\rho_o = \frac{m}{zwh} \tag{4.8}$$

$$\rho_1 = \frac{m}{xwh} \tag{4.9}$$

By combining these equations the following is achieved:

$$\frac{\rho_o}{\rho_1} = \frac{x}{z} = \frac{x}{x+y} \equiv \xi \tag{4.10}$$

The wave and foam front velocities are described in equations 4.11 and 4.12:

$$u_f = \frac{y}{\Delta t} \tag{4.11}$$

$$u_w = \frac{x + y}{\Delta t} \tag{4.12}$$

Since the wave travels faster than the foam front compresses, during some time, *Δt*, the pressure wave will pass through the entire foam thickness but the foam front will lag behind. This point in time is chosen to complete the derivation. The symbol *Δt* is the point in time when the blast wave passes through the sample thickness, but the foam front compresses at some lower rate.

The velocity equations are combined.

$$u_w = \frac{x + u_f \Delta t}{\Delta t} \tag{4.13}$$

$$x = (u_w - u_f)\Delta t \tag{4.14}$$

$$\xi = \frac{x}{x + y} = 1 - \frac{u_f}{u_w} \tag{4.15}$$

Strain is the deformation length divided by the total original length.

$$\varepsilon \equiv \frac{y}{x + y} = 1 - \xi \tag{4.16}$$

$$\varepsilon = \frac{u_f}{u_w} \tag{4.17}$$

From the conservation of momentum the fully compressed stress can be expressed as a function of the yield stress and the wave and foam front velocity

$$\sigma_d = \sigma_y + \rho_o u_f u_w \tag{4.18}$$

$$\sigma_d = \sigma_y + \frac{\rho_o {u_f}^2}{\varepsilon} \tag{4.19}$$

Equation 4.19 provides the stress where the foam is completely densified, or all the cells are crushed with respect to yield stress, original density, foam face velocity, and strain. Not surprisingly, the original foam density, strain and foam front velocity are the components, since the equation considers the densification of foam. Since the yield stress at high strain rate tests is unknown in this project, the maximum stress found in equation 4.18 can not be accurately calculated here.

In Chapter 3, the evidence that impacts and blasts affect the front of hybrid layered composite foam samples was discussed. High speed camera videos show this phenomenon during impact test. The front layer of a composite sample densifies before the rest. Li, *et al*. explored this phenomena in foam under a blast pressure wave.[26] Li, *et al.* argued that local physical quantities are changed through wave propagation. Since the blast pressure wave travels faster than the foam face under blast conditions the front of a layered composite must experience a change in stress, strain and density before the rest of the material. The thickness and number of different samples is not a factor determining what part of a foam sample will be affected initially. The sample facing the blast will experience densification first. Moreover, Sadot and Paul, *et al.* suggest the effect of strain rate on material properties is greater at high strain rate and sometime unnoticed at low strain rates.[3, 7, 8, 11, 26, 27]

4.3.3 Impact and Blast Testing Comparison

Impact and blast intensity can be compared in many ways. Directly comparing the kinetic energy of the impact sled to the energy released during a blast may seems like the obvious choice, but this approach will cause confusion. Unlike impact tests, the energy of a blast includes chemical and thermal energy. Upon detonation of a mass of C4, energy is released in through heat, pressure, sound and other forms. Instead of energy, comparing the pressure experienced by the foam face under impact and blast conditions provides more meaningful analysis.

Pressure resulting from impact is calculated conservation of momentum. First, the impulse, or force of impact multiplied by the impact duration equals the change in momentum during collision.[21]

$$J = F\Delta t = m\Delta v \tag{4.20}$$

The resulting force is divided by the area of the impacter to find pressure or stress. For this calculation, the duration of the collision is estimated using the high speed camera. The high speed camera acquires images at 1000 frames per second. Since the impact event can be viewed in a single frame, the duration is approximated as 0.001s. Of course, this calculation is based on a direct impact between the impact sled and target mass, not a collision with a foam sample attached to the impacter. This way the full force of the impacter is estimated. When foam is tested, the duration is about 0.005 - 0.012s. The impact sled mass and average velocity before impact were 34 kg (74.5 lbs.) and 8.81 m/s (28.9 ft/s) respectively. This results in an impact pressure of about 12.9 MPa (1871 psi).

Next, the blast pressure is estimated using equations 4.6 - 4.8. The specific heat ratio is approximately 1.25. The Mach number is found using the speed of sound at about 286.5 m (940 ft) above sea level, 233.5 m/s (759 ft/s), where the tests are performed in Richmond, Kentucky. The detonation velocity, 8,340 m/s (27,363 ft/s), is the speed of the pressure wave acting out from the explosive mass.[3, 23] The resulting Mach number is 35.7. These values are entered in equation 4.7 resulting in an overpressure 1390.3 times the ambient pressure. If the ambient pressure is 1 atm, the resulting overpressure is 140.9 MPa (20,426 psi). This result is 128 MPa (18,555 psi) greater than the pressure of the impact tester.

It should be noted that the pressure resulting from blasts can described in several ways. Since explosives are often used in excavation, much of the literature explaining their use assumes explosives are pressed into rock. Detonation pressure, listed in Table 4.2, describes the pressure when explosives are detonated surrounded by rock. Since blast pressure waves reflect off hard surfaces, explosions in containers have higher pressure

than explosions in open air. Blast tests for this project were performed in open air, and the energy from the blast wave traveled freely in all directions away from the explosive mass. [3, 5, 25]

4.3.4 Blast Sample Selection

Blast testing simulates the conditions that will ultimately exist in the field. Dry wall covered the face of each foam sample to simulate the front layer of a commercial wall. For hybrid composite layered samples, each layer was glued to the next with Liquid Nails (Macco Adhesives, ICI Paints, Strongsville, Ohio, USA), an adhesive often used in paneling construction.

The Ben Gurion University research group mentioned that at least a 7.62 cm (3") thick panel of aluminum foam is required to protect a concrete wall from a blast. Impact testing concurred with this estimate. Therefore, several blast testing samples included hybrid composite layered samples of 3 – 2.54 cm (1") foams.

Carbon foam was positioned directly behind the dry wall façade, since the front layer will receive the brunt of the blast and may be exposed to flame, radiation or chemical attack. Typically, a 2.54 cm (1") 8 lb. PU layer followed carbon foam and 2.54 cm (1") 4 lb. PU finished the hybrid composite layered sample. The 4 lb. PU sample touched the concrete wall. For comparison, some samples were only 5.08 cm (2") thick, or contained only 2 – 2.54 cm (1") samples. Also, some tests used only dry wall to protect the wall. These tests provided evidence that the C4 blast was capable of destroying the wall.

Chapter 5 Results

5.1 Compression Testing Results

Several material properties were gained from compression testing including yield stress and elasticity. Of course, the actual response in the event of a blast cannot be completely determined by compression testing. As discussed in Chapter 3, the yield stress of foam is dependent on strain rate. Since the strain rate during a blast is much greater than during a compression test, the yield stress during a blast may be expected to be much greater as well.

The yield stress and elastic modulus for each type of foam is listed in Table 5.1. Five 2.54 cm (1") cube samples were tested in compression. The average of the five samples is shown in Figures 5.1 -5.6. The results of each specimen are shown in the appendix.

Table 5.1 Yield Stress and Elastic Modulus of Each Foam Sample

Sample	Yield Stress (MPa)	Elastic Modulus (MPa)	Average Strain Energy Density (MPa (J/cu m))
4 lb. PU	0.42	9.4	0.187
4 lb. Ceno	0.28	10.7	0.195
4 lb. UFA	0.41	19.4	0.186
8 lb.PU	1.25	29.3	0.590
8 lb. Ceno	1.47	58.9	0.772
8 lb. UFA	1.06	43.8	0.431
16 lb. PU	4.59	148.7	2.251
16 lb. Ceno	3.65	130.8	1.888
16 lb. UFA	2.64	108.9	1.077
KFOAML	3.90	173.2	1.390
KFOAML1	1.85	165.6	0.885
KFOAMLF	0.30	19.8	0.147
KFOAMLF1	0.41	25.8	0.191
Polystyrene Foam	0.18	7.2	0.117

The stress-strain curves for the 3 different polyurethane densities are shown in Figures 5.1 – 5.3.

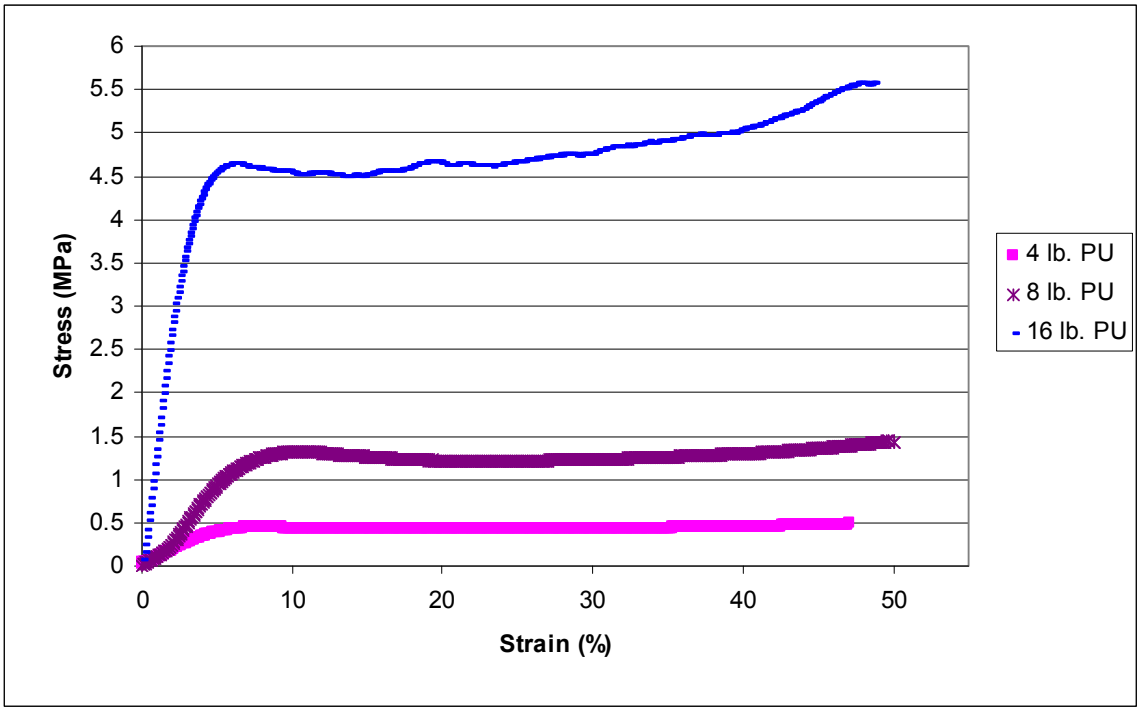

Figure 5.1 Average Stress-strain Results for 3 Different Densities of Polyurethane Densities

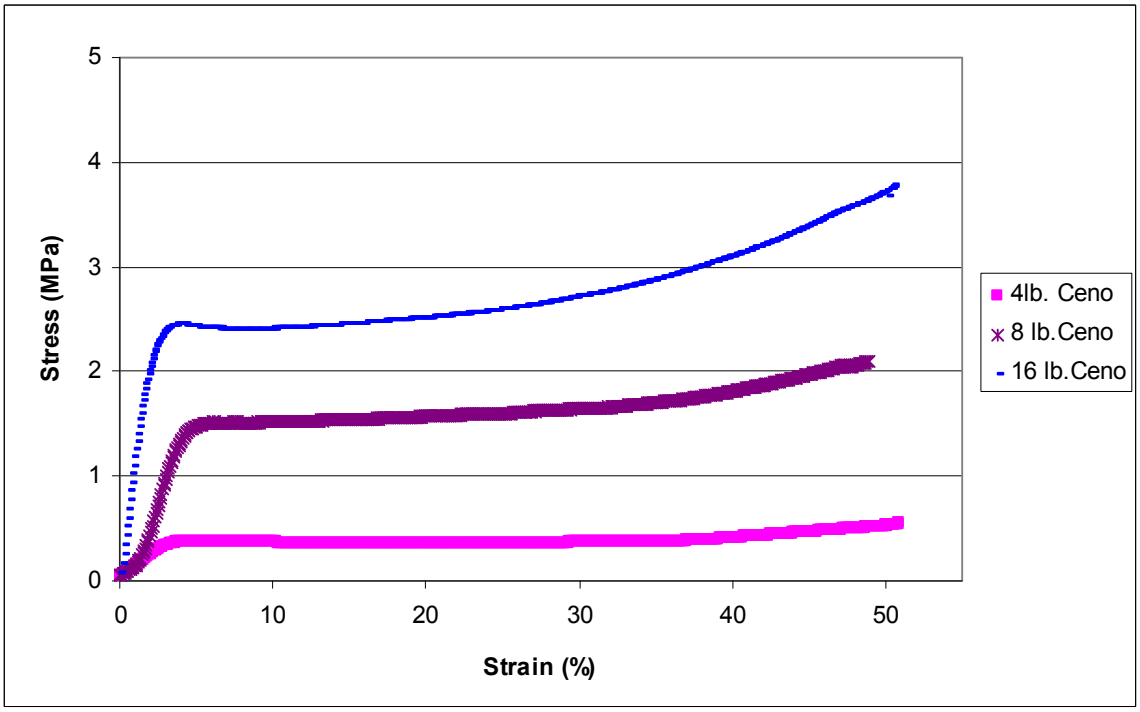

Figure 5.2 Average Stress-strain Results for 3 Different Foam Densities Polyurethane with Cenospheres

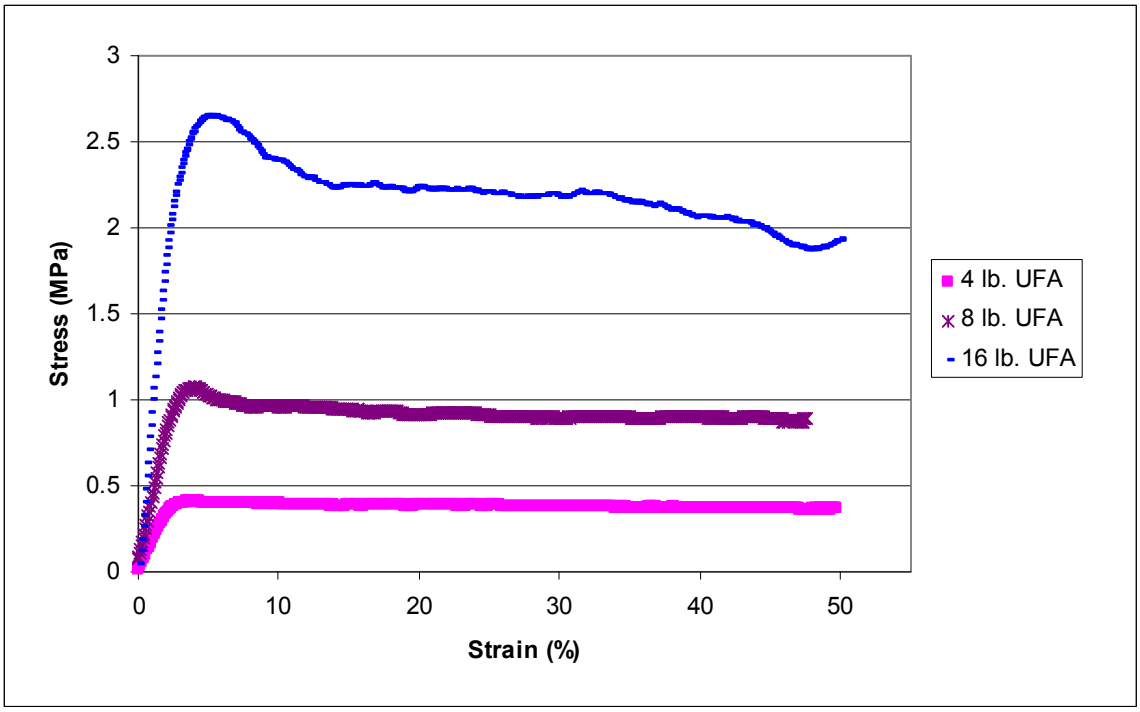

Figure 5.3 Average Stress-strain Results for Three Different Densities of Polyurethane Foam with Cenospheres

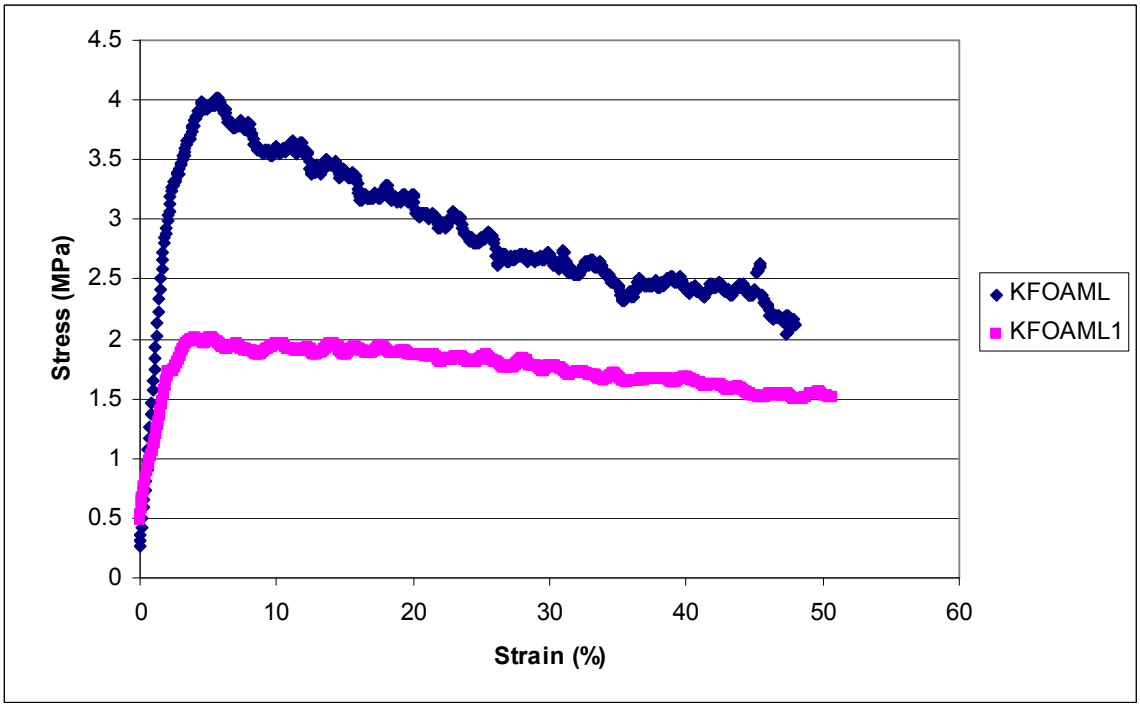

Figure 5.4 Stress-strain Curves for KFOAML & KFOAML1

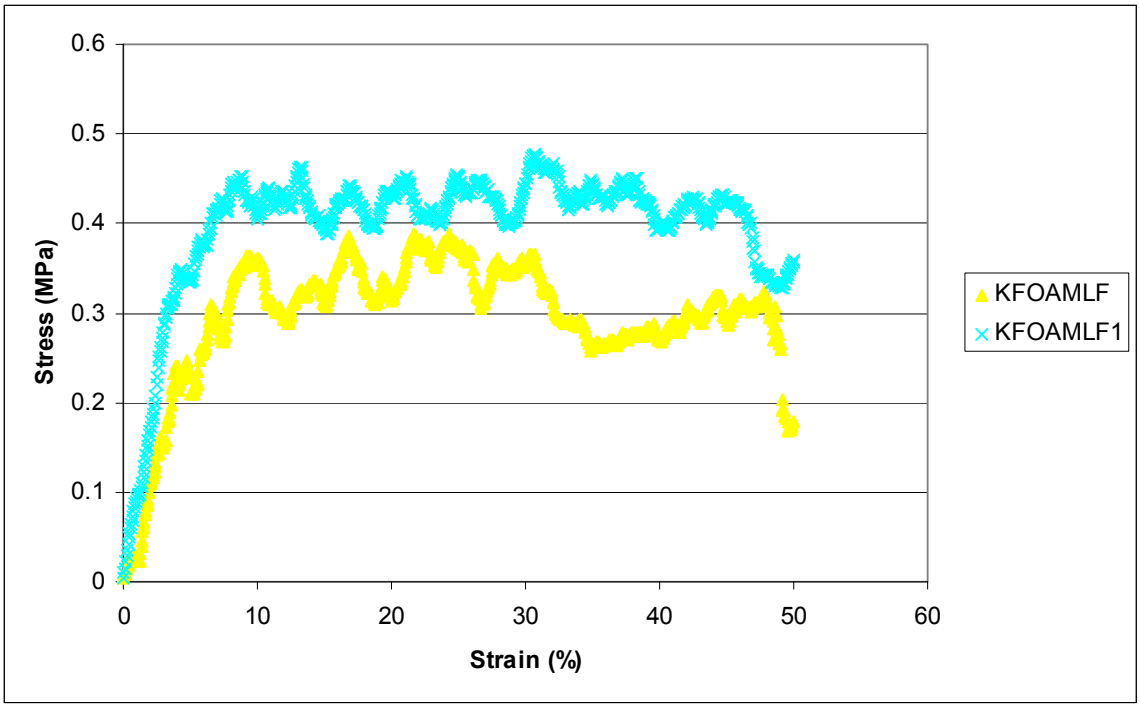

Figure 5.5 Stress-strain Curves for KFOAMLF & KFOAMLF1

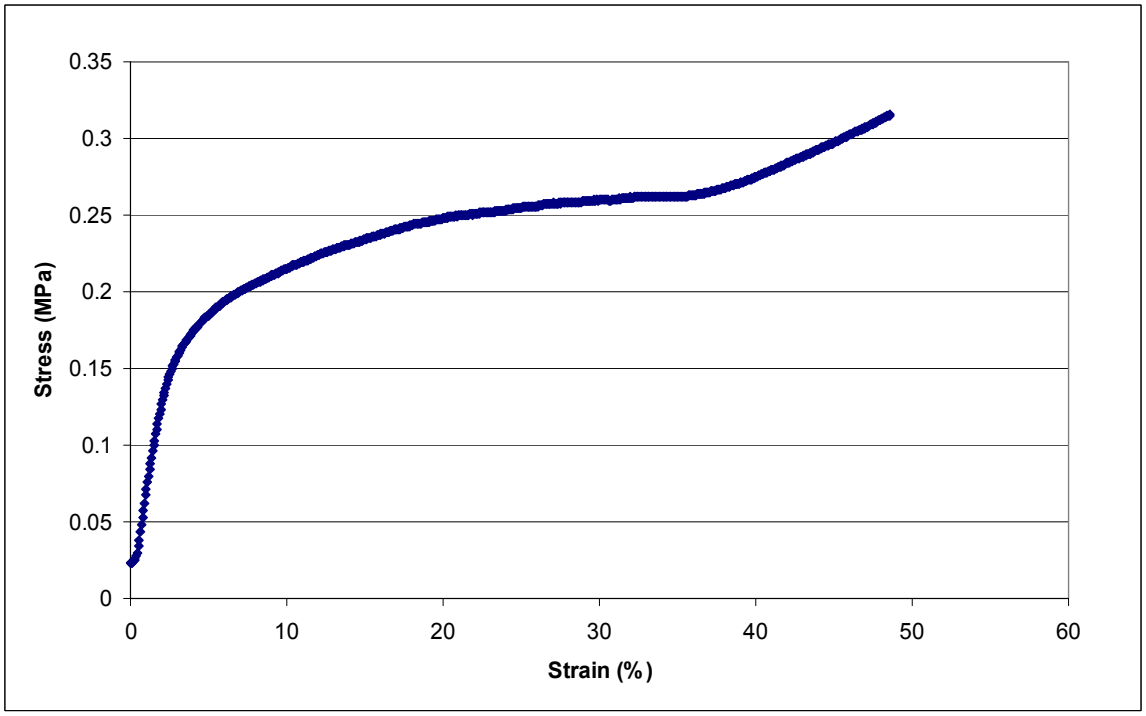

Figure 5.6 Average Stress-strain Results from Polystyrene Foam

Figures 5.7 – 5.9 show the strain-strain results for polyurethane again. Here the curves are grouped according to density so that the effect of non-flammable additives can be easily distinguished.

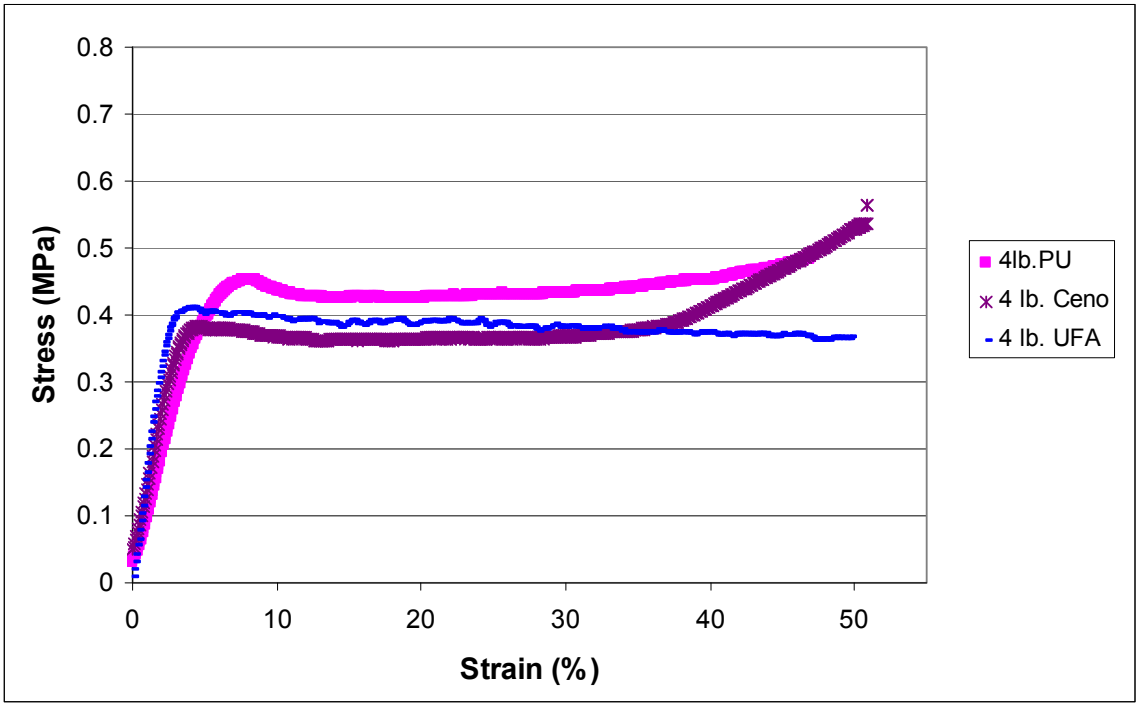

Figure 5.7 Average Stress-strain Curves for Three Types of 4 lb. Polyurethane Foam

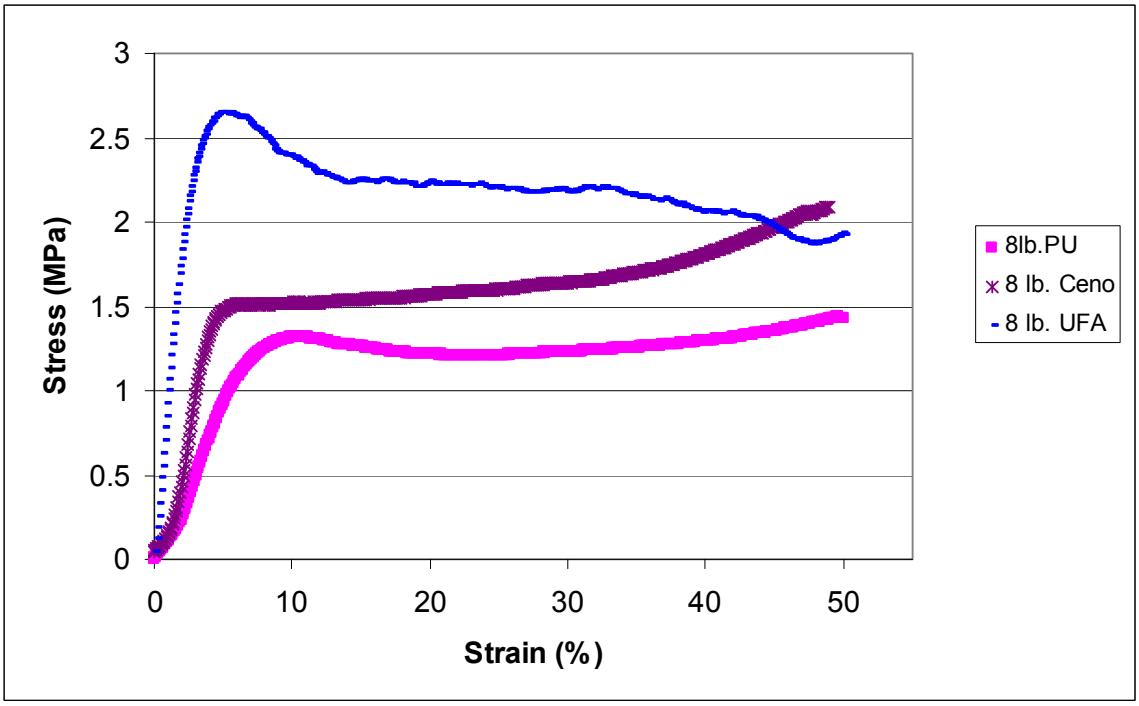

Figure 5.8 Average Stress-strain Curves for Three Types of 8 lb. Polyurethane Foam

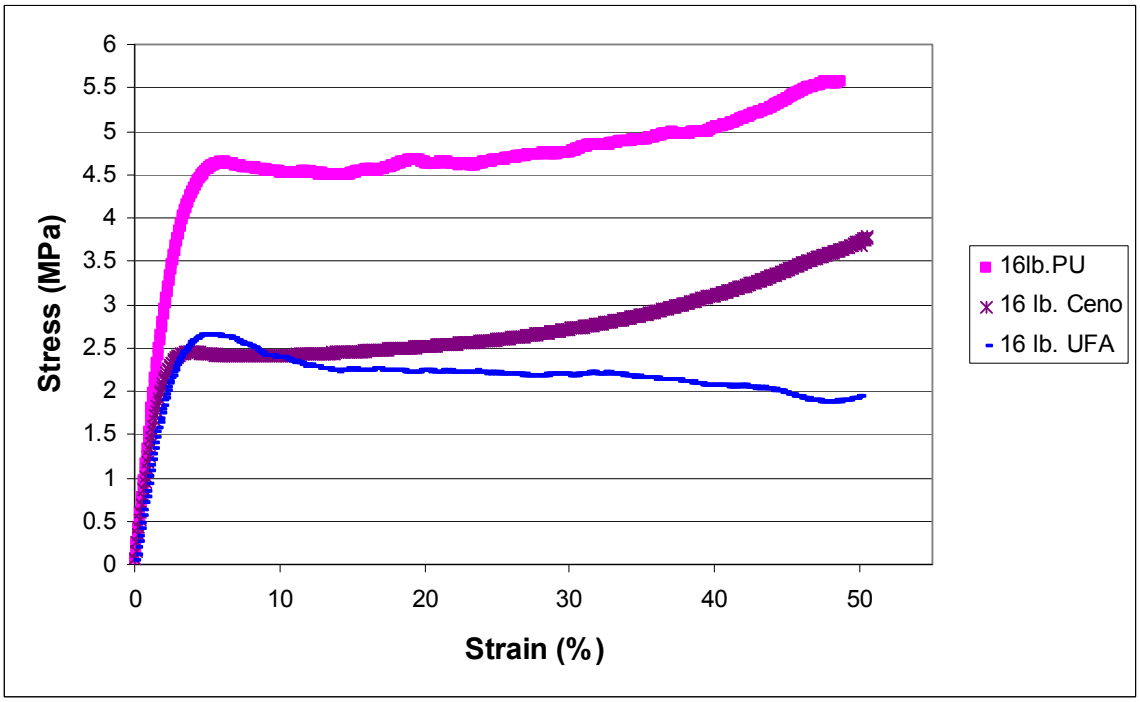

Figure 5.9 Average Stress-strain Curves for Three Types of 16 lb. Polyurethane Foam

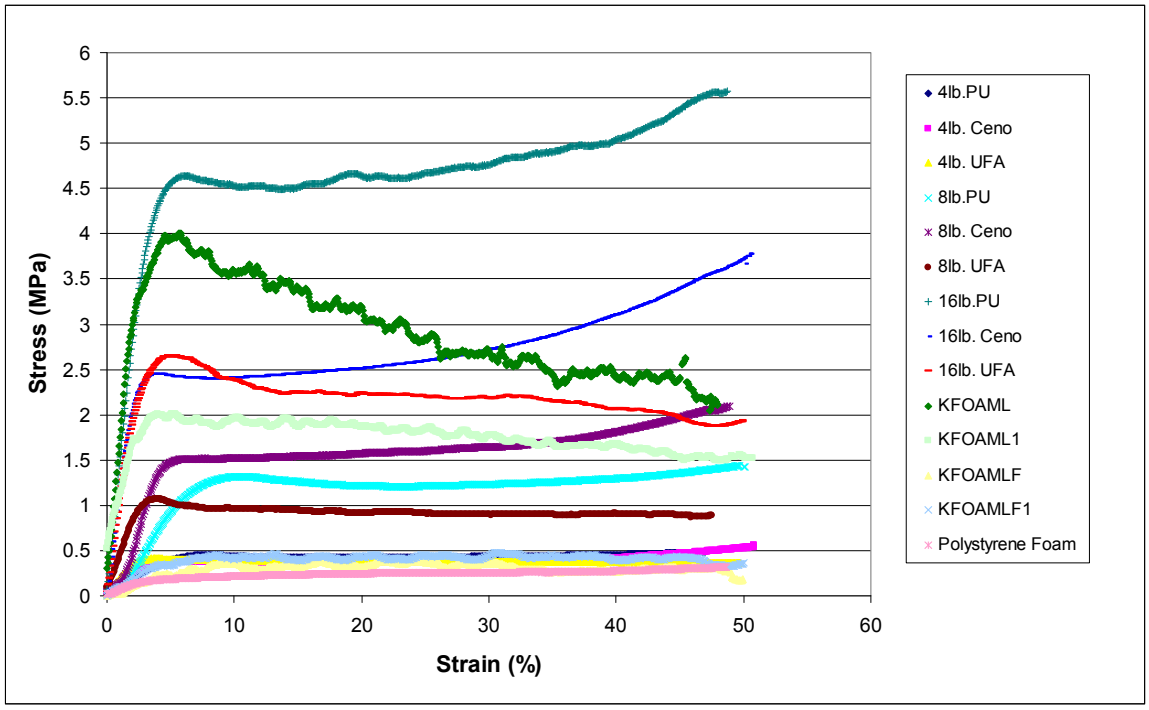

Figure 5.10 Average Stress-strain Results for All Samples

5.2 Cell Survey & Mechanical Behavior Results

In Chapter 3, the fundamentals of cellular solid mechanics were discussed. To spread light on the cellular structure of the samples used in this project, each type of foam was examined under a microscope. Five images were taken from a 1 cm (0.39") square surface of each sample using a microscope (Leica Microsystem GmbH, Wetzlar, Germany) and Advanced Spot camera (Advanced Spot, Diagnostic Instruments Inc., Sterling Heights, Michigan, USA). Three ligament, edge and cell diameter size measurements were taken from each image for a total of 45 measurements for each sample. Cell structure survey results were compared to the compression test results to illustrate the relationship between cell structure and mechanical properties. Figure 5.11 – 5.16 display these results.

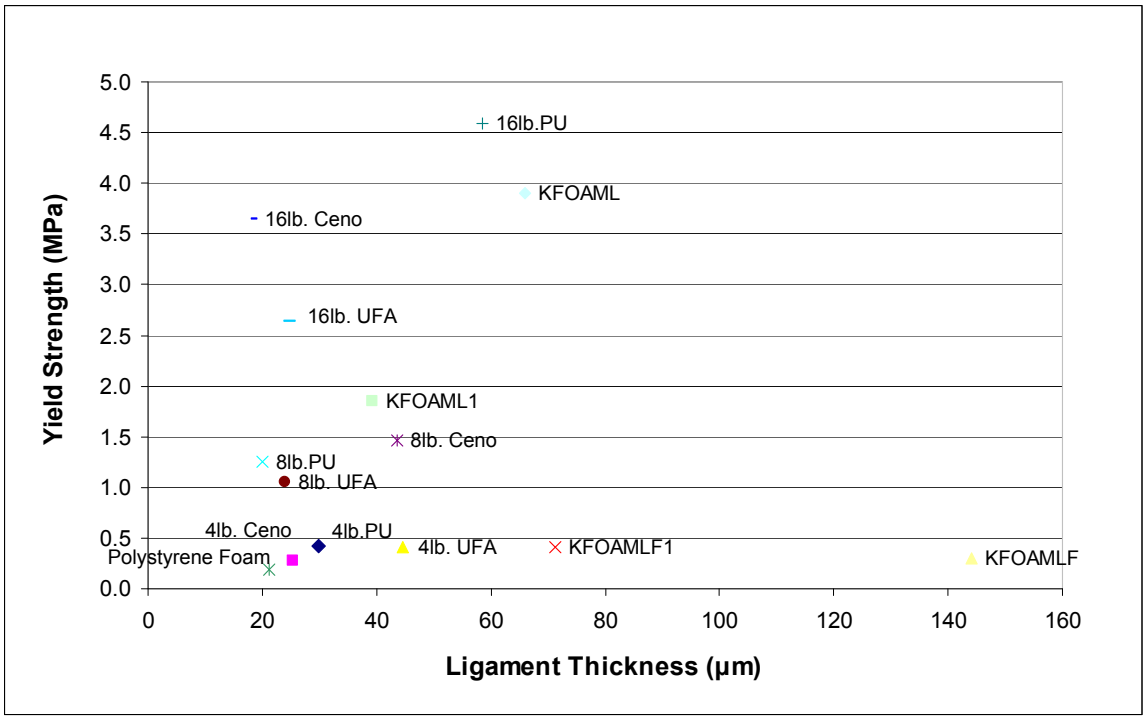

Figure 5.11 Average Ligament Thickness v. Average Yield Strength

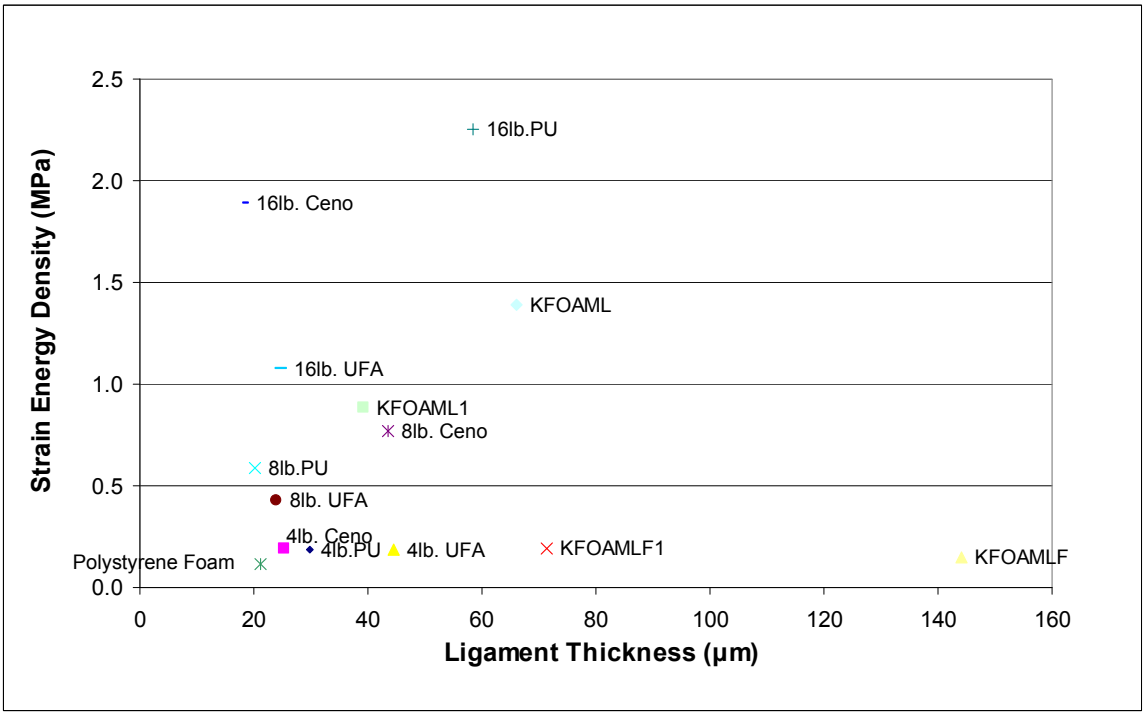

Figure 5.12 Average Ligament Thickness v. Average Strain Energy Density

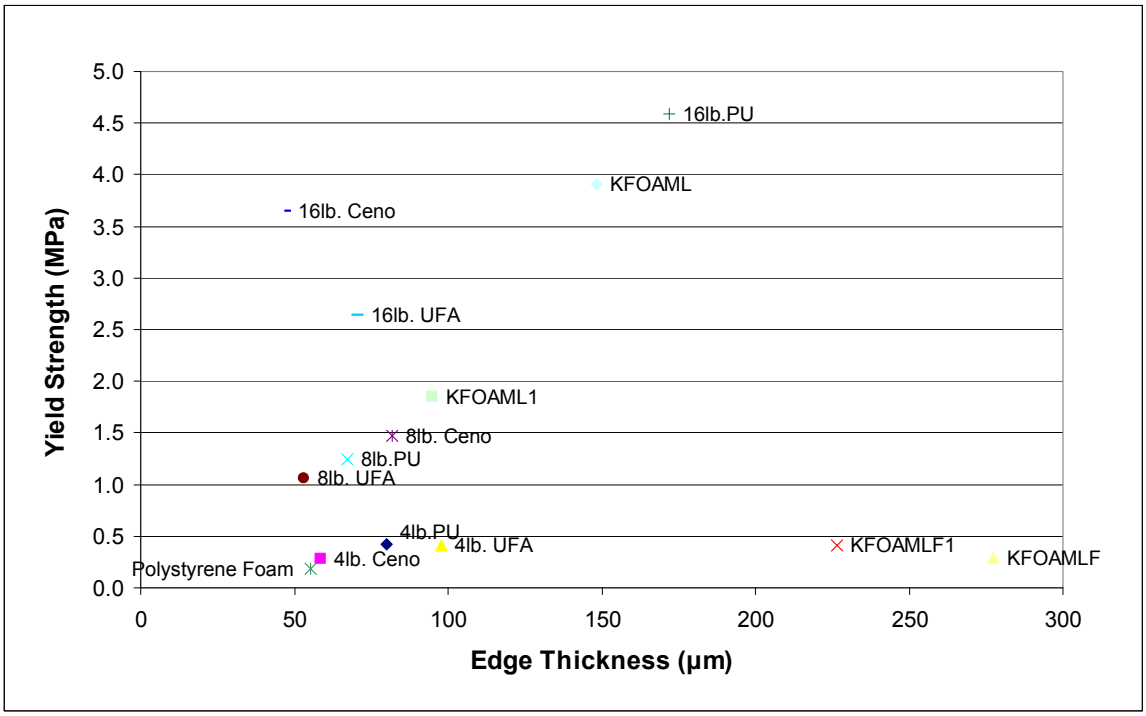

Figure 5.13 Average Edge Thickness v. Average Yield Strength

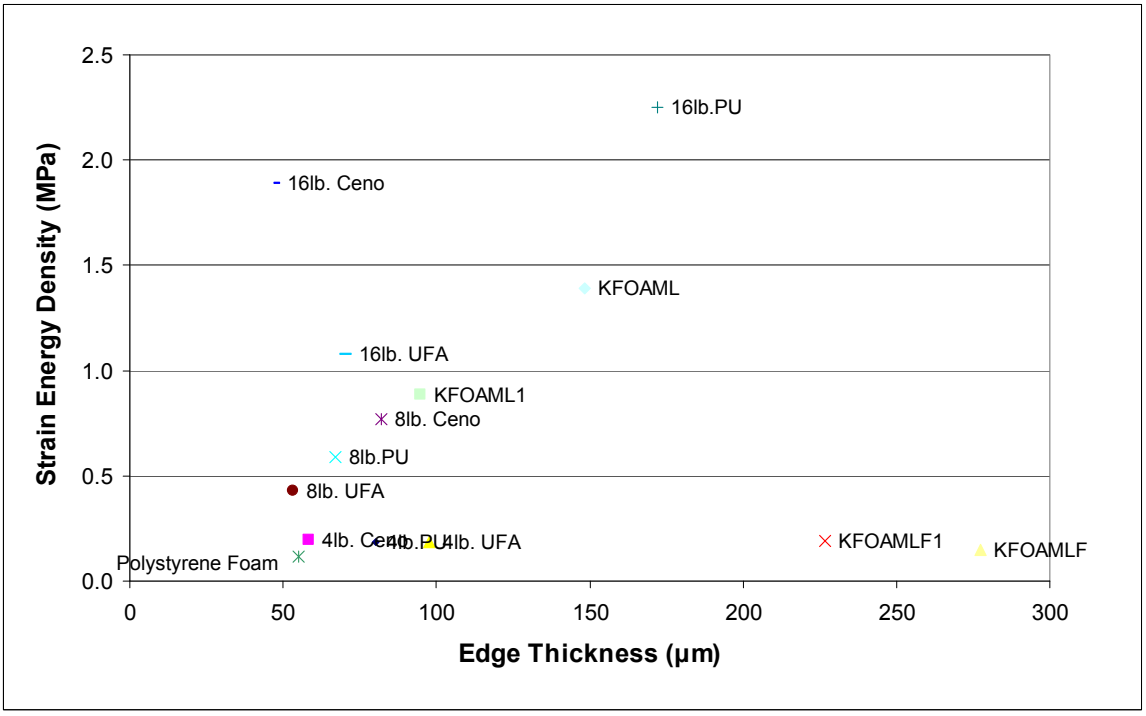

Figure 5.14 Average Edge Thickness v. Average Strain Energy Density

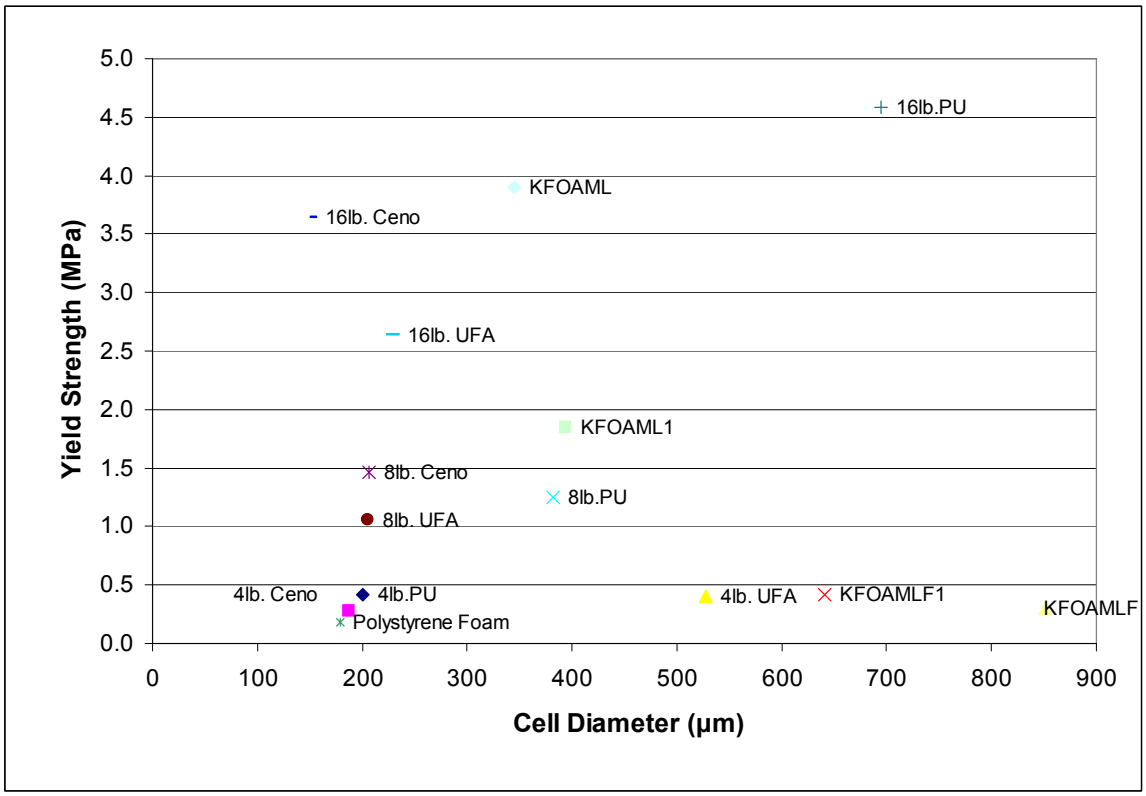

Figure 5.15 Average Cell Diameter v. Average Yield Stress

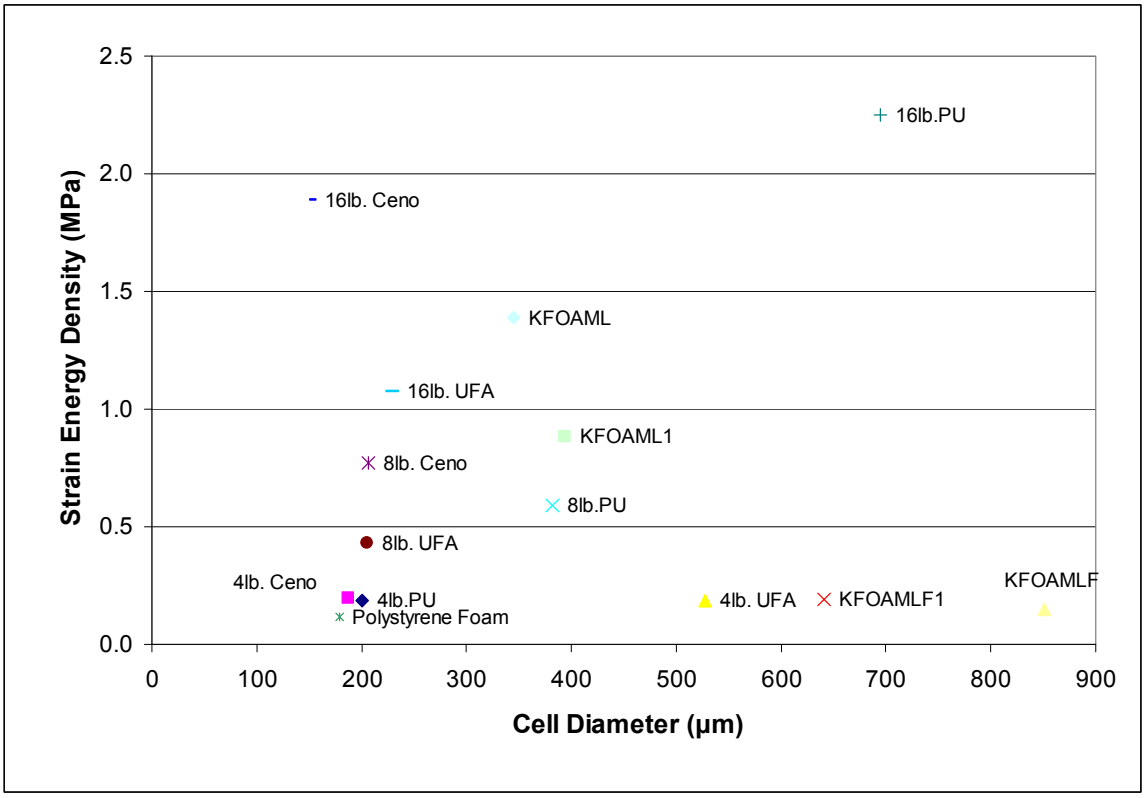

Figure 5.16 Average Cell Diameter v. Average Strain Energy Density

The plots showing edge and ligament thickness against yield strength and strain energy density exhibited a pattern. In general, thick edges and ligaments result in higher yield strengths and strain energy densities. Of course, there are some exceptions to this trend. KFOAMLF and KFOAMLF1 show high average ligament and edge thickness but low yield strength and strain energy densities. Material properties dominate the behavior over cell geometry in this case. KFOAMLF and KFOAMLF1 are brittle. The 16 lb. PU samples have relatively small edge and ligament thickness but high yield strength and strain energy density. This sample stands out for its strong materials properties independent of cell structure.

5.3 Impact Testing Results

Initial impact tests were performed on 2.54 cm (1") thick, 15.24 cm X 15.24 cm (6" X 6") square samples of polystyrene foam, polyurethane foam and each type of carbon foam. Next, 5.08 cm (2") and 7.62 cm (3") thick hybrid layered composite samples were tested.

As mentioned in Chapter 4, the kinetic energy of the impact sled before, and the speed of the target after collision were measured. The initial velocity of the sled was about 8.81 m/s (28.9 ft/s). The target's velocity varied. Tables 5.2 – 5.4 show the percent of energy absorbed or lost to the environment or the difference between the kinetic energy of the impact sled before collision and the kinetic energy of the target mass after collision divided by the kinetic energy of the impact sled before collision.

$$Percent\ of\ Total\ Energy\ Lost = \frac{KE_{Impact\ Sled} - KE_{Target\ Mass}}{KE_{Impact\ Sled}} * 100 \qquad (5.1)$$

Table 5.2 Impact Test Results for 1” Thick Samples

Sample	Percent of Total Energy Lost or Absorbed
1" Polystyrene Foam	72.3%
1" KFOAMLF1	78.0%
1" KFOAML	80.0%
1" KFOAML1	81.0%
1" KFOAMLF	81.1%
1" 8 lb. PU	82.9%

Table 5.3 Impact Test Results for 2” Thick Samples

Inner Sample	Outer Sample	Percent of Total Energy Lost or Absorbed
1" 8 lb. PU	1" KFOAML	74.6%
1" Polystyrene Foam	1" KFOAML	74.6%
1" 8 lb. PU	1" KFOAML1	79.7%
1" Polystyrene Foam	1" KFOAML1	79.7%
1” KFOAML	2" KFOAML	81.0%
1” KFOAML1	1” KFOAML1	81.1%
1" 8 lb. PU	1" 8 lb. UFA	81.5%
1” 8 lb. PU	1” 8 lb. PU	85.8%

Table 5.4 Impact Test Results for 3” Thick Samples

Inner Sample	Outer Sample	Percent of Total Energy Lost or Absorbed
1" Polystyrene Foam	2" KFOAML	72.5%
1" Polystyrene Foam	2" KFOAML1	74.1%
2" 4 lb. PU	1" 8 lb. Ceno	77.6%
1" 8 lb. PU	2" KFOAML	80.7%
1" 8 lb. PU	2" KFOAML1	81.0%

5.4 Blast Testing Results

Ultimately, blast testing results were evaluated on a pass/fail system. Images of the mock wall after the explosion are shown in Figures 5.7 – 5.22. The concrete wall frame was

tipped forward to reveal damage before the photographs were taken. Additional images of each blast tests are found in the appendix.

Figure 5.17 Result of Blast 1 – Drywall Only (Broken – Fail)

Figure 5.18 Result of Blast 2 – 2 Layers of Drywall (Broken – Fail)

Figure 5.19 Result of Blast 3 – 2 Layers of Drywall and 16 Gage Steel (Broken – Fail)

Figure 5.10 Result of Blast 4 – Polystyrene Foam, and 2 layers of Drywall (Cracked – Fail)

Figure 5.11 Result of Blast 5 – 4 lb. Ceno & 8 lb. Ceno & KFOAML1 (Intact – Pass)

Figure 5.12 Result of Blast 6 – 4 lb. Ceno & 8 lb. Ceno & KFOAML (Intact – Pass)

Figure 5.13 Result of Blast 7 – 4 lb. Ceno & 8lb. UFA & KFOAML (Intact – Pass)

Figure 5.14 Result of Blast 8 – 4 lb. Ceno & 8 lb. UFA & KFOAML1 (Intact – Pass)

Figure 5.15 Result of Blast 9 – 4 lb. UFA & 8 lb. UFA & KFOAMLF (Intact – Pass)

Figure 5.16 Result of Blast 10 – 4 lb. UFA & 8 lb. UFA & KFOAMLF1 (Broken – Fail)

Figure 5.17 Result of Blast 11 – Polystyrene Foam & 8 lb. Ceno & KFOAML1 (Broken – Fail)

Figure 5.18 Result of Blast 12 – 4 lb. UFA & KFOAML1 (Broken – Fail)

Figure 5.19 Result of Blast 13 – 4 lb. UFA & KFOAML (Cracked – Fail)

Figure 5.30 Result of Blast 14 – 8 lb. Ceno & KFOAML1 (Broken – Fail)

Figure 5.31 Result of Blast 15 – 8 lb. Ceno & KFOAMLF1 (Cracked – Fail)

Figure 5.32 Result of Blast 16 – 8 lb. Ceno & 4 lb. Ceno (Cracked – Fail)

Table 5.5 summarizes the results of the blast testing. The blast test results were evaluated as "Broken," "Cracked," or "Intact."

Table 5.5 Summary of Blast Testing Results

Blast #	Sample	Blast Test Results
1	Drywall Only	Broken
2	Drywall & Drywall	Broken
3	Drywall & Drywall & 16 Ga. Steel	Broken
4	Polystyrene Foam & Drywall & Drywall	Cracked
5	4 lb. Ceno & 8 lb. Ceno & KFOAML1	Intact
6	4 lb. Ceno & 8 lb. Ceno & KFOAML	Intact
7	4 lb. Ceno & 8 lb. UFA & KFOAML	Intact
8	4 lb. Ceno & 8 lb. UFA & KFOAML1	Intact
9	4 lb. UFA & 8 lb. UFA & KFOAMLF	Intact
10	4 lb. UFA & 8 lb. UFA & KFOAMLF1	Broken
11	Polystyrene Foam & 8 lb. Ceno & KFOAML1	Broken
12	4 lb. UFA & KFOAML1	Broken
13	4 lb. UFA & KFOAML	Cracked
14	8 lb. Ceno & KFOAML1	Broken
15	8 lb. Ceno & KFOAMLF1	Cracked
16	8 lb. Ceno & 4 lb. Ceno	Cracked

5.5 Simulated Blast Test and Correlating Impact and Blast Test Results

To correlate the results of the impact test with the blast tests, a mock wall was built in place of the target mass. The set of samples tested during blast tests were repeated using the impact sled and mock wall in place of the target block. The results of the impact sled striking the mock wall were categorized as "Broken," "Cracked," or "Intact" to match

with the blast results. Table 5.6 shows the results of blast testing and impact testing with a mock wall in place of the target block. Table 5.7 describes the condition of the blocks after impact.

Table 5.6 Summary of Results from Impact Simulation of Blast Testing

Sample	Blast Test Results	Concrete Block Impact Test Results	Match
Drywall Only	Broken	Broken	Y
Drywall & Drywall	Broken	Broken	Y
Drywall & Drywall & 16 Ga. Steel	Broken	Broken	Y
Polystyrene Foam & Drywall & Drywall	Cracked	Cracked	Y
4 lb. Ceno & 8lb. Ceno & KFOAML1	Intact	Intact	Y
4 lb. Ceno & 8 lb. Ceno & KFOAML	Intact	Intact	Y
4 lb. Ceno & 8 lb. UFA & KFOAML	Intact	Intact	Y
4 lb. Ceno & 8 lb. UFA & KFOAML1	Intact	Intact	Y
4 lb. UFA & 8 lb. UFA & KFOAMLF	Intact	Intact	Y
4 lb. UFA & 8 lb. UFA & KFOAMLF1	Broken	Intact	N
Polystyrene Foam & 8 lb. Ceno & KFOAML1	Broken	Broken	Y
4 lb. UFA & KFOAML1	Broken	Broken	Y
4 lb. UFA & KFOAML	Cracked	Broken	N
8 lb. Ceno & KFOAML1	Broken	Broken	Y
8 lb. Ceno & KFOAMLF1	Cracked	Intact	N
8 lb. Ceno & 4 lb. Ceno	Cracked	Broken	Y

Table 5.7 Summary of Results from Impact Simulation of Blast Testing Notes

Sample	Blast Test Notes	Concrete Block Impact Test Notes
Drywall Only	Structural failure; top block missing sections	Blocks were pulverized
Drywall & Drywall	Structural failure; top and middle blocks missing parts	Blocks broken into small pieces
Drywall & Drywall & 16 Ga. Steel	Structural failure; large sections of top and middle block missing	Blocks broken
Polystyrene Foam & Drywall & Drywall	Some cracks in mortar and cinder blocks	Some cracks in blocks
4 lb. Ceno & 8 lb. Ceno & KFOAML1	Intact, no obvious cracks	Intact, no obvious cracks
4 lb. Ceno & 8 lb. Ceno & KFOAML	Intact, no obvious cracks	Intact, no obvious cracks
4 lb. Ceno & 8 lb. UFA & KFOAML	Blocks remain intact. Mortar between blocks cracked.	Blocks survive impact, break due to movement after collision.
4 lb. Ceno & 8 lb. UFA & KFOAML1	Intact, no obvious damage	Intact, no obvious damage
4 lb. UFA & 8 lb. UFA & KFOAMLF	Intact, no obvious damage	Intact, no obvious damage
4 lb. UFA & 8 lb. UFA & KFOAMLF1	Failure, middle block missing	Intact, no obvious damage
Polystyrene Foam & 8 lb. Ceno & KFOAML1	Structural failure; middle block cracked and missing sections	Intact, no obvious damage
4 lb. UFA & KFOAML1	Structural failure; top and middle block destroyed	Blocks completely broken. Catastrophic failure
4 lb. UFA & KFOAML	Some cracks in mortar and cinder blocks	One block breaks.
8 lb. Ceno & KFOAML1	Structural failure; top and middle blocks cracked and parts broken off	Left block broke in compression and shear. Right block unscathed.
8 lb. Ceno & KFOAMLF1	Some cracks in top block	Intact, no obvious damage
8 lb. Ceno & 4 lb. Ceno	Some cracks in top and middle blocks	Some cracks in one of the blocks

Chapter 6 Discussion and Analysis

6.1 Compression Testing Discussion and Analysis

From section 5.1, the compression test immediately reveal foam properties. From Table 5.1, it is clear that polystyrene foam is the weakest followed by the least dense foam used in this study, 4 lb. PU. The strongest materials are KFOAML and 16 lb. PU, the densest polyurethane foam used. KFOAML, the strongest carbon foam, is produced by carbonizing foam from pitch. Unlike the other three types of carbon foam, KFOAML does not include multiwalled carbon nanotubes and is not graphitized.

From the stress-strain plots for the three densities of polyurethane, it is clear that yield stress increases with density. Plots for polyurethane foam with cenospheres and polyurethane foam with UFA concur with this observation. The 16 lb. PU plot is particularly interesting because the yield stress is more than 10 times that of 4 lb. PU. Similarly, the yield stress of 16 lb. Ceno was more than 13 times that of 4 lb. Ceno. The yield stress of 16 lb. UFA is more than 6 times greater than 4 lb. UFA. As discussed in Chapter 2, PU foam can vary from batch to batch since many parameters effect the final cellular structure. Moreover, 2.54 cm (1") cube foam samples can vary with respect to the location of the larger sample from which they are cut.

Polyurethane foam and polyurethane foam with cenospheres clearly densify, or the stress increases with increasing strain after the plateau region. However, the stress of polyurethane with UFA tampers off as it approached 50% strain. This pattern is indicative of foam that deteriorates instead of becoming denser. Ultimately, foam that crumbles will absorb less energy than one that densifies, since there will be less area under the stress-strain curve. Since five samples of each type of foam were tested the average strain-strain curve provided a typical response. The plots of all five samples for each type of foam are found in the appendix.

The stress-strain plots for KFOAML and KFOAML1 provide information about their energy absorbing behavior. Both plots are very rigid and taper off toward the end of

higher strain. The jaggedness of the curve is subdued by averaging five sample curves. This is not surprising since these two materials are much more brittle than the other samples.

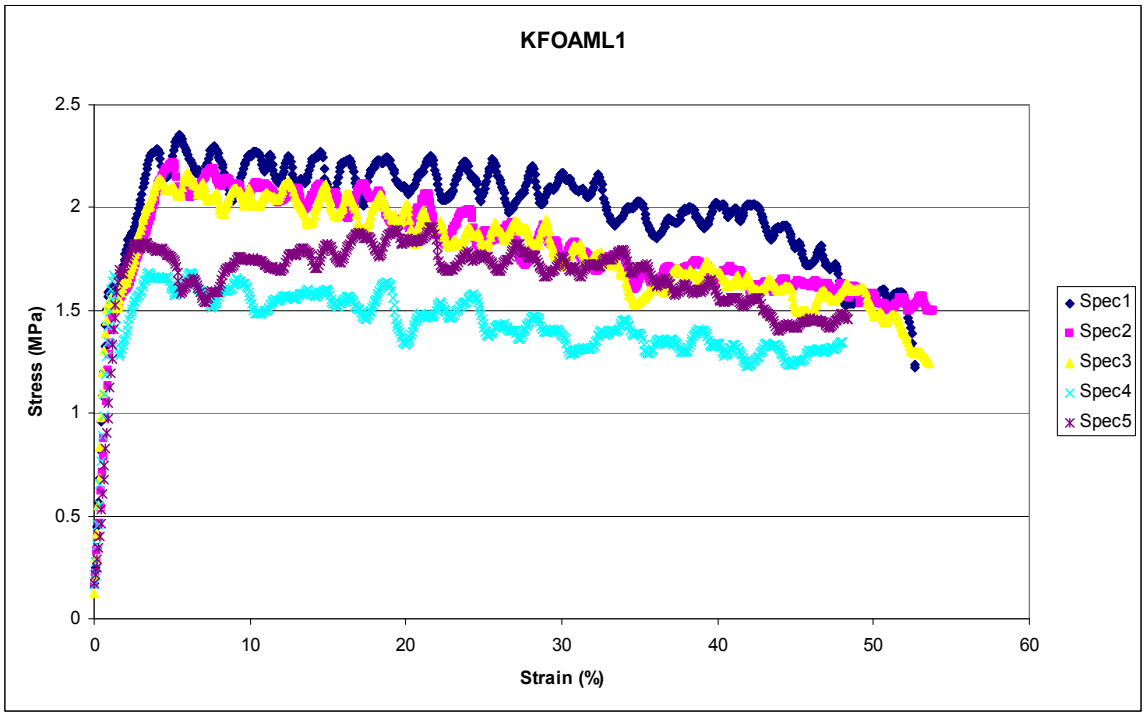

Figure 6.1 Stress-strain Plots for All Five KFOAML1 Samples

While the elastic portion of the stress-strain curve was very consistent from sample to sample, the stress path to 50% strain varies greatly. The stress path indicates KFOAML and KFOAML1 are somewhat brittle. Each peak and valley along the path shows when a cell wall fractured and allows the compression plates to move down. The peaks show when other cell walls take on the stress before failing. Although the overall curve creates a downward slope, a closer looks shows that sharp peaks and valley make up that slope.

KFOAMLF and KFOAMLF1 exhibit brittle failure patterns through the stress-strain curve. Neither material produced a clear yield stress since the stress increases after the first jump in strain. This is indicative of brittle failure. KFOAMLF and KFOAMLF1 have very large pores between cells. The peaks and valleys indicate not only the failure of sets of cell walls, but also the bending failure of the cells collapsing inside pores.

After each compression test with KFOAMLF and KFOAMLF1, the 2.54 cm (1") cube sample deteriorated to grains of material.

Stress-strain curves provide a great deal of information that can be used to evaluate the energy absorption of foam. As mentioned earlier, yield stress is directly proportional to strain rate. A different stress-strain curve exists for every strain rate. Therefore, low strain rate or compression tests will not directly provide the information necessary to choose foam for blast mitigation. However, low strain rate analysis provides information on the fundamental behavior of foam. Sometimes, the strength response can be extrapolated for high strain rate.

6.2 Impact Testing Discussion and Analysis

The impact test results provide additional information about the behavior of each type of foam. Clearly, polystyrene foam absorbs the least among the 2.54 cm (1") samples tested. Polystyrene foam exhibits different behavior than the rest of the samples since it is the only material to show elastic failure. Impact test results for polystyrene must consider that the impact sled bounced noticeable backward after collision. This reverse velocity cannot be accounted for by the velocity of the target mass.

Interestingly, the results of the impact tests did not follow what was expected based on the low strain rate compression testing. Based on the average strain energy density KFOAML should absorb the most energy during an impact; however results indicate that 8 lb. PU absorbed the most energy. Although the low rate testing method has historically provided reliable data, the results of impact testing should not be ignored. Previously, it was established that foam demonstrates a higher yield stress under higher strain rates. It was possible that 8 lb. PU experiences a higher change in yield stress than the carbon foams. This would explain the greater energy absorbed during impact testing. Unfortunately, it was not possible to provide the yield stress at this strain rate. Future tests will utilize an accelerometer (PCB 353B16, PCB Piezotronics, Depew, New York, USA) that will provide a better image for evaluating the behavior of foam during impact

tests. Chapter 7 describes this method. Table 6.1 compares the results of impact and compression tests.

Table 6.1 Foam Properties Comparison

	Modulus (MPa)	Yield Stress (MPa)	Average Strain Energy Density (MPa)	Percent Energy Absorbed or lost during Impact (%)
Polystyrene Foam	7.17	0.18	0.117	72.3%
KFOAMLF1	25.78	0.41	0.191	78.0%
KFOAML	173.18	3.90	1.390	80.0%
KFOAML1	165.57	1.85	0.885	81.0%
KFOAMLF	19.81	0.30	0.147	81.1%
8 lb. PU	29.29	1.25	0.590	82.9%

Table 6.1 shows a continuing trend with 5.08 cm (2") thick samples as found with 2.54 cm (1") samples. A 5.08 cm (2") thick sample of 8 lb. PU absorbed more energy than combinations of carbon foams and carbon foam with 8 lb. PU.

Despite the addition of 5.08 cm (2") of carbon foam, 2.54 cm (1") polystyrene foam samples dominated the behavior of two of the 7.62 cm (3") thick samples. Both samples with polystyrene foam absorbed less than 75% of the energy. Again, samples with 8 lb. PU absorbed more than others.

6.3 Blast Testing Discussion and Analysis

Among all the tests performed, blast testing were the most decisive when determining the ability for foam to protect concrete walls. Blast testing required the assistance of an explosion expert, Dr. Tom Thurman, and the labor of 6 people or more to set up samples, record data and clear debris. Since blast testing required such a large investment, only a select group of samples were tested. Sixteen blast tests were performed on the materials of interest.

As discussed earlier, photos were taken before, and immediately after the blast. Next, a photo was taken after the mock wall was tilted parallel with the ground to reveal cracks in

the mock wall. With this information, the blast test results fell into one of three categories: “Survived,” “Cracked,” or “Failed.” “Survived” indicated that the wall appeared the same before and after the blast and was structural sound. “Cracked” meant that some visible damage occurred on the surface of the wall but the wall remained mostly intact. “Failed” described a wall that broke into smaller pieces that spilled out when tipped over.

From the first three blasts, it was clear that the charge was capable of destroying the wall. The first three tests were an experimental control. Drywall, a double layer of drywall and drywall with a steel face, all failed decisively. The steel faced sample provided an interesting look at the dynamics of an explosion. The 16 gage (0.0598 inch or 0.235 mm) steel could neither absorb the energy of the blast nor deflect the pressure wave, resulting in the destroyed wall. The 1.27 cm (1/2”) thick steel that provided the backstop for the mock walls, deflected the pressure wave from the blast. This allows only the 30.48 cm (1’) square section to experience the blast pressure.

Nine of the sixteen tests resulted in “Cracked” or “Survived” results. The five “Survived” walls were covered with 3 – 2.54 cm (1”) samples, starting with 4 lb. PU and 8 lb. PU with nonflammable additives. Next, carbon foam faced with drywall finished the protective layer. The remaining “Cracked” walls were combinations of 2 – 2.54 cm (1”) samples faced with drywall. Table 5.2 clearly illustrated this information

Static compression tests determined the yield stress at the weakest part of a cinder block to be about 6.9 MPa (1000 psi). In general, foam samples must absorb enough energy so that the pressure reaching the concrete wall was less than 6.9 MPa (1000 psi).

The “Cracked” walls showed some visible damage but remained structurally sound when tipped over. The first “Cracked” wall sample was particularly interesting. A single 2.54 cm (1”) thick square foot of polystyrene foam faced with drywall protected the wall from serious damage. Moreover, from the images in the appendix it is clear that the polyurethane itself survived the explosion and evidence of the center of the blast was

seen on the polystyrene foam sample. Strangely, a wall protected by polystyrene foam, 8 lb. Ceno, and KFOAML1 was destroyed in another test. It was likely that the survival of the mock wall when protected only with polystyrene foam and drywall can be attributed to experimental error. That particular mock wall was probably constructed differently than other walls. Also, it is possible that the explosive charge moved away from the mock wall during the polystyrene foam test since the charge was suspended in air and was susceptible to wind.

Discovering that 7.62 cm (3") foam layers protected the mock wall best concurred with blast testing studies at the Ben Gurion University. Their findings suggested that at least 7.62 cm (3") of aluminum foam would be needed to protect concrete structures. Although, carbon and polyurethane based foams have different properties than aluminum foam, the assertion that a layer of foam greater than 2.54 cm (1") or 5.08 cm (2") was needed to protect concrete structures alludes to the mechanics of pressure wave mitigation by foam. Chapter 7 discusses further study in this area.

In general, 5.08 cm (2") protective layers did not mitigate the pressure wave from a blast enough to protect the wall. One 7.62 cm (3") sample, 4 lb. UFA, 8 lb. UFA and KFOAMLF1, failed. This failure can be attributed to the low yield strength and brittleness of KFOAMLF1.

The behavior of hybrid composite layered foam samples was discussed at length in Chapter 3. In high strain rate tests, composite foam layered samples exhibited the behavior of the layer facing the impact first. This phenomenon provided the rational for selecting layers of carbon foam followed by a medium density and low density polyurethane based foam. Carbon foam was selected as the front of composite sample because it can offer protection against chemicals, radiation and electromagnetic interference unlike 16 lb. PU that exhibits similar strength. Carbon foam mitigated the initial pressure of the blast. Once this initial mitigation takes place, the lower density layers were crushed and the mock wall was protected.

During the sixth blast, the blast pressure impacted a hybrid composite layered foam sample made of 4 lb. Ceno, 8 lb. Ceno, KFOAML, and drywall. Damage to the front carbon foam layer was evident and the low density 4 lb. Ceno sample was crushed as shown in Figure 3.19. This result alluded to the progress of the blast pressure wave through the composite layered sample. The concrete wall survived during this blast. Hybrid composite foam layered samples with carbon foam as a face followed by low density polyurethane layers frequently protected the mock wall. This pattern indicated a protective mechanism where the blast wave was attenuated by the failure of the carbon foam and the remaining pressure wave was mitigated by the weaker foam.

6.4 Simulated Blast Test Discussion and Analysis

Once the blast testing was performed, a mock wall was built at the end of the impact tester to establish whether the 8.81 m/s (28.9 ft/s) impact collision could simulate the destruction of a blast. All the samples tested during blasting were repeated using the impact tester. Results from the impact and blast tests were categorized as “Intact,” “Cracked,” or “Broken.” “Intact” indicates that after the impact the cinder block wall showed no signs of damage. “Cracked” describes when the blocks endure some visible damage but remained structurally sound. Finally, the description “Broken” means the wall was destroyed and broke into smaller pieces. Table 5.3 summarizes these results.

The blast and impact comparison results are encouraging. In every case except two, the impact test result matched that of the blast testing. From a practical standpoint, this shows that impact tests, which are less expensive and can be performed quickly, may be used to roughly predict the effects of a small blast. Earlier the pressure resulting from impact was found to be 12.9 MPa (1871 psi) and the pressure from blast was calculated as 140.9 MPa (20,426 psi).

The two cases that did not match were the 4 lb. UFA, 8lb. UFA, and KFOAMLF1 and 8lb. Ceno & KFOAMLF1 samples. In both cases, the mock wall remained intact during the impact test but failed during the explosion. This can be attributed to the energy absorbing quality of different samples of the same type of foam. As mentioned earlier,

each batch of foam developed a different cellular structure; therefore no two samples have the same exact structural properties. In the same way, each mock wall has different characteristics. Since some inherent inconsistency exists in the material properties, some experimental error is inevitable.

Chapter 7 Concluding Remarks

7.1 Project Summary

The need to uncover materials capable of preventing catastrophic damage to buildings and loss of life in the event of an explosion motivated this project. This need, combined with desire to reveal the full potential of a novel material, carbon foam, motivated this study. Project requirements determined what materials would be tested. Carbon foam was compared to polyurethane foam of different densities mixed with flame retardant coal combustion by-products. Polyurethane-based samples were tested for flammability and compared to carbon foam and polystyrene foam.

Background research of energy absorption by cellular solids and blast testing revealed a rich history of material research and testing methods. The work of Lorna J. Gibson and Michael F. Ashby provided the backbone for understanding the fundamentals of cellular solids. Previous energy absorption research was reviewed. One project at the Ben Gurion University stood out for its similarity in scope and objective.[2, 6, 8]

Two foam mechanical characteristics guided the selection and construction of samples for blast testing. First, the response of hybrid composite layered foam samples was determined by the layer of foam facing the blast. Therefore, strong carbon foam was selected to absorb the brunt of the blast as the top layer and protect against other threats such as chemicals and radiation. Second, gas released during the formation of foam results in the development of elongated pores in the material. Foam samples showed the greatest yield strength along the major axis of these pores.

Since the strength and energy absorbing characteristics are determined by the material and cell structure, the project aimed to test both. Each material of interest was examined under a microscope to provide an image of the basic cell structure. Since foam yield stress varied with strain rate, the foam samples were tested in three strain rate regimes.

Low strain rate or compression testing provided a view of the material behavior of each sample. Yield stress, elasticity and energy absorption at low strain rate were obtained. Next, middle strain rate or impact testing was performed. This allowed the energy absorption of each sample to be compared with an impact of about 9 m/s (29.3 ft/s). High strain rate or blast testing revealed whether samples would successfully protect a concrete wall during an explosion. Finally, impact tests were repeated to correlate the results from impact and blast testing.

The results of all tests and investigations were analyzed and summarized. Several points were determined. Polystyrene foam and polyurethane foam cannot offer the necessary flame resistance for blast protection. Polyurethane foam mixed with coal combustion by-products, cenospheres and ultra-fine fly ash, are noticeably more resistant to flame than polyurethane alone. In general, a layer of protection of at least 7.62 cm (3") is needed to protect a concrete cinder block wall from a small blast. The most effective samples tested included a base layer of 4 lb. polyurethane with either UFA or cenospheres, followed by 8 lb. polyurethane with either UFA or cenospheres and a carbon foam KFOAML or KFOAML1 face.

Repeating impact tests with samples identical to blast testing revealed nearly the same results. In the future, impact tests may offer a quicker and cheaper method for determining whether a type of foam is a good candidate for blast protection.

7.2 Future work

The Carbon Group at the Center for Applied Energy Research (CAER) continues to work with carbon foam. Modifying the foam to protect buildings and vehicles from flying debris will be the next step of the project. CAER will investigate a number of coatings to protect the foam from debris and the elements.

Additional steps could be made to improve the impact tester as a measuring tool. Recently, an accelerometer (PCB 353B16, PCB Piezotronics, Depew, New York, USA)

and data acquisition device and software (NI 9233 Data Acquisition Device and LabView Signal Express, National Instruments, Austin, Texas, USA) were acquired to measure the deceleration impulse experienced during an impact. This device measures the force experienced by the impact sled during collision at 10,000 data points per second. The accelerometer should prove useful in quantifying impact test results. [28] Other impact testing methods may be considered as well. Modifying the impact sled device so that different velocities could be achieved at collision would enhance the capabilities of this tool.

Increasing the fundamental understanding of foam would be a completely different direction for the future of this project. As mentioned before, foam behavior is determined by cellular geometry and the material making up the foam. Recent advances in studying micro-scale parameters may help advance the understanding of foam mechanics.

The evidence from this study that at least 7.62 cm (3") thick foam samples were needed to mitigate the effect of a blast suggests that further investigation in the mitigation of pressure wave by cellular solids may offer an optimum cellular structure. A great deal of literature exists on the mitigation of sound waves by different types of foam. A similar approach could be performed with pressure waves from a blast.

Similarly, the behavior of foam under high strain impacts has been understood largely through empirical observations. The actual material mechanics that cause foam to have a higher yield stress at higher strain rates is not well documented. Studying the change of material properties at high strain rates would help unlock the phenomena of time dependent material properties.

Appendix

A) Compression Testing Stress-strain Plots for All Specimens

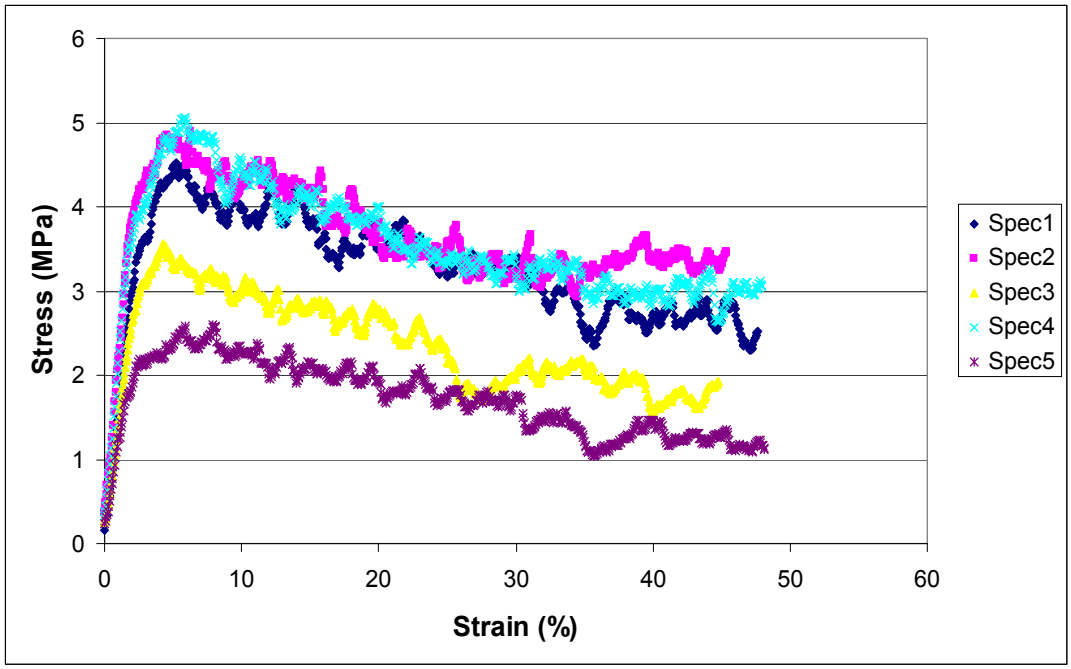

Figure A.1 Stress-strain Curves of KFOAML Specimens

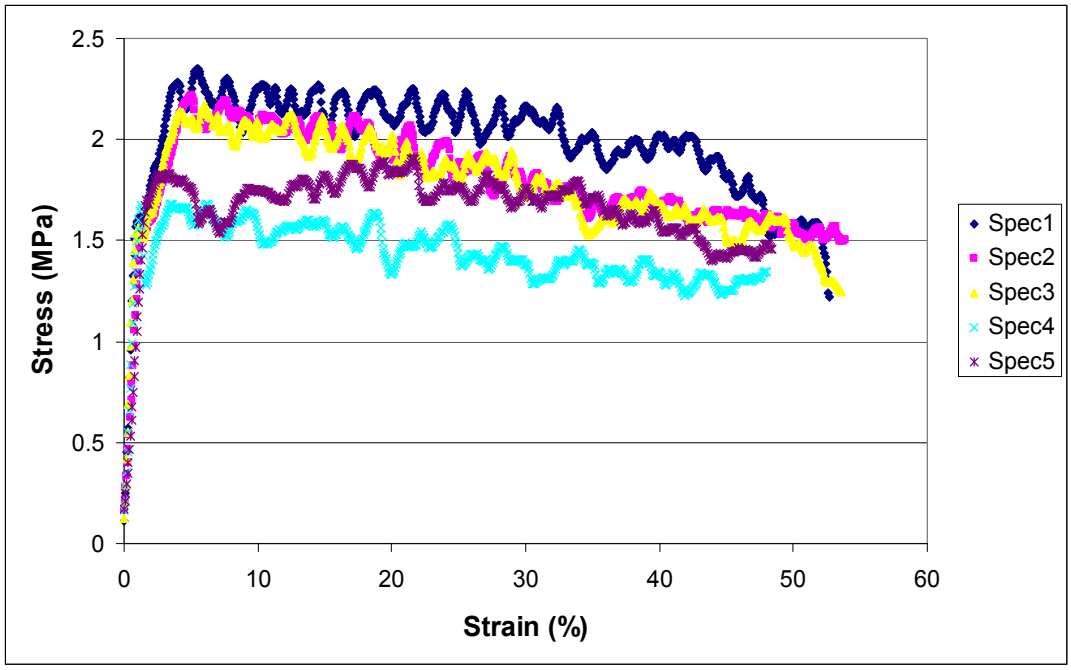

Figure A.2 Stress-strain Curves of KFOAML1 Specimens

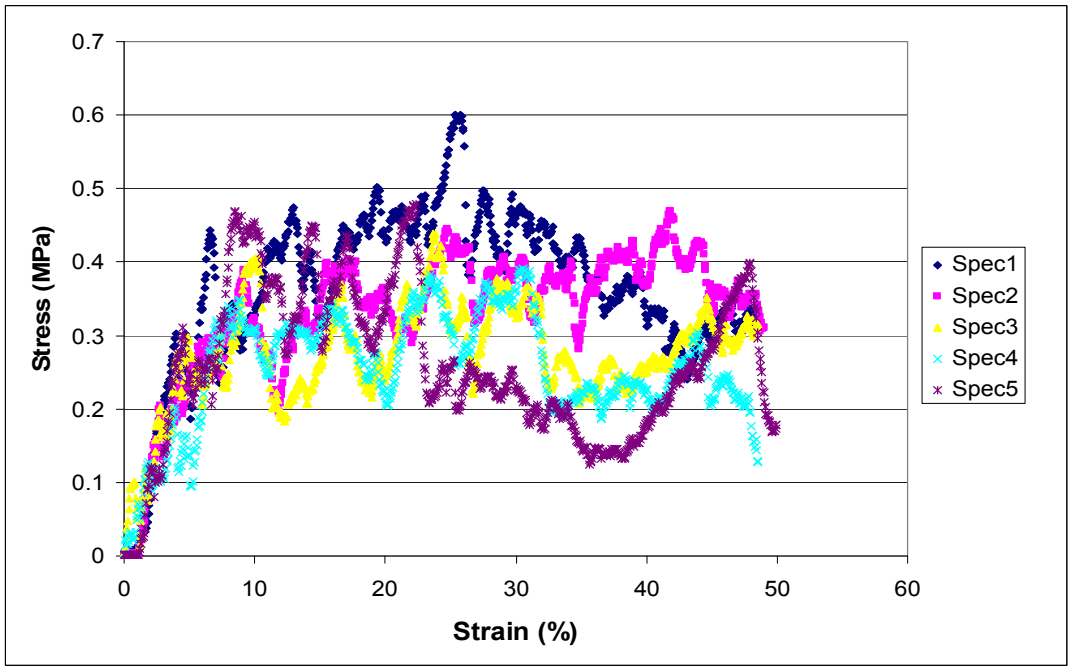

Figure A.3 Stress-strain Curves of KFOAMLF Specimens

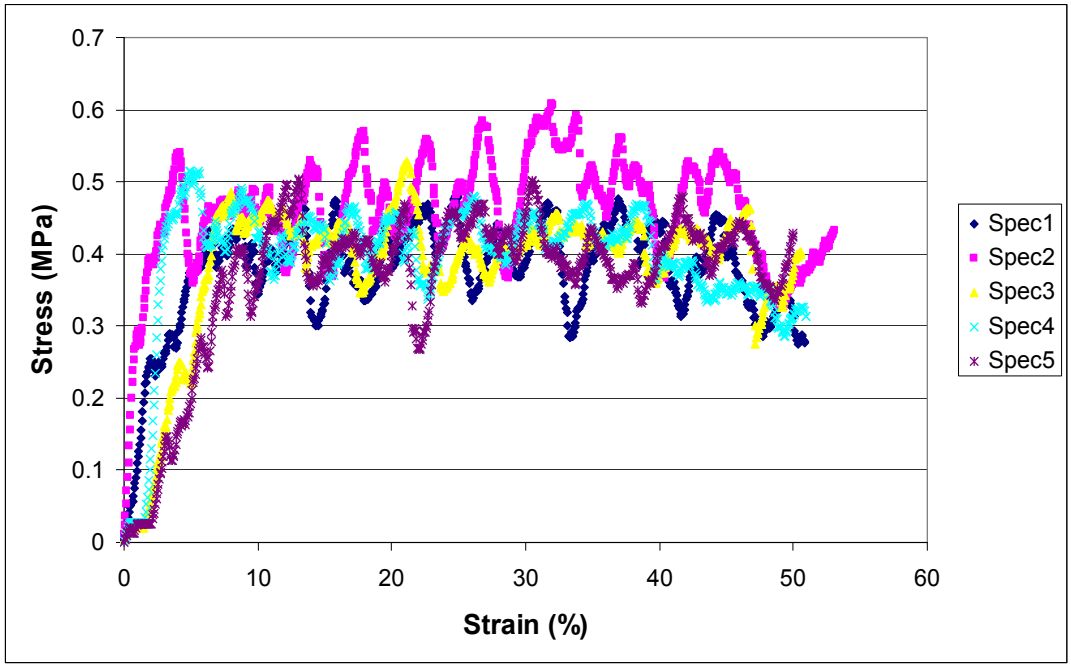

Figure A.4 Stress-strain Curves of KFOAMLF1 Specimens

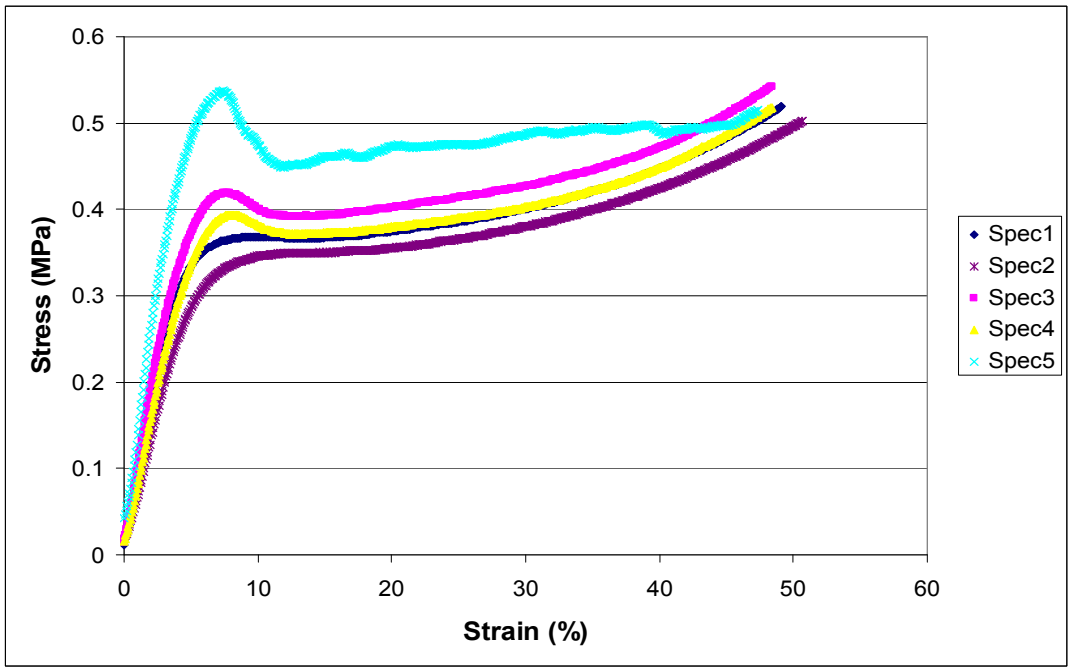

Figure A.5 Stress-strain Curves of 4 lb. PU Specimens

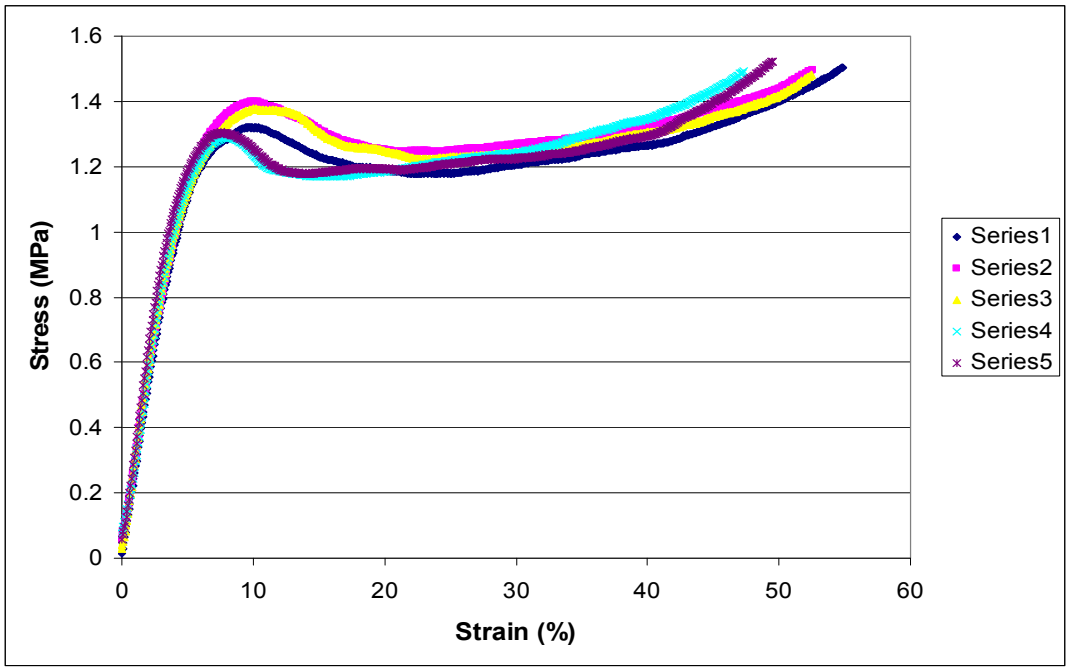

Figure A.6 Stress-strain Curves of 8 lb. PU Specimens

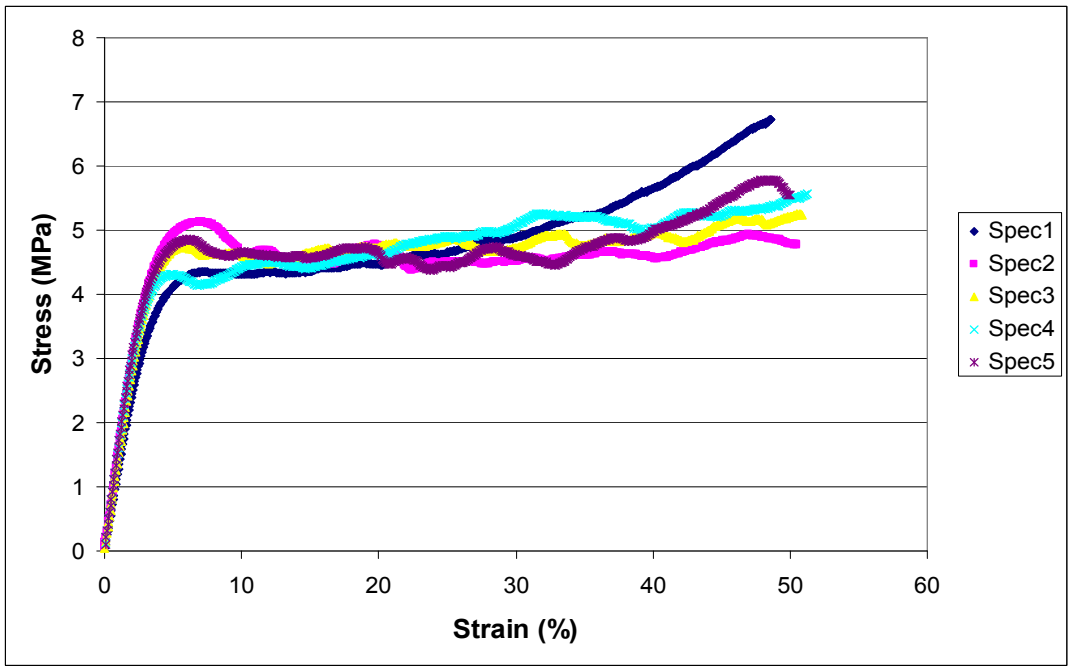

Figure A.7 Stress-strain Curves of 16 lb. PU Specimens

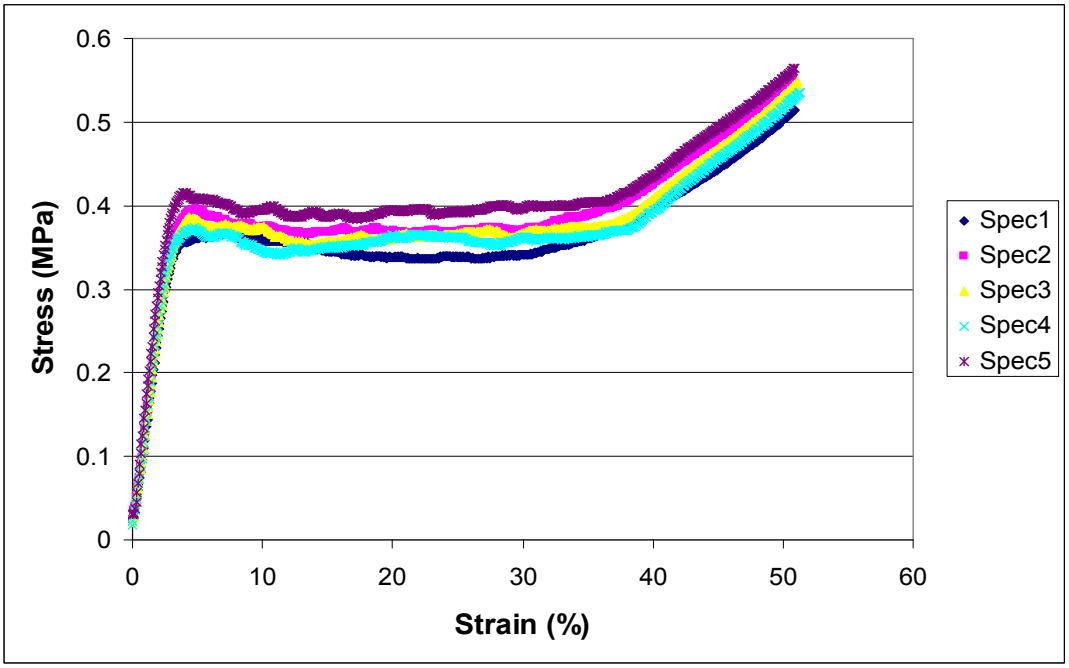

Figure A.8 Stress-strain Curves of 4 lb. Ceno Specimens

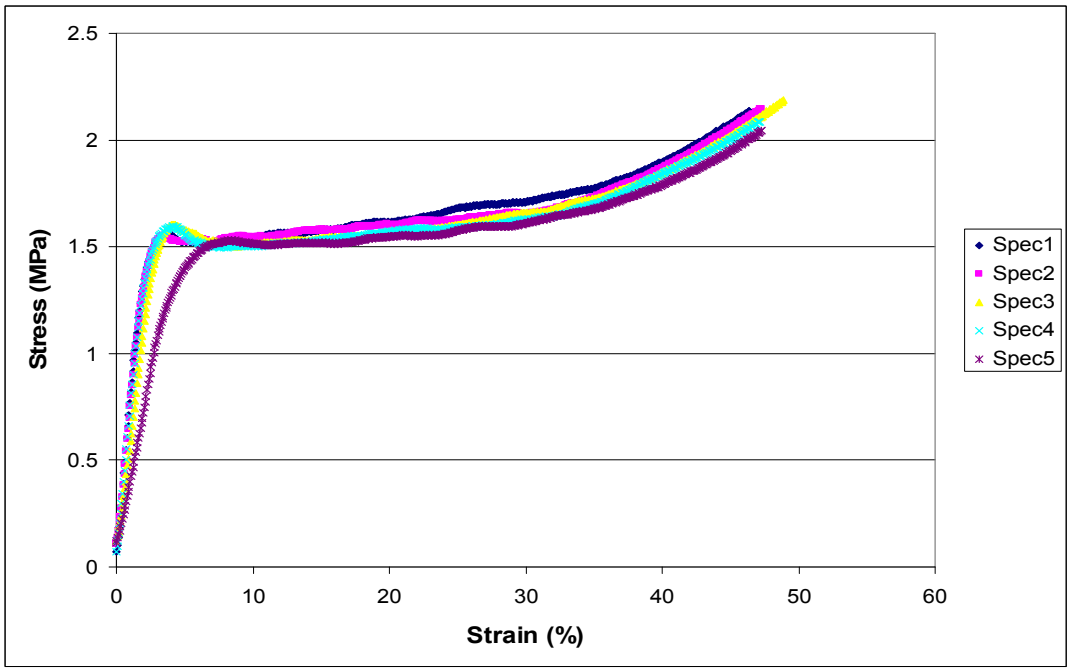

Figure A.9 Stress-strain Curves of 8 lb. Ceno Specimens

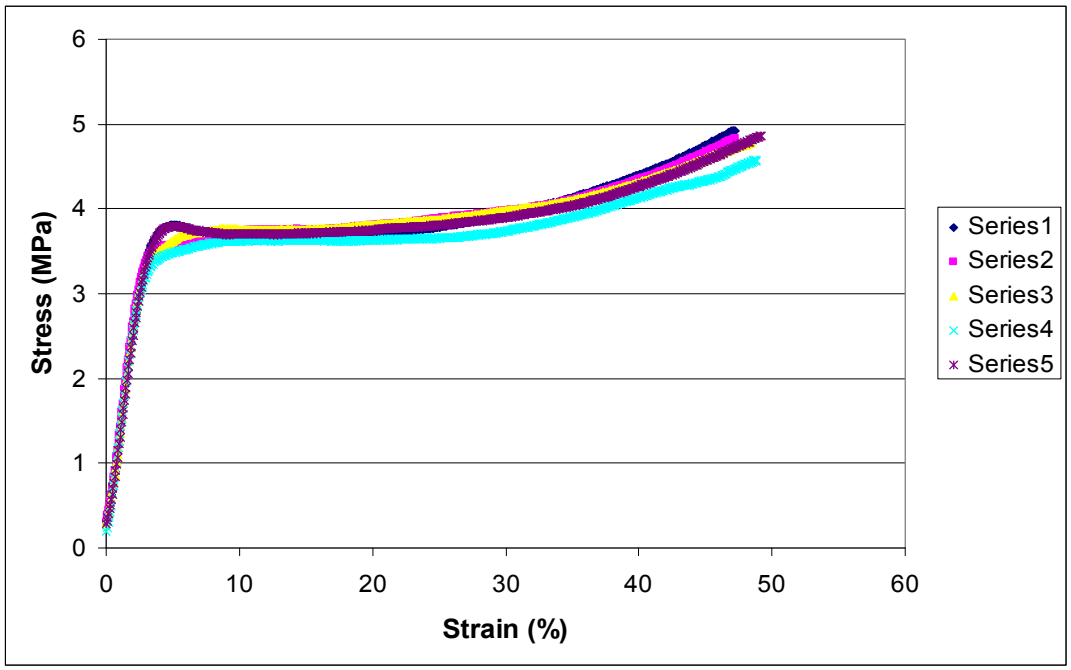

Figure A.10 Stress-strain Curves of 16 lb. Ceno Specimens

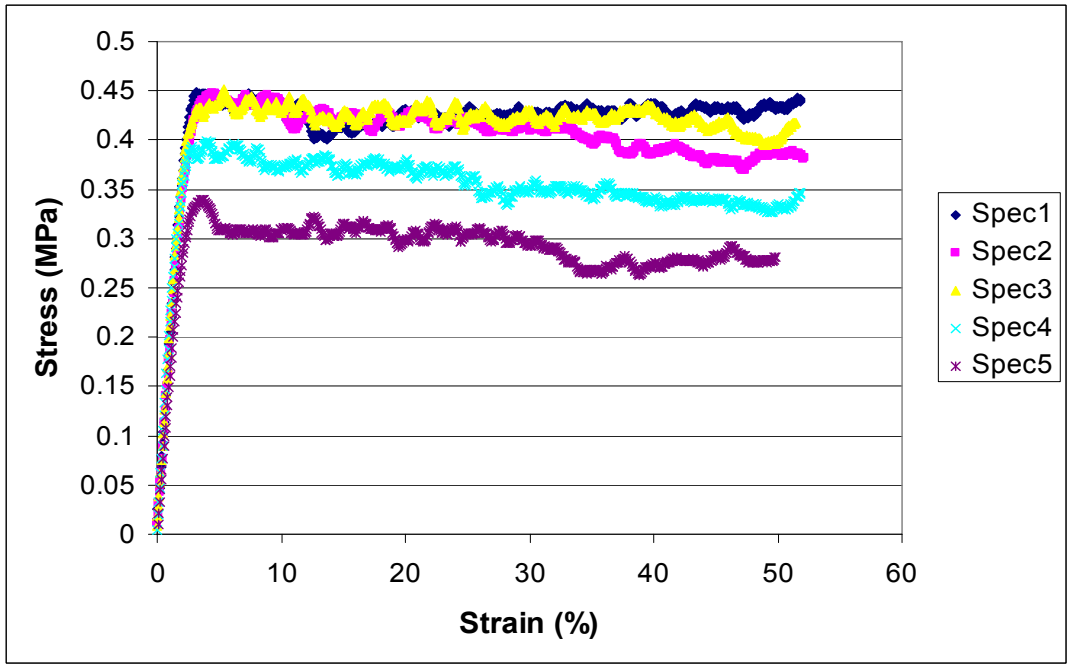

Figure A.11 Stress-strain Curves of 4 lb. UFA Specimens

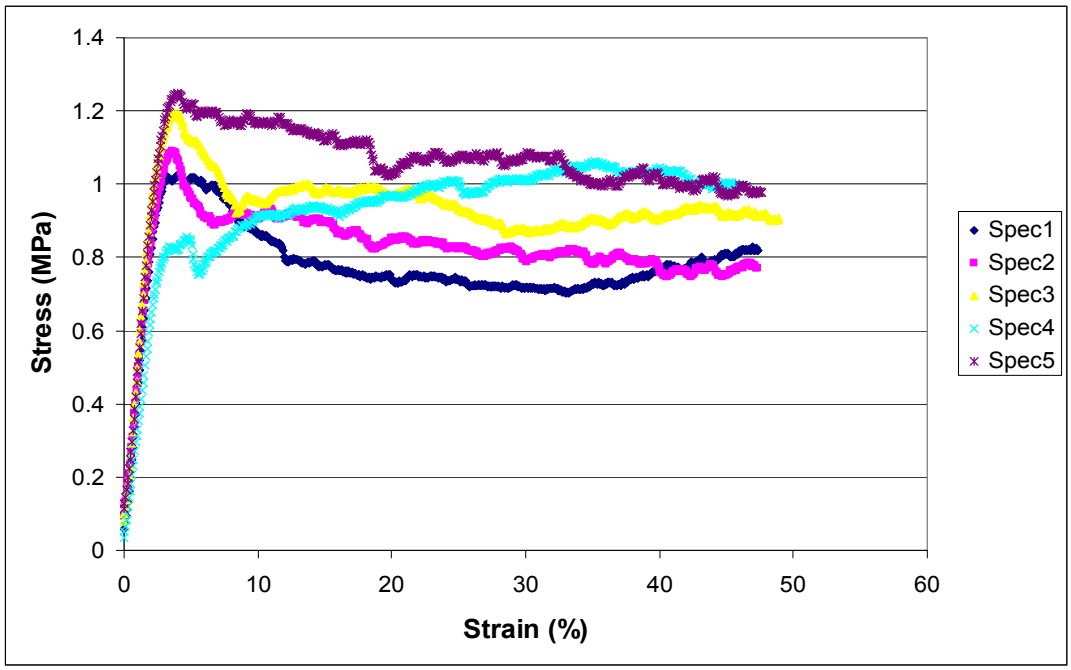

Figure A.12 Stress-strain Curves of 8 lb. UFA Specimens

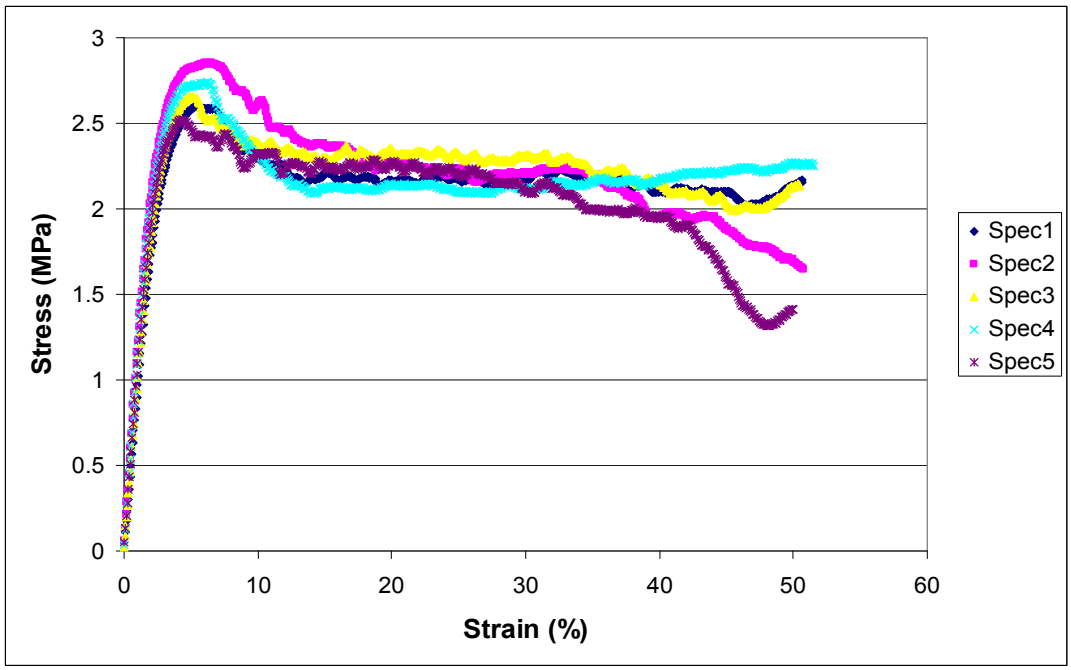

Figure A.13 Stress-strain Curves of 16 lb. UFA Specimens

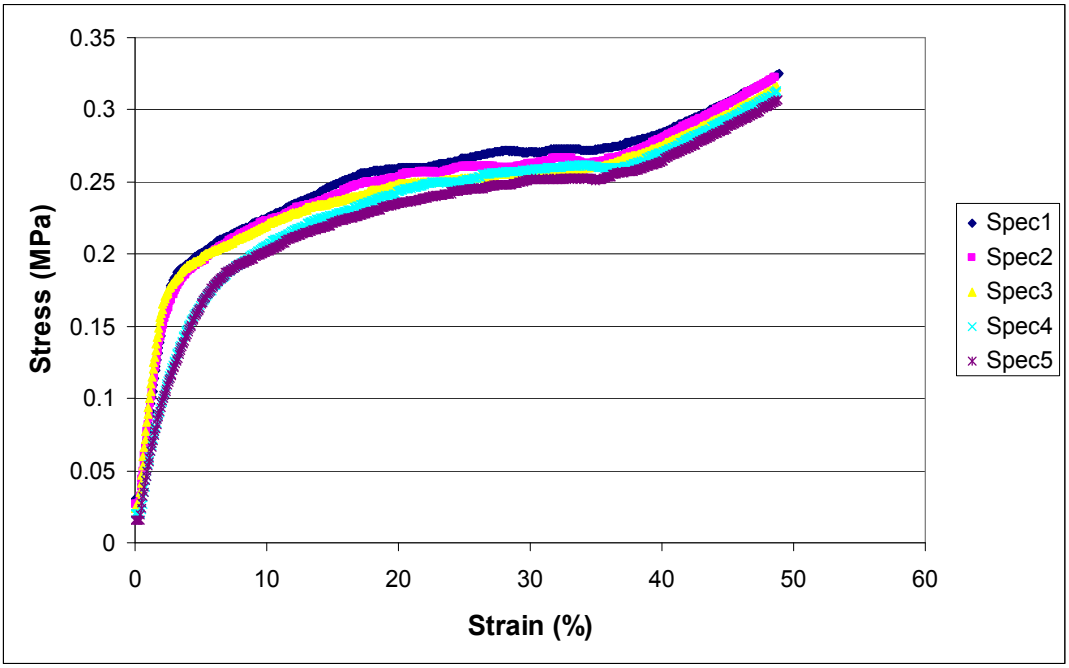

Figure A.14 Stress-strain Curves of Polystyrene Foam Specimens

B) Compression Testing Data for All Specimen

Table B.1 KFOAML Compression Test Data

Specimen Name	Modulus (MPa)	Yield Stress (MPa)
KFOAML - 1	163.2	4.31
KFOAML - 2	214.7	4.81
KFOAML - 3	145.0	3.53
KFOAML - 4	215.9	4.63
KFOAML - 5	127.0	2.24
Average	173.2	3.90
Standard Deviation	40.54	1.05

Table B.2 KFOAML1 Compression Test Data

Specimen Name	Modulus (MPa)	Yield Stress (MPa)
KFOAML1 - 1	199.0	2.07
KFOAML1 - 2	131.8	1.91
KFOAML1 - 3	217.2	1.87
KFOAML1 - 4	167.1	1.59
KFOAML1 - 5	112.7	1.81
Average	165.6	1.85
Standard Deviation	43.92	0.18

Table B.3 KFOAMLF Compression Test Data

Specimen Name	Modulus (MPa)	Yield Stress (MPa)
KFOAMLF - 1	19.40	0.241
KFOAMLF - 2	14.69	0.209
KFOAMLF - 3	25.74	0.260
KFOAMLF - 4	16.42	0.336
KFOAMLF - 5	22.81	0.440
Average	19.8	0.297
Standard Deviation	4.53	0.092

Table B.4 KFOAMLF1 Compression Test Data

Specimen Name	Modulus (MPa)	Yield Stress (MPa)
KFOAMLF - 1	19.35	0.269
KFOAMLF - 2	37.29	0.475
KFOAMLF - 3	15.87	0.436
KFOAMLF - 4	40.61	0.509
KFOAMLF - 5	15.77	0.376
Average	25.8	0.413
Standard Deviation	12.17	0.094

Table B.5 4 lb. PU Compression Test Data

Specimen Name	Modulus (MPa)	Yield Stress (MPa)
4 lb. PU - 1	8.09	0.357
4 lb. PU - 2	6.98	0.325
4 lb. PU - 3	9.73	0.406
4 lb. PU - 4	7.85	0.387
4 lb. PU - 5	13.39	0.513
Average	9.21	0.398
Standard Deviation	2.54	0.071

Table B.6 8 lb. PU Compression Test Data

Specimen Name	Modulus (MPa)	Yield Stress (MPa)
8 lb. PU - 1	27.27	1.231
8 lb. PU - 2	28.87	1.283
8 lb. PU - 3	30.23	1.226
8 lb. PU - 4	28.28	1.252
8 lb. PU - 5	31.79	1.255
Average	29.29	1.249
Standard Deviation	1.76	0.023

Table B.7 16 lb. PU Compression Test Data

Specimen Name	Modulus (MPa)	Yield Stress (MPa)
16 lb. PU - 1	126.4	4.181
16 lb. PU - 2	150.2	4.997
16 lb. PU - 3	143.9	4.724
16 lb. PU - 4	160.9	4.298
16 lb. PU - 5	162.1	4.741
Average	148.7	4.588
Standard Deviation	14.6	0.339

Table B.8 4 lb. Ceno Compression Test Data

Specimen Name	Modulus (MPa)	Yield Stress (MPa)
4 lb. Ceno - 1	12.56	0.360
4 lb. Ceno - 2	13.03	0.394
4 lb. Ceno - 3	12.95	0.382
4 lb. Ceno - 4	13.67	0.373
4 lb. Ceno - 5	16.08	0.409
Average	13.66	0.384
Standard Deviation	1.41	0.019

Table B.9 8 lb. Ceno Compression Test Data

Specimen Name	Modulus (MPa)	Yield Stress (MPa)
8 lb. Ceno - 1	76.77	1.550
8 lb. Ceno - 2	73.16	1.529
8 lb. Ceno - 3	56.83	1.584
8 lb. Ceno - 4	74.37	1.596
8 lb. Ceno - 5	36.64	1.472
Average	63.55	1.546
Standard Deviation	16.98	0.049

Table B.10 16 lb. Ceno Compression Test Data

Specimen Name	Modulus (Mpa)	Yield Stress (MPa)
16 lb. Ceno - 1	129.6	3.807
16 lb. Ceno - 2	133.5	3.566
16 lb. Ceno - 3	131.5	3.592
16 lb. Ceno - 4	132.3	3.463
16 lb. Ceno - 5	127.0	3.802
Average	130.8	3.646
Standard Deviation	2.6	0.153

Table B.11 4 lb. UFA Compression Test Data

Specimen Name	Modulus (MPa)	Yield Stress (MPa)
4 lb. UFA - 1	19.65	0.443
4 lb. UFA - 2	18.48	0.448
4 lb. UFA - 3	20.53	0.435
4 lb. UFA - 4	21.52	0.395
4 lb. UFA - 5	16.63	0.334
Average	19.36	0.411
Standard Deviation	1.89	0.048

Table B.12 8 lb. UFA Compression Test Data

Specimen Name	Modulus (MPa)	Yield Stress (MPa)
8 lb. UFA - 1	43.87	1.016
8 lb. UFA - 2	45.41	1.031
8 lb. UFA - 3	49.90	1.168
8 lb. UFA - 4	32.18	0.855
8 lb. UFA - 5	47.75	1.210
Average	43.82	1.056
Standard Deviation	6.90	0.140

Table B.13 16 lb. UFA Compression Test Data

Specimen Name	Modulus (MPa)	Yield Stress (MPa)
16 lb. UFA - 1	97.0	2.551
16 lb. UFA - 2	117.0	2.784
16 lb. UFA - 3	101.0	2.641
16 lb. UFA - 4	119.3	2.689
16 lb. UFA - 5	110.5	2.515
Average	108.9	2.636
Standard Deviation	9.76	0.108

Table B.14 Polystyrene Foam Compression Test Data

Specimen Name	Modulus (MPa)	Yield Stress (MPa)
Polystyrene Foam- 1	7.893	0.197
Polystyrene Foam - 2	8.229	0.190
Polystyrene Foam - 3	9.304	0.192
Polystyrene Foam - 4	5.201	0.169
Polystyrene Foam - 5	5.207	0.169
Average	7.167	0.183
Standard Deviation	1.866	0.013

C) Blast Testing Photographs

Figure C.1.a, b , c, d Blast 1 – Drywall Only (Clockwise from upper left) (a) Front of dry wall only sample before blast test; (b) C4 charge positioned in front of the foam sample held in position by tape; (c) Front of foam sample immediately after blast; (d) Mock wall condition after foam sample and steel plate were removed.

Figure C.2.a, b, c, d Blast 2 - Drywall & Drywall (Clock-wise from upper left) (a) Front of two layers of drywall before blast test; (b) Front of foam sample immediately after blast; (c) Condition of mock wall after removing foam sample and steel plate.

Figure C.3.a, b, c, d Blast 3 - Drywall & Drywall & 16 Ga. Steel (Clock-wise from upper left) (a) C4 charge positioned with tape in front of two layers of drywall and a 16 gage sheet of steel before blast; (b) Condition of foam sample immediately after blast; (c) Front of mock wall after blast and after wall was tilted parallel with ground; (d) Appearance of mock wall after foam sample and steel plate are removed. Some adhesive is visible.

Figure C.4.a, b, c, d, e Blast 4 - Polystyrene foam & Drywall & Drywall (Clockwise from upper left) (a) Front of two layers of drywall and one layer of polystyrene foam before blast, (b) Foam front immediately after blast, (c) Mock wall condition after foam sample and steel plate are removed. Some adhesive is visible, (d) Up close view of mock wall shows cracks in concrete blocks.

Figure C.5.a, b, c, d, e Blast 5 - 4lb.Ceno & 8lb.Ceno & KFOAML1 (Clockwise from upper left) (a) Front of foam sample before blast; (b) Front of foam sample immediately after blast; (c) Front of foam sample and steel plate after blast. Some adhesive is visible; (d) Thickness of entire hydbrid composite sample. Area of blast damage was clearly off center.

Figure C.6.a, b, c, d Blast 6 - 4lb.Ceno & 8lb.Ceno & KFOAML (Clockwise from upper left) (a) Front of foam sample before blast; (b) Front of mock wall immediately after blast. Some adhesive is visible; (c) Side view of foam sample remains after blast; (d) Front of mock wall after blast and after removing foam sample and steel plate.

Figure C.7.a, b, c, d, e Blast 7 - 4lb.Ceno & 8lb.UFA & KFOAML (Clockwise from upper left) (a) Front of foam sample before blast; (b) Front of mock wall immediately after blast. Some adhesive is visible; (c) Condition of composite hybrid foam sample after blast; (d) Front of mock wall after removing foam sample and steel plate; (e) Up close view of mock wall area behind foam sample after blast.

Figure C.8.a, b, c, d Blast 8 - 4lbCeno & 8lbUFA & KFOAML1 (Clockwise from upper left) (a) Front of foam sample before blast; (b) Front of foam sample after blast; (c) Front of mock wall after removing foam sample and steel plate. Some adhesive is visible; (d) Front of mock wall after blast.

Figure C.9.a, b, c, d Blast 9 - 4lb.UFA & 8lb.UFA & KFOAMLF (Clockwise from upper left) (a) Front of foam sample before blast; (b) Condition of experimental set-up area after 9 blasts; (c) Front of mock wall after foam sample and steel plate are removed after blast; (d) Front of mock wall after blast.

Figure C.10.a, b, c, d Blast 10 -4lb.UFA & 8lbUFA & KFOAMLF1 (Clockwise from upper left) (a) Front of foam sample before blast, (b) Front of mock wall after blast; (c) Front of mock wall after foam sample and steel plate are removed after blast; (d) Front of mock wall after was tilted parallel with the ground.

Figure C.11.a, b, c, d Blast 11 - Polystyrene & 8lb.Ceno & KFOAML1 (Clockwise from upper left) (a) Side view of front of foam sample before blast; (b) Front of mock wall after blast; (c) Front of mock wall after foam sample and steel plate were removed after blast; (d) Front of mock wall after blast after wall was tilted parallel with ground.

Figure C.12.a, b, c, d Blast 12 - 4lb. UFA & KFOAML1 (Clockwise from upper left) (a) Front of foam sample before blast; (b) Front of mock wall after blast; (c) Front of mock wall after blast.

Figure C.13.a, b, c, d Blast 13 - 4lb.UFA & KFOAML (Clockwise from upper left) (a) Front of foam sample before blast; (b) Front of mock wall after blast; (c) Front of mock wall up close after foam sample and steel plate are removed after blast; (d) Front of mock wall after blast.

Figure C.14.a, b, c, d, e, f Blast 14 - 8lb.Ceno & KFOAML1 (Clockwise from upper left) (a) Front of foam sample before blast; (b) Front of mock wall before blast; (c) Front of mock wall after blast; (d) Mock wall after tilting parallel with ground after blast; (e) Front of mock wall immediately after blast; (f) Front of foam sample immediately after blast.

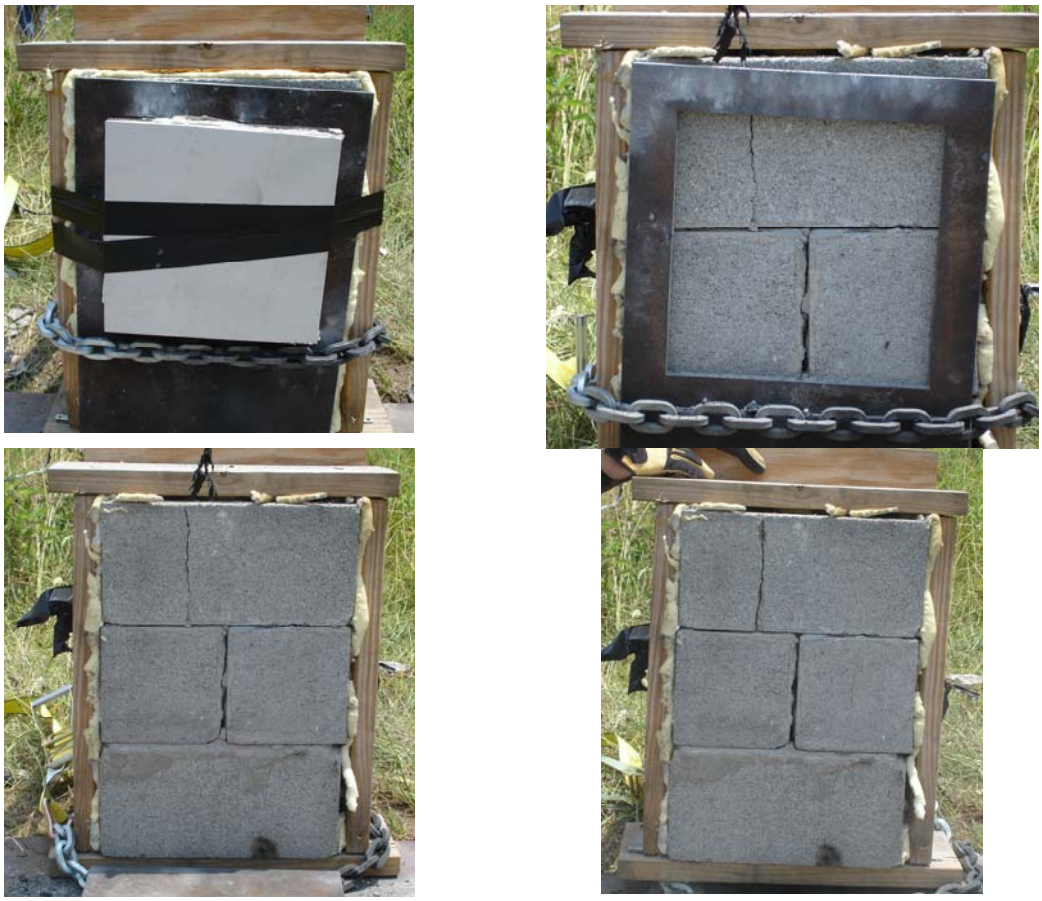

Figure C.15.a, b, c, d Blast 15 - 8lb. Ceno & KFOAMLF1 (Clockwise from upper left) (a) Front of foam sample before blast; (b) Front of mock wall immediately after blast; (c) Front of mock wall after tilting parallel with the ground after blast; (d) Front of mock wall immediately after blast.

Figure C.16.a, b, c, d Blast 16 - 8lb.Ceno & 4lb.Ceno (Clockwise from upper left) (a) Front of foam sample before blast; (b) Front of mock wall after blast. Some adhesive is visible; (c) Front of mock wall up close after blast; (d) Front of mock wall after tilting parallel with ground after blast.

Bibliography

[1] Chertoff MaM, J. H. III. The National Plan for Research and Development In Support of Critical Infrastructure Protection. In: Policy DoHSaOoSaT, ed. Washington, DC 2004.

[2] Schenker A, Anteby I, Nizri E, Ostraich B, Kivity Y, Sadot O, et al. Foam-Protected Reinforced Concrete Structures under Impact: Experimental and Numerical Studies. Journal of Structural Engineering. 2005;131:1233.

[3] [cited; Available from: **www.koppers.com**

[4] Klett J. ORNL High Conductivity Graphite Foams. Oak Ridge National Laboratory 2003.

[5] Çengel YA, Boles MA. Thermodynamics: an engineering approach: McGraw-Hill 2002.

[6] Gibson LJ, Ashby MF. Cellular Solids: Structure and Properties: Cambridge University Press 1997.

[7] Paul A, Ramamurty U. Strain rate sensitivity of a closed-cell aluminum foam. Materials Science & Engineering A. 2000;281(1-2):1-7.

[8] Sadot O, Anteby I, Harush S, Levintant O, Nizri E, Ostraich B, et al. Experimental Investigation of Dynamic Properties of Aluminum Foams. Journal of Structural Engineering. 2005;131:1226.

[9] Jang BZ, Chen LC, Wang CZ, Lin HT, Zee RH. Impact Resistance and Energy Absorption Mechanisms in Hybrid Composites. Compos Sci Technol. 1989;34(4):305-35.

[10] Kaiser MA. Advancements in the split Hopkinson bar test. *VPI & SU Mechanical Engineering MS 1998*. [Blacksburg, Va.: University Libraries, Virginia Polytechnic Institute and State University 1998.

[11] Lee S. Dynamic failure of blast-resistant structures subjected to impulsive loading [Thesis (Ph D , Mechanical Engineering)]: Northwestern University, 2006.

[12] Mukai T, Kanahashi H, Higashi K, Miyoshi T, Mabuchi M, Nieh TG. Experimental study of energy absorption in a close-celled aluminum foam under dynamic loading. Scripta Materialia(USA). 1999;40(8):921-7.

[13] Medding JA, Love BJ. Evaluation of collisional damage in polystyrene foam constructions using a dual hammer impact test. Polymer Engineering & Science. 1996;36(9):1286-9.

[14] Ramachandra S, Sudheer Kumar P, Ramamurty U. Impact energy absorption in an Al foam at low velocities. Scripta Materialia. 2003;49(8):741-5.

[15] Tan PJ, Reid SR, Harrigan JJ, Zou Z, Li S. Dynamic Compressive Strength Properties of Aluminium Foams. Part 11-'Shock'model and Comparison with Experimental Data. J Mech Phys Solids. 2005;53:2206-30.

[16] Akay M, Hanna R. A comparison of honeycomb-core and foam-core carbon-fibre/epoxy sandwich panels. Composites. 1990;21:325-31.

[17] Reid SR, Peng C. Dynamic uniaxial crushing of wood. International Journal of Impact Engineering. 1997;19(5-6):531-70.

[18] Jahsman WE. STATIC AND DYNAMIC MATERIAL BEHAVIOR OF SYNTACTIC FOAM. Mechanical Behavior of Materials Under Dynamic Loads. 1968.

[19] Gere JM, Timoshenko SP. Mechanics of materials: Brooks/Cole Pacific Grove, CA 2001.
[20] Maiti SK, Gibson LJ, Ashby MF. Deformation and energy absorption diagrams for cellular solids. ACTA METALLURG. 1984;32(11):1963-75.
[21] Fishbane PM, Gasiorowicz S, Thornton ST. Physics for scientists and engineers: Prentice Hall Upper Saddle River, NJ 1996.
[22] Bjerketvedt D, Bakke JR, Van Wingerden K. Gas explosion handbook. Journal of Hazardous Materials. 1997;52(1):1-150.
[23] Nordin JS. Explosion. PEAC - Aristatek:10.
[24] Lewis B, Von Elbe G. Combustion, flames and explosions of gases: Academic Press New York 1961.
[25] Benson T. Speed of Sound. 2007 [cited; Available from: **www.lerc.nasa.gov**
[26] Li QM, Reid SR. About one-dimensional shock propagation in a cellular material. International Journal of Impact Engineering. 2006;32(11):1898-906.
[27] Taylor J. Detonation in Condensed Explosives: Clarendon Press 1952.
[28] Forrest D. Careful Planning Improves Impact Testing. Hewlett-Packard Realtime Update. 1995:1-5.

Vita

Bradley E. Toon
Born November 12, 1980 in Louisville, Kentucky, USA

Education

Bachelor of Science, Mechanical Engineering, August 1999 – May 2003
Saint Louis University, Saint Louis, Missouri, USA

Professional Positions Held

Research Assistant, August 2006 – Present
Center for Applied Energy Research
University of Kentucky, Lexington, Kentucky, USA

Project Design Engineer, December 2003 – August 2006
Industrial Solutions Group, Inc.
Cincinnati, Ohio, USA

Student Intern, May 2002 – August 2002
Department of Energy, Argonne National Labs, Process Evaluation Group
Argonne, Illinois, USA

Cooperative Student, May 2001 – August 2001
Louisville Gas and Electric (Now: E.On-US), Gas Storage Group
Muldraugh, Kentucky, USA

Scholastic Honors

Certified Engineer Intern (Passed Fundamentals of Engineering Exam)
State of Ohio, October 2005
Summa Cum Laude Graduate, Saint Louis University
Department of Mathematics Award for Excellence, Saint Louis University